VIBRATION FATIGUE ANALYSIS OF STRUCTURES UNDER BROADBAND EXCITATION

A THESIS SUBMITTED TO
THE GRADUATE SCHOOL OF NATURAL AND APPLIED SCIENCES
OF
MIDDLE EAST TECHNICAL UNIVERSITY

BY

BİLGE KOÇER

IN PARTIAL FULFILLMENT OF THE REQUIREMENTS
FOR
THE DEGREE OF MASTER OF SCIENCE
IN
MECHANICAL ENGINEERING

JUNE 2010

Approval of the thesis:

VIBRATION FATIGUE ANALYSIS OF STRUCTURES UNDER BROADBAND EXCITATION

submitted by **BİLGE KOÇER** in partial fulfillment of the requirements for the degree of **Master of Science in Mechanical Engineering Department, Middle East Technical University** by,

Prof. Dr. Canan Özgen _____
Dean, Graduate School of **Natural and Applied Sciences**

Prof. Dr. Suha Oral _____
Head of Department, **Mechanical Engineering**

Assoc. Prof. Dr. Serkan Dağ _____
Supervisor, **Mechanical Engineering Dept., METU**

Asst. Prof. Dr. Yiğit Yazıcıoğlu _____
Co-Supervisor, **Mechanical Engineering Dept., METU**

Examining Committee Members:

Asst. Prof. Dr. Ergin Tönük _____
Mechanical Engineering Dept., METU

Assoc. Prof. Dr. Serkan Dağ _____
Mechanical Engineering Dept., METU

Asst. Prof. Dr. Yiğit Yazıcıoğlu _____
Mechanical Engineering Dept., METU

Asst. Prof. Dr. Ender Ciğeroğlu _____
Mechanical Engineering Dept., METU

Dr. Volkan Parlaktaş _____
Mechanical Engineering Dept., Hacettepe University

Date: 24 – 06 – 2010

I hereby declare that all information in this document has been obtained and presented in accordance with academic rules and ethical conduct. I also declare that, as required by these rules and conduct, I have fully cited and referenced all material and results that are not original to this work.

Name, Last name : Bilge, Koçer

Signature :

ABSTRACT

VIBRATION FATIGUE ANALYSIS OF STRUCTURES UNDER BROADBAND EXCITATION

Koçer, Bilge
M.S., Department of Mechanical Engineering
Supervisor: Assoc. Prof. Dr. Serkan Dağ
Co-Supervisor: Asst. Prof. Dr. Yiğit Yazıcıoğlu

June 2010, 117 pages

The behavior of structures is totally different when they are exposed to fluctuating loading rather than static one which is a well known phenomenon in engineering called fatigue. When the loading is not static but dynamic, the dynamics of the structure should be taken into account since there is a high possibility to excite the resonance frequencies of the structure especially if the loading frequency has a wide bandwidth. In these cases, the structure's response to the loading will not be linear. Therefore, in the analysis of such situations, frequency domain fatigue analysis techniques are used which take the dynamic properties of the structure into consideration. Vibration fatigue method is also fast, functional and easy to implement.

In this thesis, vibration fatigue theory is examined. Throughout the research conducted for this study, the ultimate aim is to find solutions to problems arising from test application for the loadings with nonzero mean value bringing a new perspective to mean stress correction techniques. A new

method is developed to generate a modified input loading history with a zero mean value which leads in fatigue damage approximately equivalent to damage induced by input loading with a nonzero mean value. A mathematical procedure is proposed to implement mean stress correction to the output stress power spectral density data and a modified input loading power spectral density data is obtained. Furthermore, this method is improved for multiaxial loading applications. A loading history power spectral density set with zero mean but modified alternating stress, which leads in fatigue damage approximately equivalent to the damage caused by the unprocessed loading set with nonzero mean, is extracted taking all stress components into account using full matrixes. The proposed techniques' efficiency is discussed throughout several case studies and fatigue tests.

Keywords: Vibration Fatigue, Mean Stress Correction, Power Spectral Density, Finite Element Method.

ÖZ

YAPILARIN GENİŞ BANTLI TAHRİK ALTINDA TİTREŞİM KAYNAKLI YORULMA İNCELEMELERİ

Koçer, Bilge
Yüksek Lisans, Makine Mühendisliği Bölümü
Tez yöneticisi: Doç. Dr. Serkan Dağ
Yardımcı tez yöneticisi: Yrd. Doç. Dr. Yiğit Yazıcıoğlu

Haziran 2010, 117 sayfa

Yapılar statik yükleme yerine dalgalanan bir yüklemeye maruz kaldıklarında, davranışları tamamen değişiklik gösterir. Bu husus, mühendislikte sıklıkla karşılaşılan bir durum olup yorulma olarak adlandırılır. Yükleme statik olmaktan ziyade dinamik ise yapı dinamiği de göz önünde bulundurulmalıdır çünkü özellikle yükleme frekans bandı genişse yapının rezonans frekanslarını tahrik etme olasılığı yüksektir. Bu tür durumlarda, yapının yüklemeye karşı tepkisi doğrusal olmayacaktır. Bu yüzden, bu tarz problemlerin incelenmesinde, yapının dinamik özelliklerini de dikkate alan frekans temelli yorulma analiz teknikleri kullanılır. Ayrıca, titreşim kaynaklı yorulma yöntemi hızlı, kullanışlı ve uygulaması kolaydır.

Bu tezde, titreşim kaynaklı yorulma teorisi incelenmektedir. Bu çalışma için gerçekleştirilen araştırma sürecinde esas amaç, ortalama değeri sıfırdan farklı yüklemeler için test uygulamalarından kaynaklanan problemleri, ortalama gerilme düzeltme tekniklerine yeni bir bakış açısı getirerek çözmektir. Ortlaması sıfır olmayan bir girdi yükünün sebep olduğu

yorulma hasarına yakın bir hasar meydana getirecek ve ortalaması sıfır olacak şekilde modifiye edilmiş bir girdi yükü oluşturmak için yeni bir yöntem geliştirilmiştir. Ortalama gerilme düzeltme formülünü çıktı gerilme güç spektrum yoğunluk datasına uygulamak için matematiksel bir prosedür önerilmiştir ve modifiye edilmiş girdi yükleme güç spektrum yoğunluk datası elde edilmiştir. Ayrıca bu yöntem, çok yönlü yükleme uygulamaları için de kullanılacak şekilde geliştirilmiştir. Ortalaması sıfır olmayan işlenmemiş girdi yükü setinin yarattığı yorulma hasarına yakın bir hasar oluşturacak ve ortalaması sıfır olacak şekilde dalga değerleri modifiye edilmiş bir yükleme güç spektrum yoğunluk seti bütün gerilme elemanlarını dikkate alarak ve tüm matrisleri kullanarak elde edilmiştir. Önerilen tekniklerin etkinliği çeşitli örnek çalışmalarla ve yorulma testleriyle değerlendirilmiştir.

Anahtar kelimeler: Titreşim Kaynaklı Yorulma, Ortalama Gerilme Düzeltmesi, Güç Spektrum Yoğunluk, Sonlu Eleman Metodu

To my dear family,

with love and gratitude...

ACKNOWLEDGEMENTS

I am very thankful to my thesis supervisors, Assoc. Prof. Dr. Serkan Dağ, and Asst. Prof. Dr. Yiğit Yazıcıoğlu, whose valuable guidance, technical support, and contributions throughout this study enabled me to complete this thesis work successfully and gave me enthusiasm in developing new techniques in scientific studies.

I am pleased to express my special thanks to my family for their endless support and help, especially to my mother who supported me morally throughout my life. I also heartily thank to my fiancé, and colleague, Mehmet Ersin Yümer, with my deepest appreciation for his understanding, encouragement and willing assistance.

I am also grateful to TÜBİTAK-SAGE, especially to Structural Mechanics Division, for their technical guidance in academic studies. I would like to thank to Dr. A. Serkan Gözübüyük and Dr. Özge Şen who inspired me to achieve new solutions to the problems arising from test applications. Also, I sincerely thank to my colleagues Ahmet Akbulut and Harun Davut Kendüzler for their help in manufacturing test equipments.

Lastly, I offer my regards to my colleagues and friends who supported me in any respect during the completion of this thesis.

TABLE OF CONTENTS

LIST OF FIGURES

FIGURES

LIST OF TABLES

TABLES

LIST OF SYMBOLS

S	: Stress
N, n	: Number of cycles
a	: Crack size
S_a	: Alternating stress amplitude
S_r	: Stress range
S_m	: Mean stress
$S_{\max}$	: Maximum stress amplitude
$S_{\min}$	: Minimum stress amplitude
R	: Stress ratio
b	: Basquin exponent
C	: Material constant
S_o	: Fatigue limit
S_e	: Endurance limit
K_i	: Stress concentration factor
K_f	: Fatigue strength concentration factor
q	: Notch Sensitivity
k_a	: Surface condition modification factor
k_b	: Size modification factor
k_c	: Load modification factor
k_d	: Temperature modification factor
k_e	: Reliability factor
k_f	: Miscellaneous-effects modification factor

$S_e^{'}$: Laboratory test specimen endurance limit

S_a : Alternating stress

$S_a^{'}$: Equivalent alternating stress

S_m : Mean stress

S_u : Ultimate tensile strength

S_y : Tensile yield strength

$E[D]$: Expected damage

PSD : Power spectral density

T_p : Period

$y(t)$: Time history

A_o, A_n, B_n : Fourier coefficients

PSD : Power spectral density

$y(f)$: Frequency spectrum of time history

FFT : Fast Fourier Transform

$IFFT$: Inverse Fourier Transform

$H(f)$: Transfer function

$H^*(f)$: Complex conjugate of transfer function

$G_r(f)$: Response stress PSD

$G_i(f)$: Input acceleration PSD

$p(S)$: Probability density function (PDF) of rainflow stress ranges

m_n : The nth spectral moment of the PSD of stress

$E(P)$: Expected number of peaks per second

$E(0)$: Expected number of upward zero crossings per second

γ : Irregularity factor

$G_{rm}(f)$: Modified output stress PSD

$G_{im}(f)$: Modified input acceleration PSD

$\{\sigma(f)\}$: Output stress vector

$\{a(f)\}$: Input acceleration vector

$\{\sigma_m(f)\}$: Modified output stress vector

$\lfloor G_{\sigma_m}(f) \rfloor$: Modified output stress PSD matrix

$\lfloor G_{a_m}(f) \rfloor$: Modified input acceleration PSD matrix

CHAPTER 1

INTRODUCTION

The aerospace industry's increasing demands for durability, safety, reliability, long life and low cost lead in high interest in studies for improving strength, quality, productivity, and longevity of components in engineering science. Consequently, these products should be designed and tested for sufficient fatigue resistance over a desired range of product populations to satisfy the needs.

1.1 Metal Fatigue Damage

The behavior of machine parts becomes totally different when they are subjected to fluctuating loading rather than static one. Often, machine members fail under the excitation of repeated or alternating stresses; yet the most careful analysis shows that the actual maximum stresses are well below the ultimate strength of the material, and quite frequently even below the yield strength. The most distinguishing characteristic of these failures is that the stresses repeat in a cyclic manner very large number of times. Such a failure is called a fatigue failure [1]. In other words, metal fatigue is the progressive and localized structural damage that occurs when a material is subjected to alternating, cyclic, varying loading.

1.1.1 Properties of Fatigue Failure

A fatigue failure looks like a brittle fracture, since the fracture surfaces are flat and perpendicular to the stress axis without necking occurring. However, fracture characteristics of fatigue failure are quite different from the static brittle fracture in the aspect that fatigue failure comes out in stages (Figure 1.1). In Forsyth's notation [2], [3], Stage I is the initiation of one or more microcracks and this stage's crack propagation is an extension of the initiated microcrack without change of direction. Hence, a Stage I crack propagates within a slip band that is on a plane of high shear stress (Figure 1.2). The term fatigue crack initiation sometimes involves Stage I fatigue crack growth. A Stage I crack turns into a Stage II crack as it achieves a critical length. It changes its direction and starts to propagate normal to the maximum principal tensile stress. After the transition, Stage II, the crack propagates throughout the majority of the cross section. More descriptive terms, microcrack and macrocrack, are sometimes used, for Stage I and II, respectively. Similarly, unqualified references to fatigue crack propagation refer to macrocrack propagation. After two preceding stages, finally, the cross section so shrinks that even one load cycle is sufficient to constitute the conditions for failure. This process is sometimes called Stage III and can be resulted from crack propagation by brittle fracture, ductile collapse or both.

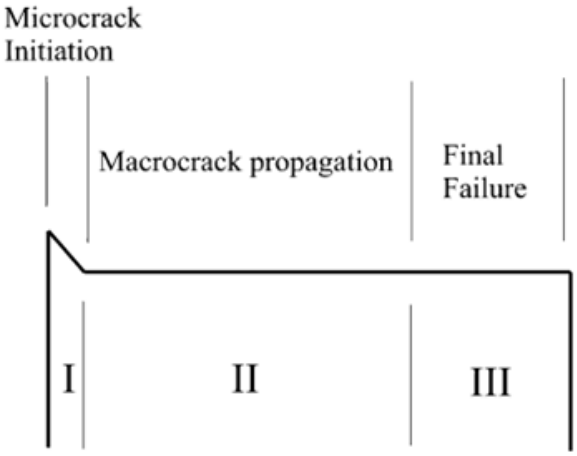

Figure 1.1 – Schematic section through a fatigue fracture showing the three stages of crack propagation [4].

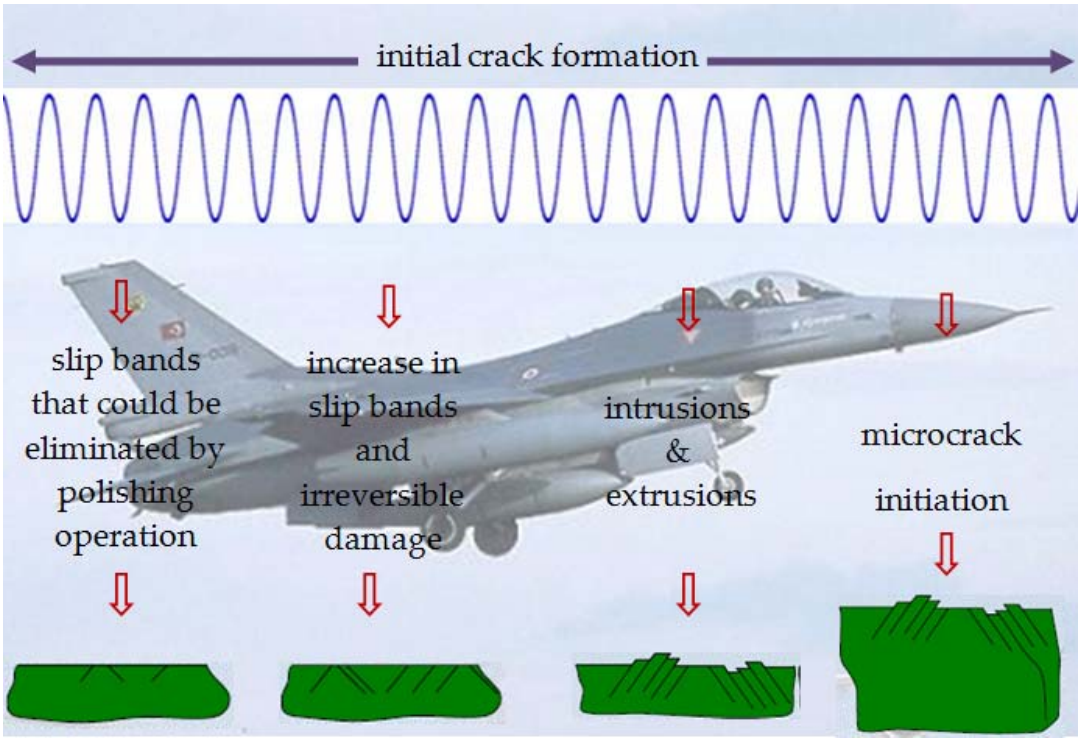

Figure 1.2 – Stage I: Crack Initiation

Most of the static failures give a visible warning in advance, such as developing a large deflection due to the exceeding of yield strength of the material, before the total fracture occurs. However, fatigue failures are sudden and total usually without a warning, therefore dangerous. Figure 1.3 shows a post fatigue failure surface at the point of failure. Figure 1.4 shows a failure crack which occurs for a railway component.

Figure 1.3 –A fatigue failure surface [52]

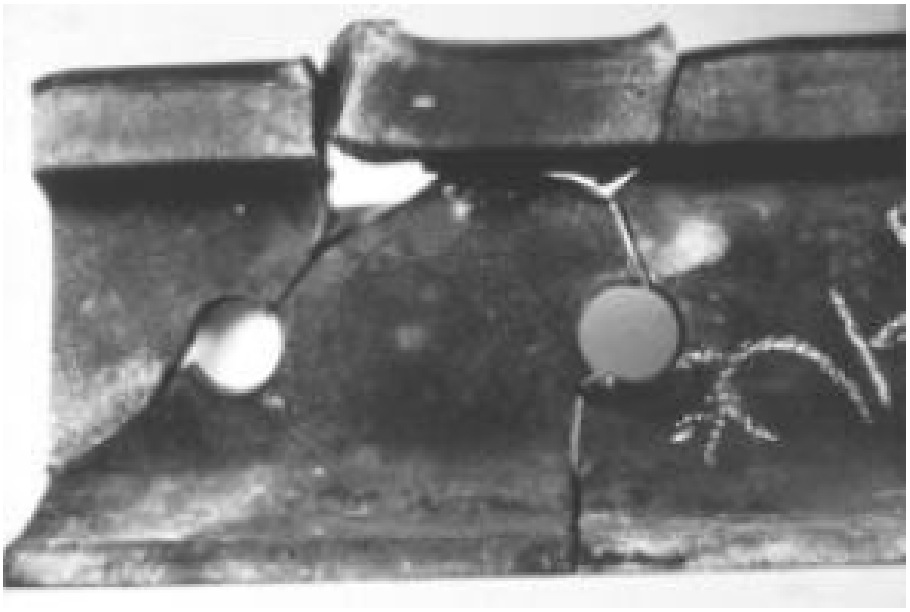

Figure 1.4 –Failure of a railway track component [52]

1.1.2 Major Fatigue Damage Accidents During In Service

The first known disastrous fatigue failure accident is the France railway accident takes place in 1842 [5]. The body of the leading engine falls down since the front axle of the front, four wheeled engine collapses suddenly because of metal fatigue. Then, the second engine breaks up. Follower carriages pass over ruin which starts a fire and results in major loss of life. These kinds of failures occurring on railway transportation push scientists start extensive examinations on the nature of metal fatigue [5], [6], [7].

Comet I aircraft G-ALYP disintegrates after 3680 flight hours and 1286 flight cycles at 30,000 feet altitude in 1954 since fatigue crack initiates at the corner of automatic direction finding window [8].

A Boeing 707-300 run by DAN-Air loses the control of pitch, then, the right hand horizontal stabilizer and elevator separates in-flight after 16,723 flight cycles and 47,621 hours in 1977 (Figure 1.5). The rear spar top chord and is exposed to long-term fatigue damage. Besides, the redundant fail safe structure cannot support the flight loads for a period long enough to enable the fatigue crack to be detected during a routine inspection [8].

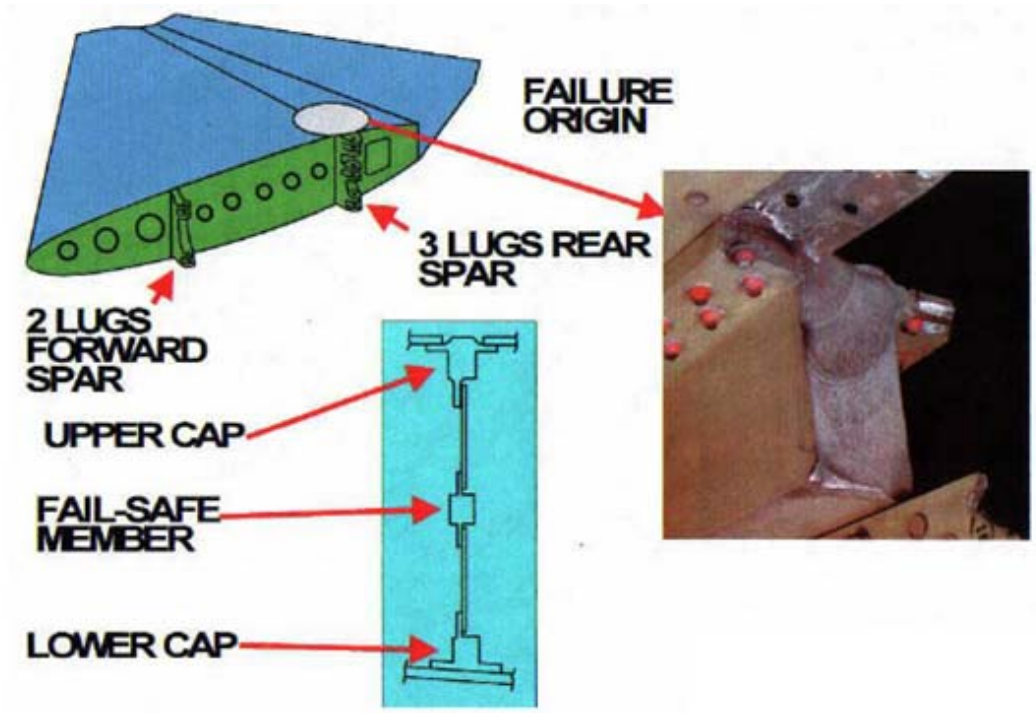

Figure 1.5 – Lusaka Accident, 1977 [8]

Left engine and pylon of Douglas DC-10 No.22, operated by American Airlines, separates from the wing as the airplane lifts off the run-way on take-off and the airplane crashes, in Chicago, in 1979. The accident

investigation [9] shows that captain's control panel is disabled when the engine separates. The severed hydraulic lines allowed the slats on the left wing to gradually retract. The stall speed on the left wing increases noticeably. As the aircraft's speed decreases, the left wing aerodynamically stalls due to its clean configuration, while the right wing continues to gain lift while its slats are still in takeoff position. Since one wing stalls and the other wing generates full lift continuously, the airplane eventually rolls past a 90° bank, and falls down to ground (Figure 1.6 - Figure 1.7). The reason of the crash is stated as the crack which occurs due to improper maintenance.

a)  b) 

Figure 1.6 – Chicago Accident, 1979: a) An amateur photo, as the aircraft rolling past a 90° bank angle, b) explosion as the airplane impacts [9]

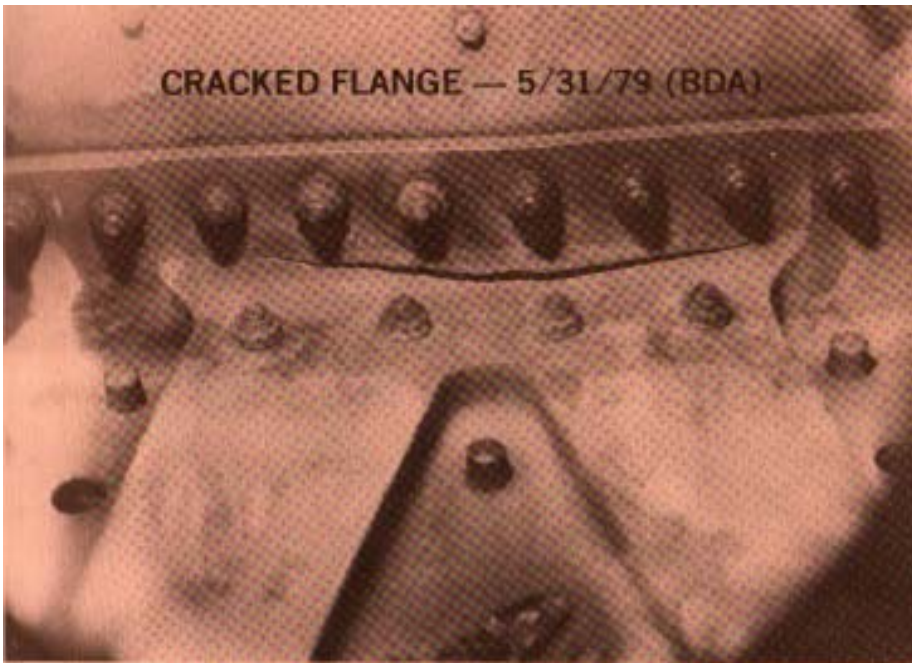

Figure 1.7 – A Cracked Flange of American Airplane [8]

Boeing 737-200 aircraft MSN 152 belonging to Aloha Airlines is exposed to explosive decompression at 24,000 feet altitude after 89,681 flight cycles in 1988 (Figure 1.8). The accident is caused by fatigue failure which takes place in lap splice at one of the stringers that is a cold bonded and riveted joint. Fatigue failure occurs because of knife edge effect due to deep countersunk and therefore subsequent multiple site damage [8].

Figure 1.8 – Aloha Accident, 1988 [10]

1.2 Scope of the Thesis

Lifetime prediction assessment for components under random loading is an important concern in engineering. The study carried out in this thesis aims to investigate vibration fatigue approach. Throughout the research, the ultimate goal is to bring new perspectives to mean stress correction techniques and find solutions to problems arising from test applications for the loadings with nonzero mean values.

In fatigue calculations, mean stress effect resulting from the mean value of the loading can be taken into account rather easily but experimental verification is troublesome because any mean value of an acceleration excitation other than 1g in the direction of gravity is difficult to simulate with traditional testing equipments like vibration shakers. To overcome this situation, a method is developed to create a modified input loading history

with a zero mean which causes fatigue damage approximately equivalent to that created by input loading with a nonzero mean. A mathematical procedure is proposed to implement mean stress correction to the output von Mises stress power spectral density data. Furthermore, this method is extended to generate a loading history set in multi-axis with zero mean but modified alternating stress, which leads in fatigue damage approximately equivalent to the damage caused by the unprocessed loading set with nonzero mean, taking all stress components into account using full matrices. The efficiency of proposed solutions is discussed throughout several case studies and fatigue tests.

1.3 Outline of the Thesis

Chapter 1 begins with preliminary information on fatigue definition, metal fatigue mechanism, fatigue failure and the importance of design considering fatigue criterion illustrating major fatigue accidents during service.

In Chapter 2, the emphasis is on literature survey. Historical overview of fatigue theory with the milestones of the fatigue phenomenon is presented in this chapter in a chronological order. Furthermore, a subchapter is completely separated to investigate the progress in vibration fatigue approach mentioning the research and studies carried out in this field.

Chapter 3 is devoted to fatigue theory. Time domain methods and frequency domain methods are discussed. Stress life approach is examined in detail where mean stress effects on fatigue life and counting methods are

presented. Besides, stress life approach and crack propagation approach are mentioned briefly. Moreover, frequency domain vibration fatigue theory is examined in detail where narrowband solutions and wideband solutions are discussed.

In Chapter 4, a new method for generation of a loading history with zero mean is proposed, whose efficiency is discussed throughout a case study. The method aims to obtain zero mean loading for a structure, approximately equivalent in fatigue damage that is subjected to random loading with nonzero mean making use of the frequency domain fatigue calculation techniques and output stress power spectral density.

Chapter 5 is dedicated to the extension of the technique proposed in Chapter 4. The goal is to generate a loading history with zero mean for multiaxial loading. A multiaxial input loading with zero mean but modified alternating stress, which creates fatigue damage approximately equivalent to the damage caused by the unprocessed loading set with nonzero mean, is extracted by means of the frequency domain fatigue calculation techniques and output stress power spectral density. The efficiency of proposed approach is discussed throughout case studies and fatigue tests.

Finally, Chapter 6 summarizes the work done throughout the research, and evaluates the outcomes and contributions to the literature.

Schematic representation of the thesis outline is given in Figure 1.9.

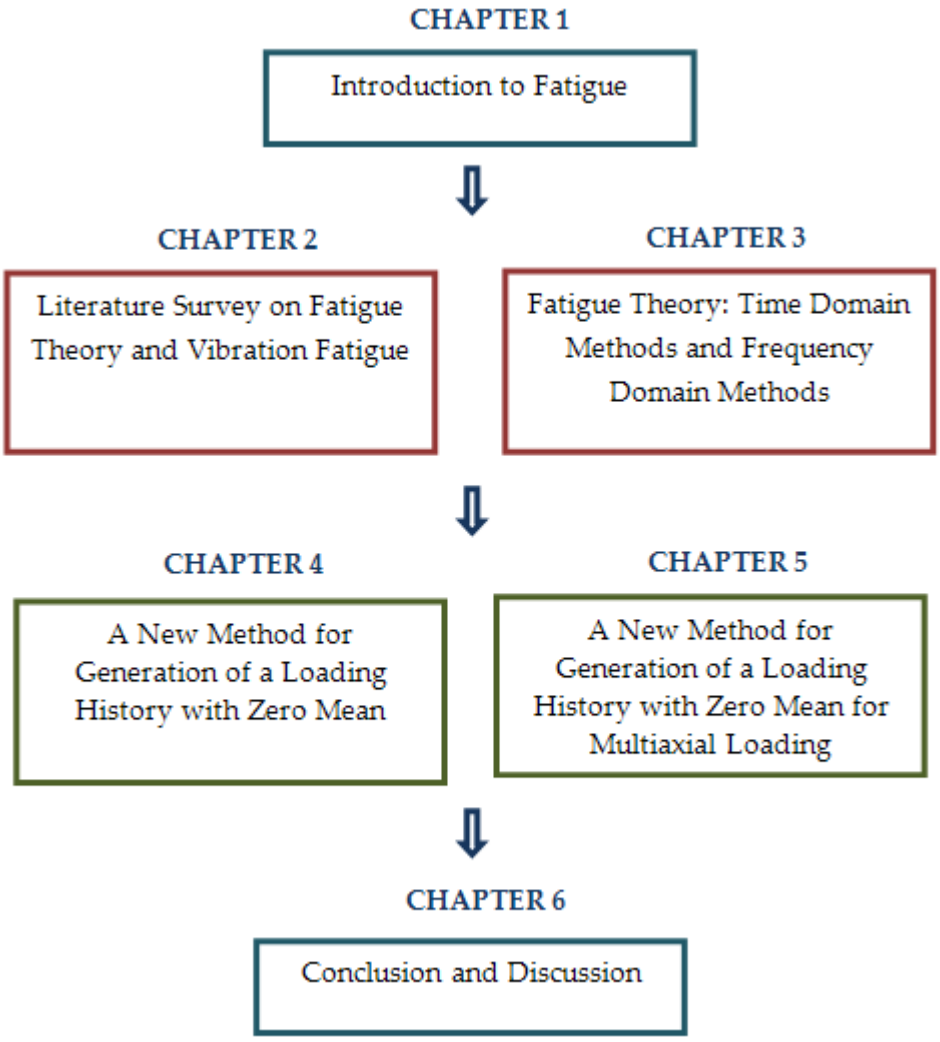

Figure 1.9– Outline of the Thesis

CHAPTER 2

LITERATURE SURVEY

2.1 Historical Overview of Fatigue

The first fatigue examinations seems to have been reported by Albert, a mining engineer, who carried out some repeated loading tests on iron chain in 1829 [11].

As railway service started to improve rapidly throughout the nineteenth century, fatigue failures of railway axles become a widespread problem. This situation requires that the cyclic loading effect should be taken into consideration. The first major impact of failures resulting from repeated stresses appears in the railway industry in the 1840s. It is recognized that railroad axles fails regularly at shoulders [12]. Then, the removal of sharp corners is recommended.

The term “fatigue” is introduced to explain failures happening due to alternating stresses in the 1840s and 1850s. The first usage of the word “fatigue” in print comes into view by Braithwaite, although Braithwaite states in his paper that it is coined by Mr. Field [13]. Then, a general opinion starts to develop in such a way that the material gets tired of bearing the load or repeating application of a load exhausts the capability of the material to carry load which survives to this day [4].

August Wöhler, a German railway engineer, sets and performs the first systematic fatigue examination from 1852 to 1870. He carries out experiments on full-scale railway axles and also on small scale torsion, bending, and axial cyclic loading test specimens for different materials. Wöhler's data for Krupp axle steel are plotted as nominal stress amplitude versus cycles to failure. This presentation of fatigue life leads in the S-N diagram. Furthermore, Wöhler indicates that the range of stress is more important than the maximum stress for fatigue failure [11], [14].

Gerber, Goodman and some other researchers examine the influence of mean stress in loading throughout 1870s and 1890s.

Bauschinger [15] points out that the yield strength in compression or tension decreases after applying a load of the opposite sign that results in inelastic deformation. It is the first indication that a single exchange of inelastic strain could alter the stress-strain behavior of metals.

Ewing and Humfrey [16] study on fatigue mechanisms in microscopic scale observing microcracks in the early 1900s. Basquin [17] represents alternating stress versus number of cycles to failure (S-N) in the finite life region as a log-log linear correlation in 1910.

Grifith [18], an important contributor to fracture mechanics, presents theoretical calculations and experiments on brittle fracture by means of glass in the 1920s. He states that the relation $S\sqrt{a}$ = constant, where S is the nominal stress at fracture and a is the crack size at fracture.

Palmgren [19] introduces a linear cumulative damage model for loading with varying amplitude in 1924. Neuber [20] demonstrates stress gradient effects at notches in the 1930s. Miner [21] formulates linear cumulative fatigue damage criterion proposed by Palmgren in 1945 which is now known as Palmgren-Miner linear damage rule.

Irwin [22] introduces the stress intensity factor K_I, which is known as the basis of linear elastic fracture mechanics and the origin of fatigue crack growth life calculations. The Weibull distribution [23] grants a two-parameter and a three-parameter statistical distribution for probabilistic fatigue life analysis and testing.

Manson-Coffin relationship [24][25] investigates the relationship between plastic strain amplitude at the crack tip and fatigue life. The idea is developed by Morrow [26]. Matsuishi and Endo [27] formulate the rainflow-counting algorithm to determine stress ranges for variable amplitude loading.

Elber [28] develops a quantitative model which figures crack closure on fatigue crack growth in 1970. Paris [29] shows that a threshold stress intensity factor could be obtained for which fatigue crack growth would not occur in 1970.

Throughout the 1980s and the 1990s, many researchers study on the complex problem of in phase and out-of-phase multi-axial fatigue, critical plane models are proposed.

2.2 Background of Vibration Fatigue

Rice [30] develops the very important relationships for the number of upward mean crossings per second and peaks per second in a random signal expressed solely in terms of their spectral moments of the power spectral density of the signal. This is the first serious effort at providing a solution for estimating fatigue damage from power spectral density.

Bendat [31] presents the theoretical basis for the so-called Narrow Band solution. The expression used for the estimation of expected value of damage is defined only in terms of the spectral moments of the power spectral density up to the fourth degree.

Many expressions are proposed to improve narrow band solution [31] and adapt it to broad band type. Most of them are developed with regards to offshore platform design where interest in the techniques has existed for many years. The methods are produced by generating sample time histories from power spectral densities using Inverse Fourier Transform techniques. Then probability density function of stress ranges is estimated empirically. The solutions of Wirsching et al. [32], Chaudhury and Dover [33], Tunna [34], Hancock [35], and Kam and Dover [35] formulas are all derived using mentioned technique. They are all expressed in terms of the spectral moments of power spectral density up to the fourth degree.

Steinberg [36] presents three band technique, based on Gaussian distribution, for fatigue failure under random vibration for electronic components. It is a simplified approach which does not require a large

computational effort. Therefore it is valuable as a time saving method. The proposed method is based on a large volume of test data that was arranged and rearranged to verify that a simplification in determining stress ranges distribution is usable to analyze random vibration fatigue failures with reasonable accuracy.

Dirlik [37] develops an empirical closed form expression for determination of the probability density function of rainflow ranges directly from power spectral density. The solution is obtained using extensive computer simulations to model the signals using the Monte Carlo technique.

Wu et al. [38] work on a group of specimens made of 7075-T651 aluminum alloy to examine the applicability of methods proposed in the estimation of fatigue damage and fatigue life of components under random loading. Fatigue test results illustrate that the fatigue damage estimated based on the Palmgren-Miner rule can be improved by applying Morrow's plastic work interaction damage rule. Furthermore, random vibration theory for narrow band process is utilized to estimate fatigue life where the probability density function of the stress amplitudes is determined by means of Rayleigh distribution for a zero-mean narrow-band Gaussian random process.

Bishop et al. [39] present a state of the art perspective of random vibration fatigue technology. Several design applications are presented. Time and frequency domain methods are investigated and compared performing finite element analysis using a model of a bracket, which is fully fixed at the position of a round hole inside. Time domain and frequency domain

calculations show agreement if a transient dynamic analysis is carried out with time domain fatigue life calculations for the excitations whose frequency range includes the natural frequencies of the specimen. Also, it is stated that the time and frequency domain processes are actually very similar. The only differences are the structural analysis approach used (time or frequency domain) and the fact that a fatigue modeler is needed as a tool to extract the rainflow cycle histogram from the PSD of stress.

Liou et al. [40] study the theory of random vibration which is incorporated into the calculation of the fatigue damage of the component subjected to variable amplitude loading making use of the fundamental stress-life cycle relationship and different accumulation rules. The purpose is to derive ready to-use formulas for the prediction of fatigue damage and fatigue life when a component is subjected to statistically defined random stresses. Morrow's plastic work interaction damage rule is considered, in particular, in the derivation in which the maximum stress peak should be taken into consideration and it gives rather accurate fatigue life prediction in the long life region and slightly conservative life in the short life region with the use of Miner's rule. Moreover, a series of fatigue tests are conducted and some of the analytical in addition to experimental results are presented to verify the applicability of the derived formulas.

Pitoiset et al. [41] make use of the frequency domain method, directly from a spectral analysis for the estimation of high-cycle fatigue damage under random vibration leading multiaxial stresses. This method is derived from a new designation of the von Mises stress as a random process which is used as an equivalent uniaxial counting variable. Also, this approach can be

generalized to include a frequency domain formulation of the multiaxial rainflow method for biaxial stress states. Furthermore, a procedure for the generation of multiaxial stress tensor histories of a given PSD matrix is described.

Petrucci [42] studies the fatigue life prediction of components and structures under random loading mainly concerning the general problem of directly relating fatigue cycle distribution to the power spectral density of the stress ranges by means of closed-form expressions that avoid expensive digital simulations of the stress process. The method illustrates that the statistical distribution of fatigue cycles depends on four parameters of the PSD calculated from spectral moments making use of numerical simulations and theoretical considerations while the present methods, proposed to obtain stress cycle distribution, are based on the use of a single parameter of the PSD which is irregularity factor. The proposed approach gives reliable estimates of the fatigue cycle distribution, with the use of the range-mean counting method, when the stress process has narrow-band derivatives.

Petrucci et al. [43] develop Petrucci's approximated method [42] for the high cycle fatigue life prediction of structures subjected to Gaussian, stationary, wide band random loading. Fatigue life of components under uniaxial stress state can directly be estimated from the stress power spectral density of any shape. In particular, approximated closed-form ralationships between the spectral moments of the stress power spectral density of the fatigue cycles of the Goodman equivalent stress, and the irregularity factor also with a bandwidth parameter are determined. The accuracy of fatigue

life predictions obtained with this method is compared with some of the frequency based techniques in literature and found to be more accurate than some of them.

Pitoiset et al. [44] deal with frequency domain methods to determine the high-cycle fatigue life of metallic structures under random multiaxial loading. The equivalent von Mises stress method is reviewed and it is assumed that the fatigue damage under multiaxial loading can be predicted by calculating an equivalent uniaxial stress on which the classical uniaxial random fatigue theory is applied. The multiaxial rainflow method, initially formulated in the time domain, can be implemented in the frequency domain in a formally similar way. The consistency of the results is verified by means of a time domain method based on the critical plane. Furthermore, it is showed that frequency domain methods are computationally efficient and correlate fairly well with the time domain method in terms of localizing the critical areas in the structure. A frequency domain implementation of Crossland's failure criterion is also proposed; it is found in good agreement and faster than its time domain counterpart.

Tovo [45] studies fatigue damage under broadband loading by reviewing analytical solutions in the literature states and verifies the relationships between various cycle counting methods and available analytical solutions of expected fatigue damage in the frequency domain. Furthermore, a new method is developed starting from knowledge of power spectral density distributions for rainflow damage estimation which gives accurate approximations of fatigue damage under both broadband and narrowband Gaussian loading. The proposed technique is based on the theoretical

examination of possible combinations of peaks and valleys in Gaussian loading and fits numerical simulations of fatigue damage well.

Siddiqui et al. [46] states that a tension leg platform, a deep water oil exploration offshore compliant system, is subjected to fatigue damage significantly because of the dynamic excitations caused by the oscillating waves and wind over its design life period. The reliability estimation against fatigue and fracture failure due to random loading considers the uncertainties associated with the parameters and procedures utilized for the fatigue damage assessment. Calculations for fatigue life estimation require a dynamic response analysis under various environmental loadings. A non-linear dynamic analysis of the platform is implemented for response calculations. The response histories are employed for the study of fatigue reliability analysis of the tension leg platform tethers under long crested random sea and associated wind. Fatigue damage of tether joints is estimated using Palmgren-Miner's rule and fracture mechanics theory. The stress ranges are described by Rayleigh distribution. First order reliability method and Monte Carlo simulation method are employed for reliability estimation. The influence of various random variables on overall probability of failure is studied through sensitivity analysis.

Tu et al. [47] conduct μBGA solder-joints' vibration fatigue failure analysis that are reflowed with different temperature profiles, and aging at 120 ^{o}C for 1, 4, 9, 16, 25, 36 days. Also, Ni3Sn4 and Cu–Sn intermetallic compound (IMC) effects are considered on the fatigue lifetime determination in this work. During the vibration fatigue tests, electrical interruption is followed continuously to see the failure of BGA solder joint. The results of the

experiments indicate that the fatigue lifetime of the solder joint firstly increases and then decreases with increasing heating factor, integral of the measured temperature over the dwell time above liquidus (183 ^{o}C) in the reflow profile. Furthermore, solder joint lifetime decreases almost linearly as fourth root of the aging time increases. According to the test results, the intermetallic compounds contribute mainly to the fatigue failure of BGA solder joints. Also, the fatigue lifetime of solder joint is shorter for a thicker IMC layer.

Benasciutti et al. [48] work on fatigue damage caused by wide-band stationary and Gaussian random loading. Expected rainflow damage is estimated approximately for a given stationary stochastic process described in frequency-domain by its power spectral density. Numerical simulations on power spectral densities with different shapes are performed in order to establish proper dependence between rainflow cycle counting, linear cumulative fatigue damage and spectral bandwidth parameters. Expected rainflow fatigue damage is taken as weighted linear combination of expected damage intensity given by the narrow-band approximation of Rychlik [49] and expected range counting damage intensity approximately obtained by Madsen et al. [50] with the weighting factor approximated using Tovo's approach [45] dependent on PSD through bandwidth parameters. Comparison is made between numerical results and some analytical prediction formulae available for fatigue damage evaluation.

Aykan [51] analyzes helicopters self-defensive system's chaff/flare dispenser bracket by applying vibration fatigue method as a part of an ASELSAN project. Operational flight tests are performed to obtain the

acceleration loading as boundary conditions. The acceleration versus time data is gathered and converted into power spectral density to obtain frequency components of the signal. Bracket is modeled in the finite element environment in order to obtain the stresses for fatigue analysis. The validity of dynamic characteristics of the finite element model is verified by conducting modal tests on a prototype. As the reliability of the finite element model is confirmed, stress transfer functions that are frequency response functions are found and combined with the loading power spectral density to acquire the response stress power spectral density. Narrow band and broad band vibration fatigue calculation techniques are applied and compared to each other for fatigue life. The fatigue analysis results are verified by accelerated life tests on the prototype. Furthermore, the effect of single axis shaker testing for fatigue on the specimen is obtained.

CHAPTER 3

FATIGUE THEORY

Fatigue is examined in two domains basically. First one is the time domain methods and the second one is the frequency domain methods which are similar in approach Figure 3.1 and explained in detail in this chapter.

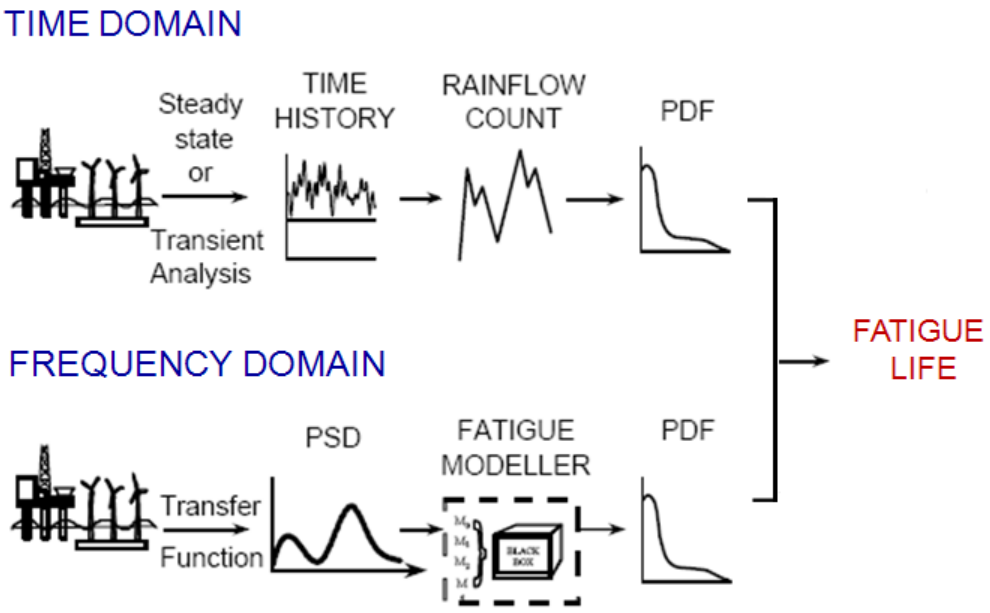

Figure 3.1 – Time Domain vs. Frequency Domain Schematic Representation

Frequency domain approach is generally more time saving when compared to time domain approach because transfer functions needed for response determination are calculated once and can be used repeatedly for different loadings. It makes calculations easier. Furthermore, when the loading is not static but dynamic, the dynamic characteristics of the structure cannot be neglected. In such situations, there is a high possibility to excite the resonance frequencies of the structure if the loading frequency has a wide bandwidth. Therefore, it cannot be assumed that the structure's response will remain linear. Frequency domain fatigue analysis methods are preferred in such situations which include the dynamics of the structure.

3.1 Time Domain Fatigue Approaches

3.1.1 Stress Life (S-N) Approach

It is the oldest of the time domain methods originated in 19th century and is still suitable and usable for most of the cases for fatigue calculations.

Figure 3.2 a) illustrates a fully reversed stress cycle with a sinusoidal form. For example, this loading condition is a typical of that observed in rotating shafts operating at constant speed and constant load. The maximum and minimum stresses are equal in magnitude but opposite in sign. Figure 3.2 b) shows a loading condition where the maximum and minimum stresses are not of equal magnitude since there is an offset in the cyclic loading. The parameters to define this type of loading are given below Figure 3.2.

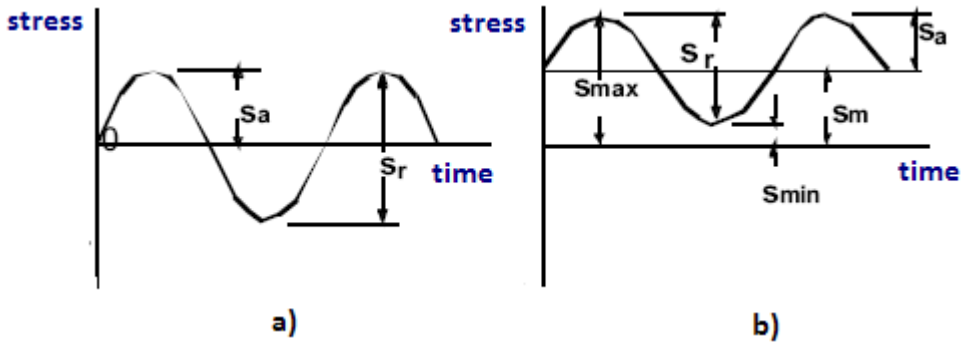

Figure 3.2 – Stress Cycles; (a) fully reversed, (b) offset

S_a	: Alternating stress amplitude
S_r	: Stress range
S_m	: Mean stress
$S_{\max}$	: Maximum stress amplitude
$S_{\min}$	: Minimum stress amplitude
R	: Stress ratio, $S_{\min} / S_{\max}$

The most common test specimen in the past is a cylinder with little changes of cross-section, and with a polished surface in the region where crack formation tends to start. It is loaded in bending and called Wöhler test which has limitations. Now, a cylinder loaded in axial tension is the preferred test specimen with free of sudden changes of geometry and also with a polished surface at the section where cracks are likely to start. Several identical specimens are examined and the number of cycles needed for total separation is accepted as N . Load, not stress, is kept constant in the test. For each specimen a nominal stress, S, is calculated from elastic formulae and the results are plotted as the un-notched $S-N$ curve which is a basic material property [52]. N is plotted on the x-axis in the logarithmic

scale while S constitutes the y-axis plotted in linear or logarithmic scale, but logarithmic is becoming the norm. The mean line in the finite-life region (10000 to 10 million cycles) is usually straight Figure 3.3, and presented with the convenient equation where the inverse slope of the line is b, namely Basquin exponent, and C is related to the intercept on the y axis.

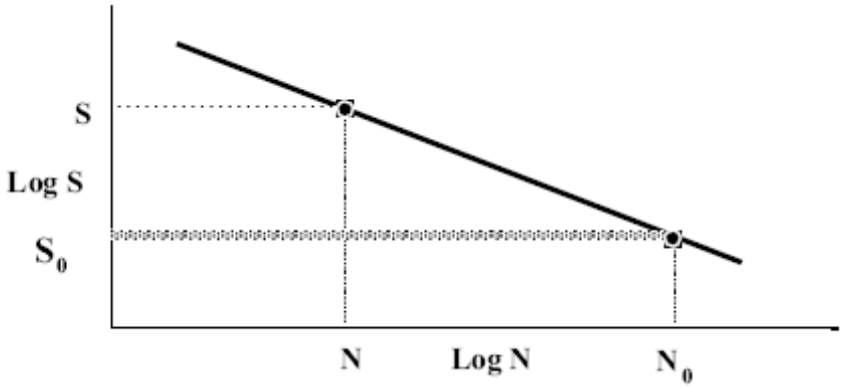

Figure 3.3 – Standard form of the material S-N curve [52]

$$N = C.S^{-b} \tag{3.1}$$

$S-N$ plot of some metals, mostly low alloy steels, is constituted from two-lines. The line may become horizontal and the material is said to have a fatigue limit, S_0, which is important when the aim is infinite life. For materials which do not show a clear fatigue limit, tests are generally terminated at between 10^7 and 10^8 cycles. The corresponding S is named as an endurance limit, S_e, at the specified N, Figure 3.4. There is no strict convention about the use of the terms fatigue limit and endurance limit,

and the original test documentation should be observed if the difference is a critical issue [52].

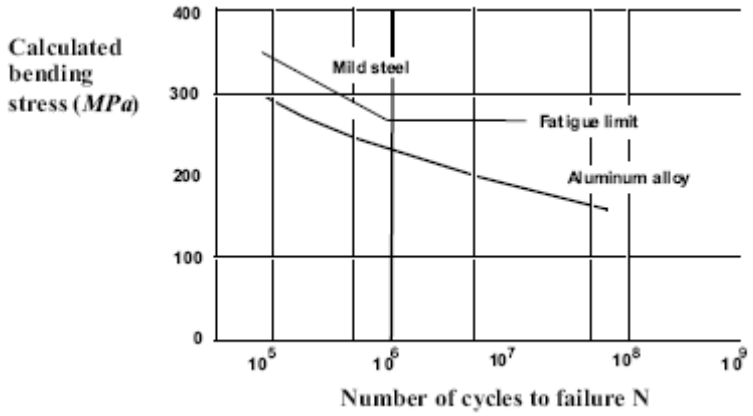

Figure 3.4 – S-N curves for ferrous and non-ferrous metals [52]

3.1.1.1 Stress Concentration and Notch Sensitivity

$S-N$ curve properties of a material are extracted for the specimens that are free from geometrical factors that cause high stress gradients and create local high stress regions. However, components designed for real life can have holes, grooves, changes of section etc. which lead in local hot spots of high stress. Then, fatigue starts at these points. Therefore, their effect must be taken into consideration in life calculations. Geometrical properties that cause high local stresses are named as notches and, the stress concentration factor, K_t, is used to handle this effect [52].

$$K_t = \frac{\text{Maximum stress in the region of the notch}}{\text{Nominal stress remote from the notch}} \tag{3.2}$$

K_f is a reduced value of K_t and generally called fatigue strength concentration factor and described by (3.3) [1].

$$K_f = \frac{\text{Maximum stress in notched specimen}}{\text{Stress in notch free specimen}} \tag{3.3}$$

Then, notch sensitivity, q, is defined as (3.4) [1].

$$q = \frac{K_f - 1}{K_t - 1} \tag{3.4}$$

For simple loading, it is convenient to reduce the endurance limit by dividing the unnotched specimen endurance limit by K_f or multiplying the reversing stress by K_f [1].

3.1.1.2 Endurance Limit Modifying Factors

It is not realistic to expect the endurance limit of a structural part to match the values obtained in the laboratory [1]. All effects of endurance limit modifying factors are investigated in the equation given below (3.5).

$$S_e = k_a k_b k_c k_d k_e k_f S_e^{'} \tag{3.5}$$

where

k_a : surface condition modification factor

k_b : size modification factor

k_c : load modification factor

k_d : temperature modification factor

k_e : reliability factor

k_f : miscellaneous-effects modification factor

$S_e^{'}$: laboratory test specimen endurance limit

S_e : endurance limit at the critical location of a machine part in the geometry and condition of use.

3.1.1.3 Mean Stress Effect

Fatigue life depends essentially on the amplitude of stress existing in the component, but a modification is needed when a mean value of stress exists. Components can carry some form of dead load before the working stresses are applied or the input loading can have a mean value. The general trend in traditional methods is such that the allowable amplitude of fatigue stress gets smaller as the mean stress becomes more tensile for a given life [52].

The basic idea is to assume that mean stress lessens the allowable applied amplitude of stress in a linear way. It is expected that any fatigue load cannot be carried when the mean stress reaches the ultimate tensile strength of the material. If fatigue strength at any mean is known, the line representing fatigue life can be defined. This is a commonly known and mostly used method and called Goodman's Rule. [52]. There are other mean stress correction approaches, like Gerber and Soderberg that modify

alternating stress according to mean stress. Mean stress correction methods' graphical representations are illustrated in Figure 3.5.

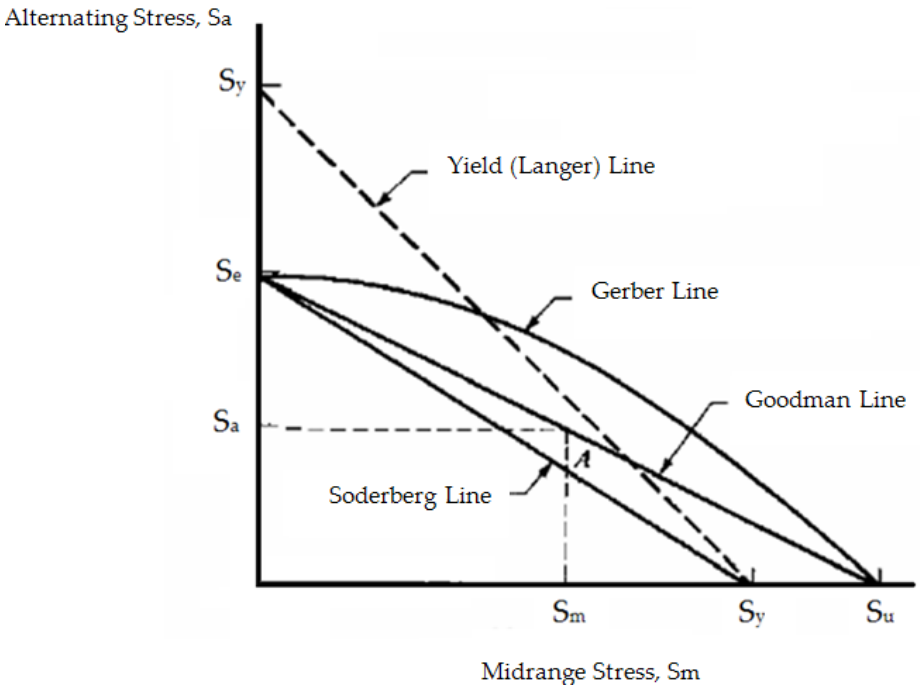

Figure 3.5 - Mean Stress Modification Methods [1]

Goodman's Model:

$$\frac{S_a}{S_a'} + \frac{S_m}{S_u} = 1 \tag{3.6}$$

Gerber's Model:

$$\frac{S_a}{S_a'} + \left(\frac{S_m}{S_u}\right)^2 = 1 \tag{3.7}$$

Soderberg's Model:

$$\frac{S_a}{S_a^{'}} + \frac{S_m}{S_y} = 1 \tag{3.8}$$

S_a : Alternating stress

$S_a^{'}$: Equivalent alternating stress

S_m : Mean stress

S_u : Ultimate tensile strength

S_y : Tensile yield strength

3.1.1.4 Variable Amplitude Loading and Fatigue Damage

The investigation of metal fatigue under variable amplitude loading is based on the study of cumulative damage. The variable amplitude time history consists of n_1 cycles of amplitude S_1, n_2 of amplitude S_2, n_3 of amplitude S_3 and so on. Usually the pattern repeats itself after a small number of stress cycles, S_n (Figure 3.6). The sequence up to S_n is then called block, and the aim is to determine the number of the blocks that can be applied until failure occurs. The method commonly used is known as Miner or Palmgren-Miner rule. According to Miner's hypothesis, linear damage accumulation is assumed. First, when the S_1 level of stress that repeats n_1 cycles is considered, the number of life cycles at stress level S_1 that would cause fatigue failure if no other stresses were present can be obtained from $S-N$ curve . Calling this number of cycles as N_1, it is assumed that n_1 cycles of S_1 use up a fraction n_1 / N_1 of the total fatigue life.

This shows the damage fraction that n_1 cycles cause. The total damage fraction for one block is obtained by doing a similar calculation for all other stresses and summing all the damage fraction results [52]. Then, expected damage, $E[D]$, is equated to this summation and set to one to calculate fatigue life (3.9). The order of stresses occurring in history is ignored in Miner's rule.

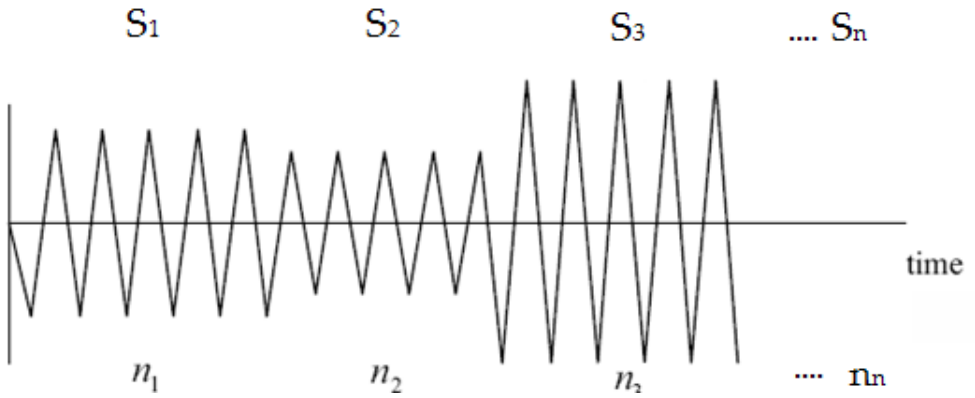

Figure 3.6 – Block Loading Sequence

$$E[D] = \sum_{i=1}^{n} \frac{n_i}{N_i} = \frac{n_1}{N_1} + \frac{n_2}{N_2} + \ldots + \frac{n_n}{N_n} = 1 \tag{3.9}$$

3.1.1.5 Counting Methods

Most of the engineering components in real life are exposed to stress responses that are more complex than shown in Figure 3.6. When individual stress cycles causing fatigue damage cannot be distinguished

easily, as in broad band random loading (Figure 3.7), a cycle counting method is needed to determine discrete cycles, and hence allow the application of Miner's rule.

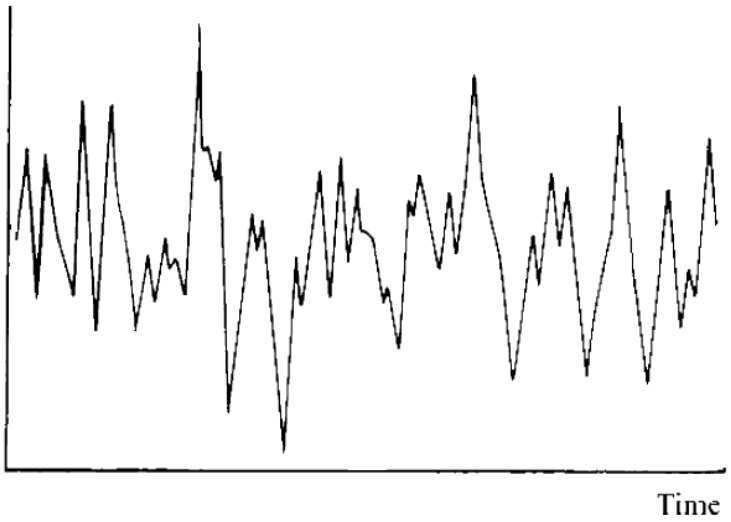

Figure 3.7 – Broadband Random Loading

Rainflow counting, peak counting, level crossing counting and range counting procedures [53] are methods commonly used to identify loading cycle occurrences, amplitudes and mean values in a time history. Development of these empirical cycle counting methods is mainly based on a trial and error, and all have shortcomings [4]. The most reasonable and widely used cycle counting method is the rainflow counting [54]. It derives its name from the first practical algorithm, developed by Matsuishi and Endo [27], in which it is imagined that water flows down the load time

history, with the axes reversed. An algorithm is developed for counting Rainflow cycles. The most common procedure is as follows [52]:

- Peaks and troughs from the time signal are extracted so that all points between adjacent peaks and troughs are discarded.
- The beginning and end of the sequence are arranged to have the same level. The simplest way is to add an additional point at the end of the signal to match the beginning.
- The highest peak is found and the signal is reordered so that this becomes the beginning and the end. The beginning and end of the original signal have to be joined together.
- Procedure is started at the beginning of the sequence and consecutive sets of four peaks and troughs are picked. A rule is applied that states,

If the second segment is shorter (vertically) than the first, and the third is longer than the second, the middle segment can be extracted and recorded as a Rainflow cycle. In this case, B and C are completely enclosed by A and D (Figure 3.8).

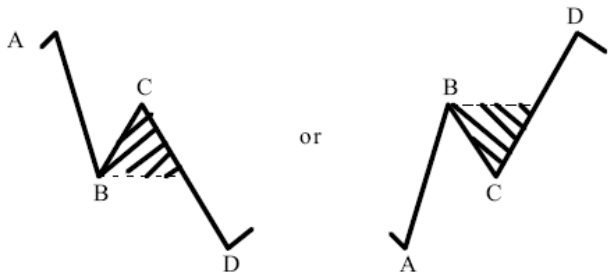

Figure 3.8 – Rainflow Cycles [52]

- If no cycle is counted then a check is made on the next set of four peaks, i.e. peaks 2 to 5, and so on until a Rainflow cycle is counted. Every time a Rainflow cycle is counted the procedure is started from the beginning of the sequence again.

An example of Rainflow cycles extraction is presented in Figure 3.9.

a)

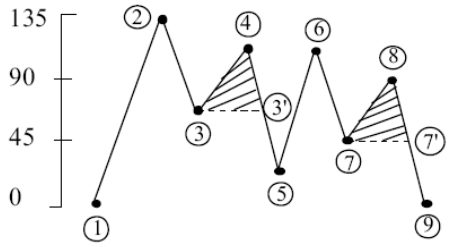

Cycles (= 2 reversals)	Range
3 – 4 – 3'	45
7 – 8 – 7'	45

b)

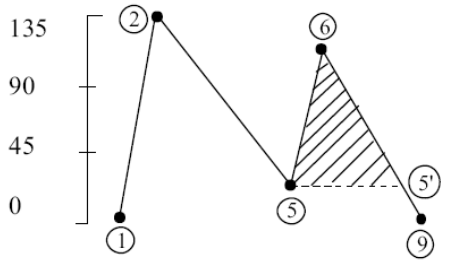

Cycles (= 2 reversals)	Range
5 – 6 – 5'	90
1 – 2 – 9	135

c)

Range	45	90	135
Reversals	4	2	2

Figure 3.9 – Rainflow Counting Example: a) Time History b) Reduced History c) Rainflow Count [52]

3.1.2 Strain Life Approach

When loading cycles are severe, another type of fatigue behavior emerges. In this regime, the cyclic loads are relatively large and lead in significant amounts of plastic deformation resulting in relatively short lives.

In this approach, Strain-Cycle curve should be used rather than Stress-Cycle curve ($S-N$) to obtain fatigue life. Strain-Cycle curve can be obtained by cyclic tests where the strain is held constant via closed loop control test equipment.

3.1.3 Crack Propagation Approach

When an initial crack exists in the structure, then crack propagation is followed. The crack growth analytical calculation is done by means of Linear Elastic Fracture Mechanics theory.

3.2 Frequency Domain Approach

When the loading is not static but dynamic, the dynamics of the structure should be taken into account. There is high possibility to excite the resonance frequencies of the structure if the loading frequency has a wide bandwidth. When this situation occurs, it cannot be assumed that the structure's response to the loading will remain linear in the frequency domain. Therefore, to overcome such situations, frequency domain fatigue analysis methods are applied which do not neglect the vibrant properties of the structure.

A general way of representing the random data in the frequency domain is using Power Spectral Density (PSD) which is an alternative way of specifying the time signal. The PSD illustrates the frequency content of the time signal. It is obtained by utilizing Fourier Transformation.

A periodic time history, $y(t)$, can be represented by the summation of a series of sine and cosine waves of different amplitude, frequency and phase which is the basis of Fourier series expansion expressed by (3.10) [55].

$$y(t) = A_0 + \sum_{n=1}^{\infty} \left\{ A_n \cos\left(\frac{2\pi n}{T_p} t \right) + B_n \sin\left(\frac{2\pi n}{T_p} t \right) \right\} \tag{3.10}$$

where T_p denotes for period and

$$A_0 = \frac{1}{T_p} \int_{-T_p/2}^{T_p/2} y(t) dt \tag{3.11}$$

$$A_n = \frac{2}{T_p} \int_{-T_p/2}^{T_p/2} y(t) \cos\left(\frac{2\pi n}{T_p} t \right) dt \tag{3.12}$$

$$B_n = \frac{2}{T_p} \int_{-T_p/2}^{T_p/2} y(t) \sin\left(\frac{2\pi n}{T_p} t \right) dt \tag{3.13}$$

A_0, A_n and B_n are Fourier coefficients which yield information about the frequency content of the time history. A_0 denotes the mean value of the time history as A_n and B_n show the amplitudes of the various sines and cosines which constitute time history when added together.

To express the time series with its frequency content, a transformation between the time and frequency domain is achieved by means of Fourier transformation. In this sense, $y(f)$ entails a description of the time history $y(t)$ in the frequency domain 'f'. The Fourier transform pair given in (3.14) and (3.15) enables transformations between the two domains effectively.

$$y(f) = \int_{-\infty}^{\infty} y(t) e^{-i(2\pi f)t} dt \tag{3.14}$$

$$y(t) = \int_{-\infty}^{\infty} y(f) e^{i(2\pi f)t} df \tag{3.15}$$

As well as the integral form, the Fourier transformation can also be depicted in a discrete form. This usage is mostly favorable because time histories are generally measured in a discrete, digitized form with equally spaced intervals in time. In these conditions, the integral form is difficult to process. Therefore, some numerical calculations are carried out on the measured time history to transform it into the frequency domain which is called Discrete Fourier Transform. The result obtained from a discrete transformation is liable to approximate the result obtained from an integral transformation as the sample length and sampling frequency increase [11]. Cooley and Tukey [56] develops a very rapid discrete Fourier transform algorithm called Fast Fourier Transform (FFT) and has a reverse process named the Inverse Fourier Transform (IFFT). The discrete form of Fourier transformation is given by

$$y(f_n) = \frac{T_p}{N} \sum_k y(t_k) e^{i\left(\frac{2\pi n}{N}\right)k} \tag{3.16}$$

$$y(t_k) = \frac{1}{T_p} \sum_n y(f_n) e^{i\left(\frac{2\pi k}{N}\right)n} \tag{3.17}$$

where T_p is the period of the function $y(t_k)$ and N is the number of data points for Fourier transform.

Random time histories can be expressed in the frequency domain under certain circumstances. A random time history cannot be periodic by definition, but it can be expressed in the frequency domain if the time history is taken from a stationary random process. A stationary time history is described as a time series whose statistics are not influenced by a shift in the time origin. In other words, the statistics which belong to time history $y(t)$ are the same as those of time history $y(t+\tau)$ for all values of τ. The statistics obtained from a sampled time history are representative of the statistics of the whole random process. Figure 3.10 illustrates the application of the Fourier transformation applied to a random time history taken from a stationary random process.

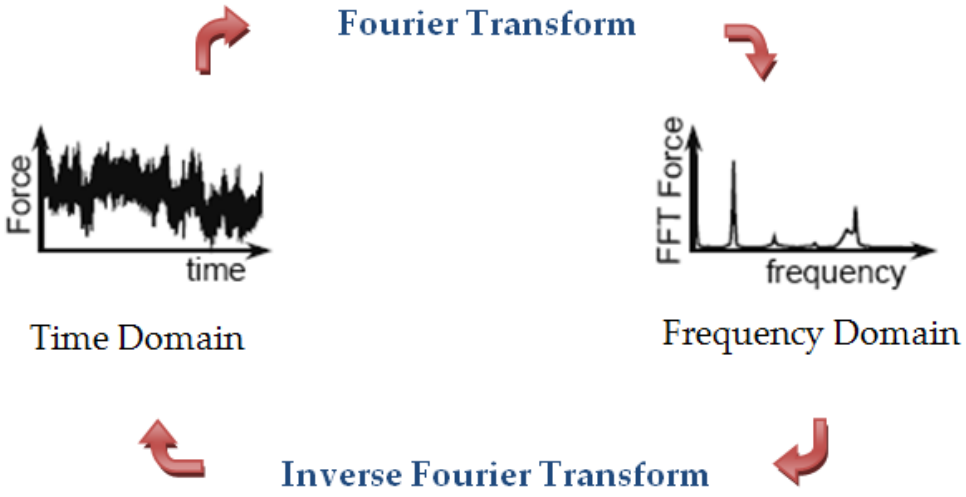

Figure 3.10 – Fourier Transformation

Power Spectral Density (PSD) is a way of illustrating the amplitude content of a time signal in the frequency domain as a spectrum. It is calculated by taking square of the modulus of the FFT and dividing by 2 times the period, T_p as shown in (3.18).

$$PSD^{def} = \frac{1}{2T_p}\left|y(f_n)\right|^2 \tag{3.18}$$

Only the amplitudes are retained in PSD but phase information is discarded.

The area under each spike in Figure 3.11 represents the mean square of the sine wave at that frequency and the total urea under the PSD curve gives the mean square of the time history.

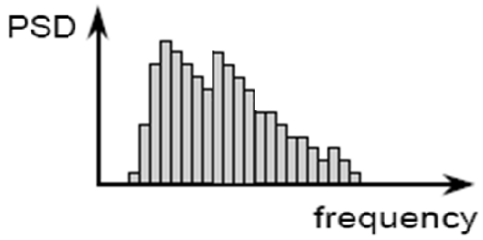

Figure 3.11 – Schematic Representation of Power Spectral Density

PSD shows the frequency content and the type of the time history. For example, a sinusoidal time signal comes out as a single spike centered at

the frequency of the sine wave on the PSD plot and the spike should be infinitely tall and infinity narrow for a pure sine function on the PSD graph in theory while it always has a finite height and finite width because a sine wave has a finite length. However, the area under the PSD graph is the interest. Broadband time history appears as a wide band peak or several peaks covering a wide range of frequencies in the PSD plot while narrowband process comes out as centered, narrow band plot when PSD is calculated. White noise includes sine waves of the same amplitude at each frequency (Figure 3.12).

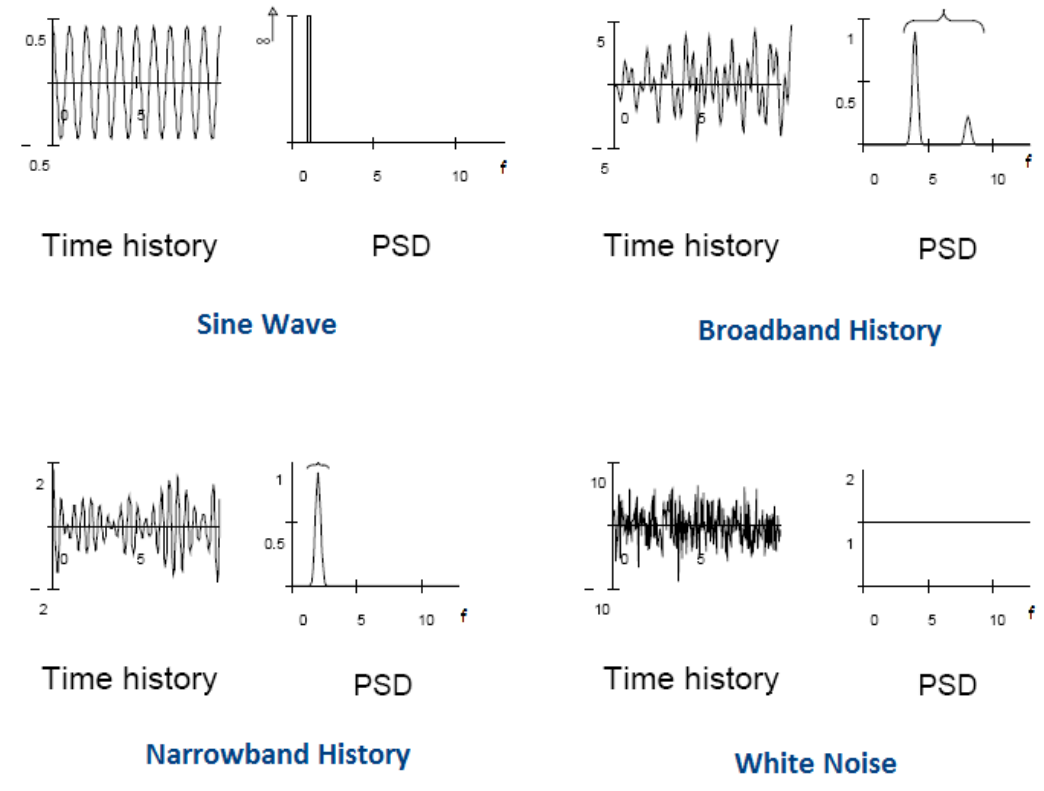

Figure 3.12 – Time Histories and PSDs

In linear systems, the output is related to the input by a linear transfer function. The response of a linear system to a single random process is obtained by means of transfer functions obtained via frequency response analysis of the structure where for each frequency a different transfer function is calculated:

$$FFT_r(f) = H(f) \times FFT_i(f) \tag{3.19}$$

where $FFT_r(f)$ and $FFT_i(f)$ stands for FFT of the response, stress in this thesis, and FFT of the input loading, acceleration in this thesis, respectively. $H(f)$ represents the transfer function of the system in frequency domain. It is convenient to obtain the response, stress, as a PSD, $G_r(f)$ (3.20). If the input, acceleration, is also expressed as PSD, $G_i(f)$, then the PSD of output is given by means of a linear transfer function, $H(f)$, its conjugate, $H^*(f)$ and input PSD in the frequency domain where $FFT_i^*(f)$ is complex conjugate of the input FFT (3.21).

$$G_r(f) = \left(\frac{1}{2T_p}\right)\left(H(f) \times FFT_i(f) \times H^*(f) \times FFT_i^*(f)\right) \tag{3.20}$$

$$G_r(f) = H(f) \times H^*(f) \times G_i(f) \tag{3.21}$$

Then, (3.21) can be rewritten in the form of (3.22), where $G_r(f)$ is equal to input PSD times modulus squared of transfer function.

$$G_r(f) = \left|H(f)\right|^2 \times G_i(f) \tag{3.22}$$

Stress PSD is directly used for vibration fatigue life calculations which will be explained in the proceeding parts of this thesis in detail.

In vibration fatigue calculations, the frequency content of the stresses is accounted for by a probability density function (PDF) of rainflow stress ranges, $p(S)$. The most convenient way, mathematically, of storing stress range histogram information is in the form of a probability density function of stress ranges Figure 3.13. The bin width, dS, and the total number of cycles recorded in the histogram, S_t, are required to transform from a stress range histogram to a PDF, or back.

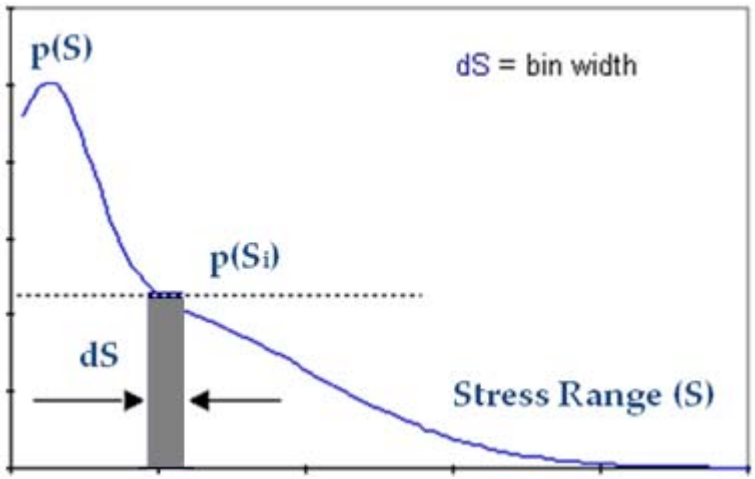

Figure 3.13 – Probability Density Function

The probability of the stress range occurring between $S_i - \frac{dS}{2}$ and $S_i + \frac{dS}{2}$ is calculated as the multiplication of $p(S_i)$ and dS while to get PDF from

rainflow histogram, each bin height is divided by $S_t dS$. Then, number of cycles at the particular stress level S, $n(S)$ is stated as in (3.23).

$$n_i(S) = p(S)dSSt \tag{3.23}$$

The total number of cycles at the stress level S that causes failure according to Woehler curve, $N(S)$, is expressed as in (3.24) where C and b stand for material constant and Basquin exponent respectively.

$$N(S_i) = \frac{C}{S^b} \tag{3.24}$$

Then, fatigue life calculation is performed by utilizing (3.25) that equates (3.26) in turn where total number of cycles in required time, S_t, is equal to $E[P]T$. T is the fatigue life in seconds and $E[D]$ is expected value of damage. Fatigue life is found setting $E[D]$ to unity. The order of stresses occurring in history is ignored in Miner's rule. However, this does not create a problem for vibration fatigue solution since the loading's statistical properties are important and the loading is random, stationary and Gaussian.

$$E[D] = \sum_i \frac{n_i(S)}{N(S_i)} = \frac{S_t}{C}\int_0^\infty S^b p(S)dS \tag{3.25}$$

$$E[D] = \sum_i \frac{n_i(S)}{N(S_i)} = E[P]\frac{T}{C}\int_0^\infty S^b p(S)dS \tag{3.26}$$

To calculate the probability density function of rainflow stress ranges, several different empirical solutions are proposed by researchers to obtain the $p(S)$ from output stress PSD and calculate fatigue life which constitutes the basis of vibration fatigue approach. Statistical properties of random history should be examined to obtain $p(S)$.

Random stress time histories can be described using statistical parameters properly. Any sample time history can be regarded as one sample from an infinite number of possible samples which can occur for the random process. Each time sample will be different but the statistics of each sample should be constant as long as the samples are reasonably long [39], [57].

Two of the most important statistical parameters are undertaken by Rice [30], which are relationships for the number of upward mean crossings per second and peaks per second in a random signal using spectral moments of the PSD. This is the first serious effort at providing a solution for estimating fatigue damage from PSDs.

The nth spectral moment of the PSD of stress, which is m_n, is defined as the summation of each strip's area times the frequency raised to the power n (3.27). It is necessary to divide the PSD curve into small stripes to make these calculations as shown in Figure 3.14.

$$m_n = \int_0^{\infty} G(f).f^n.df = \sum_{k=1}^{m} f_k^n.G_k(f_k).\delta f \tag{3.27}$$

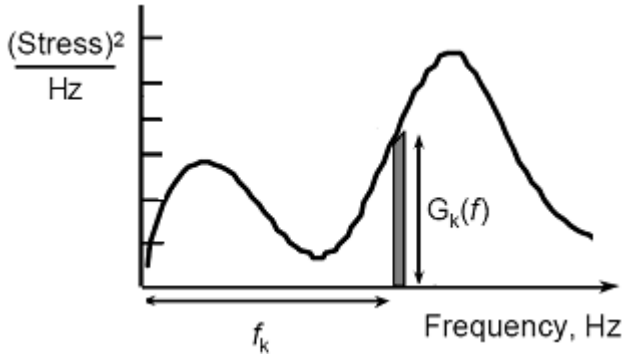

Figure 3.14 – PSD Moments Calculation

Expected number of peaks per second $E(P)$ and expected number of upward zero crossings per second, $E(0)$, in the time history, whose schematic representation are shown in Figure 3.15, are calculated using spectral moments up to 4th degree, m_0, m_1, m_2, m_3, m_4 as formulated in (3.28) and (3.29).

Figure 3.15 – Expected Zeros and Expected Peaks in the Time History

$$E[P] = \sqrt{\frac{m_4}{m_2}} \tag{3.28}$$

$$E[0] = \sqrt{\frac{m_2}{m_0}} \tag{3.29}$$

Another important statistical parameter is irregularity factor, γ, which is the ratio of expected number of zeros per second over expected number of peaks per second. It is a measure of frequency band the history cover on PSD graph in the sense that as the irregularity factor approaches to one, the process gets closer to narrow band process, and as the irregularity factor approaches to zero, the process gets closer to broadband process. In other words, a value of one corresponds to a narrow band signal which means that the signal contains only one predominant frequency while a value of zero implies that the signal contains an equal amount of energy at all frequencies.

$$\gamma = \frac{E[0]}{E[P]} = \sqrt{\frac{m_2^2}{m_0 m_4}} \tag{3.30}$$

All these statistical information gathered from the stress PSD is used for vibration fatigue calculations.

3.2.1 Narrow Band Approach

The first frequency domain method on calculating fatigue damage from PSD's is called narrow band approach. Bendat [31] assumes that all positive peaks in the time history is followed by corresponding troughs of similar magnitude regardless of whether they actually formed stress cycles, in

other words, it assumes that the PDF of peaks is equal to the PDF of stress amplitudes. Negative peaks and positive troughs in the time history are ignored. For wide band response data, the method overvalues the probability of large stress ranges. Therefore, calculated fatigue damage becomes conservative. In Figure 3.16, the time series shown is accepted as the black history instead of blue one. Probability density function calculated according to narrow band solution comes out as (3.31) and expected damage equation (3.26) turns into (3.32).

$$p(S) = \frac{S}{4m_0} e^{\frac{-S^2}{8m_0}} \tag{3.31}$$

$$E[D] = \sum_i \frac{n_i(S)}{N(S_i)} = E[P]\frac{T}{C}\int_0^\infty S^b \left[\frac{S}{4m_0} e^{\frac{-S^2}{8m_0}}\right] dS \tag{3.32}$$

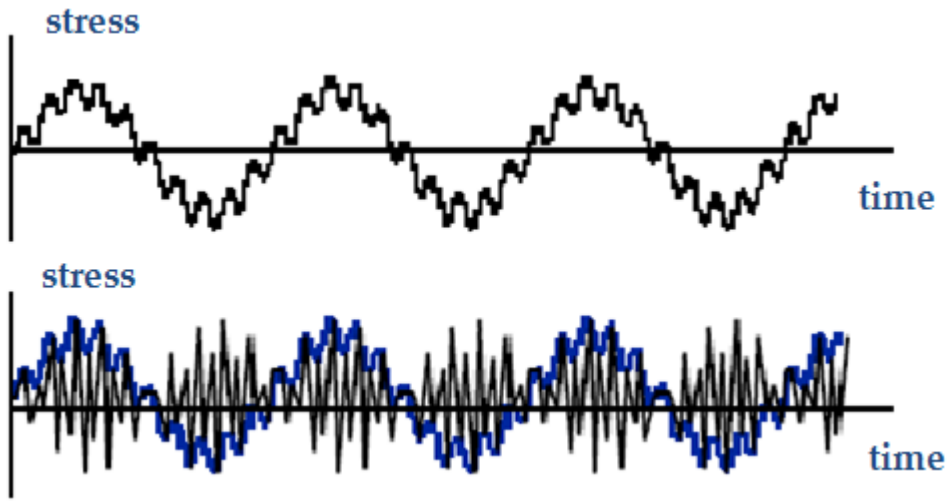

Figure 3.16 – Narrow Band Solution

3.2.2 Empirical Correction Factors

Many expressions are proposed to correct the conservatism of narrow band solution. Generally, they are constituted by generating sample time histories from PSD's by means of inverse Fourier transformation. A conventional rainflow cycle count is obtained from these data sets.

The solutions of Wirsching et al [32], Chaudhury and Dover [33], Tunna [34] and Hancock [35] are all developed making use of this approach and are all expressed in terms of the spectral moments up to the forth degree.

Wirsching's Equation:

$$E[D] = E[D]_{NB}\left(a(b) + (1 - a(b))(1 - \varepsilon^{c(b)})\right) \tag{3.33}$$

where

$$a(b) = 0.926 - 0.033b \tag{3.34}$$

$$c(b) = 1.587b - 2.323 \tag{3.35}$$

$$\varepsilon = \sqrt{1 - \gamma^2} \tag{3.36}$$

Hancock's Equation:

$$S_h{}^b = \left(2\sqrt{2m_0}^{\,b}\right)^b \left[\gamma\Gamma\left(\frac{b}{2} + 1\right)\right] \tag{3.37}$$

This solution is proposed in the form of an equivalent stress range parameter, S_h, where

$$S_h^b = \int S^b p(S) dS \tag{3.38}$$

Chaudhury and Dover Equation:

$$E[D] = E[P]\frac{T}{C}S_h{}^b \tag{3.39}$$

Tunna Equation:

$$p(S) = \frac{S}{4\gamma m_0}e^{\frac{-\delta^2}{8\gamma m_0}} \tag{3.40}$$

3.2.3 Steinberg's Solution

Steinberg [36] proposes a three-band technique as a rough estimation for the fatigue damage calculation. This method is based on the Gaussian distribution. The instantaneous stress values in the time history are assumed for the 3 bands where σ stands for standard deviation:

- 1σ values occur 68.3% of the time
- 2σ values occur 27.1% of the time
- 3σ values occur 4.33% of the time

Therefore, the fatigue damage is estimated based on these three stress levels. This approach is a very simple solution based on the assumption that no stress cycles occur with ranges greater than 6 rms values. The distribution of stress ranges is then specified to follow a Gaussian distribution. This method is preferred in the electronics industry, as a tool for comparison.

3.2.4 Dirlik's Empirical Formulation

A better approach is to approximate PDF directly from the PSD without using the narrow band approach as a starting point because PDF of rainflow stress ranges is the issue controlling fatigue life. Dirlik [37] develops an empirical closed form expression for the PDF of rainflow ranges, which is obtained using extensive computer simulations to model the signals using the Monte Carlo technique. Dirlik's solution is illustrated in the equation [11].

$$p(S_i) = \frac{\frac{D_1}{Q} e^{-\frac{Z_i}{Q}} + \frac{D_2 Z_i}{R^2} e^{-\frac{Z_i^2}{2R^2}} + D_3 Z_i e^{-\frac{Z_i^2}{2}}}{2\sqrt{m_0}} \tag{3.41}$$

where

$$Z_i = \frac{S_i}{2\sqrt{m_0}} \qquad \gamma = \frac{E[0]}{E[P]} \qquad E[0] = \sqrt{\frac{m_2}{m_0}} \qquad E[P] = \sqrt{\frac{m_4}{m_2}} \qquad x_m = \frac{m_1}{m_0}\sqrt{\frac{m_2}{m_4}}$$

$$D_1 = \frac{2(x_m - \gamma^2)}{1+\gamma^2} \qquad D_2 = \frac{1-\gamma-D_1+D_1^2}{1-R} \qquad D_3 = 1 - D_1 - D_2$$

$$Q = \frac{1.25(\gamma - D_3 - D_2 R)}{D_1} \qquad R = \frac{\gamma - x_m - D_1^2}{1-\gamma-D_1+D_1^2}$$

Dirlik's empirical formula for the PDF of rainflow stress ranges is shown to be far superior, in terms of accuracy, then the previously available correction factors for narrow band solution conservatism [59].

CHAPTER 4

A NEW METHOD FOR GENERATION OF A LOADING HISTORY WITH ZERO MEAN

When a component is subjected to an excitation that has a nonzero mean, this mean value could have a noteworthy effect on the stresses and thus on the fatigue life of the component. In fatigue calculations, mean stress effect can be taken into consideration rather easily but experimental verification is troublesome since with traditional testing equipment like vibration shakers, any mean value of an acceleration excitation other than 1g in the direction of gravity is difficult to simulate. In the content of this thesis study, a method is developed to create a modified input loading history with a zero mean which causes fatigue damage approximately equivalent to that created by input loading with a nonzero mean. For this purpose, a mathematical procedure is developed to apply mean stress correction to the output von Mises stress power spectral density data. A modified input acceleration power spectral density is generated by means of transfer functions calculated via frequency response analysis. This will enable to perform fatigue tests. The mathematical approach developed to modify the output von Mises stress power spectral density takes the multi-axial stresses into account at the point of consideration and provides the needed input loading power spectral density. The corrected input with zero mean value enables experimental verification while the mean value, other than 1g, of the input cannot be applied in standard vibration tests.

Time domain fatigue life calculation techniques directly utilize mean stress correction methods to amplify the stress ranges to take the mean stress effect into account. In frequency domain fatigue life calculation approaches, when the power spectral density of the stress is determined, only the variable stress part is considered, however, the constant mean component is ignored [60]. In this study, the mean stress correction is accomplished on von Mises stress power spectral density to be able to include the loading's bias effect. Goodman correction technique is preferred to Gerber since it is reported in [61] that Gerber relationship generally gives higher fatigue lives compared to the experimental results. Dirlik method is chosen for application of vibration fatigue approach. According to [59], Dirlik approach leads to better results in comparison to the corresponding time domain and frequency response methods.

An aluminum (2024 T4) plate fixed and excited at one end is used for the implementation which is shown schematically in Figure 4.1, whose dimensions are given in Table 4.1. The base excitation leads to a fully three dimensional multi-axial state of stress in the plate.

It is shown that the developed method is useful in creating a modified input acceleration data with a zero mean that can simulate damage for a selected point in the structure under consideration. Equivalent input loading obtained by means of the aforementioned method is convenient and conservative for experimental applications. Besides being a time saving method, it is suitable to be implemented for any type of loading.

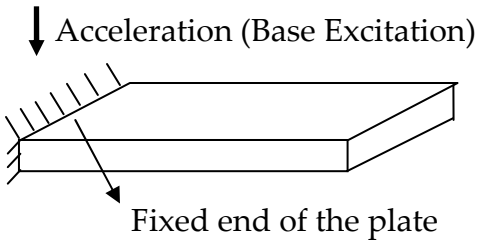

Figure 4.1 – Plate Subjected to Base Excitation

Table 4.1 – Dimensions of the Plate

Length	750 mm
Width	100 mm
Thickness	5 mm

4.1 Theory

The developed method to calculate zero mean loading for a structure, approximately equivalent in fatigue damage, which is subjected to random loading with nonzero mean, is based on the frequency domain fatigue calculation techniques.

To compute a zero mean input acceleration PSD, which is mentioned as the modified acceleration input PSD, $G_{im}(f)$, first of all, mean stress correction is performed on the von Mises stress output PSD, $G_r(f)$. Goodman's mean stress correction shown in Equation (3.6) is used to obtain the modified output stress PSD, $G_{rm}(f)$. Note that Goodman's formula is widely used for

mean stress correction for stress amplitude modification [62], but in this study it is utilized to correct PSD of von Mises stress output data. If the PSD is split into equal strips, the area of each strip can be utilized to obtain an equivalent sine wave. The amplitude of each equivalent sine wave is equal to the square root of the area times $\sqrt{2}$. This is because of the fact that the root mean square of a sine wave is equal to its amplitude divided by $\sqrt{2}$, and the root mean square of each strip in the PSD is equal to the square root of its area [39]. In this study, the stress PSD value, $G_r(f)$, is multiplied by the corresponding frequency resolution and the square root of it is taken and multiplied with $\sqrt{2}$ to obtain the alternating stress amplitude, S_a, for each frequency. Then, mean stress correction is performed with (3.6) to calculate the modified alternating stress amplitude, S_a'. Afterwards, the calculations are carried out in the reverse direction to reach modified output stress PSD, $G_{rm}(f)$.

Theoretically, there should be an input acceleration PSD that results in the modified output stress PSD, $G_{rm}(f)$, when applied to the structure since the transfer function of the structure remains the same regardless of input type. This physical relation can be represented by the following equation which is rewritten from (3.21) for a different input-output couple.

$$G_{rm}(f) = H(f) \times H^*(f) \times G_{im}(f) \tag{4.1}$$

According to (3.21);

$$H(f) \times H^*(f) = G_r(f) x G_i(f)^{-1} \tag{4.2}$$

and from (4.1);

$$H(f) \times H^{*}(f) = G_{rm}(f) x G_{im}(f)^{-1} \tag{4.3}$$

To obtain $G_{im}(f)$, (4.2) and (4.3) are equated to each other and re-ordered which results in:

$$G_{im}(f) = \left[G_{rm}(f)^{-1} x G_{r}(f) x G_{i}(f)^{-1} \right]^{-1} \tag{4.4}$$

The variables in equation (4.4) are vectors, which in turn makes regular matrix inversion impossible. Therefore, the inverse calculations in equation (4.4) are carried out by using pseudo-inverse. A corrected input loading with zero mean but modified alternating stress, which creates fatigue damage approximately equivalent to the damage caused by the unprocessed loading with nonzero mean, is extracted by means of this technique. It should be noted that, this approach is focusing to find a modified loading that simulates damage for a selected point on the structure, which in turn will be acceptable in the vicinity of that point only.

4.2 Case Study

The proposed correction method is demonstrated on an application analyzed according to the method presented in Section 4.1.

The plate shown in Figure 4.1 is excited from its cantilevered base with stationary, Gaussian, random, 10 second acceleration time history with a non-zero mean value of 3 g, as shown in Figure 4.2. Power spectral density

of the input is also shown in Figure 4.3. The input loading consists of harmonics that possess different amplitudes with broadband frequency range, up to 2000 Hz, involving the first 20 of the natural frequencies of the specimen. The deformation patterns include bending and torsional mode shapes that induce a multi-axial stress state in the structure.

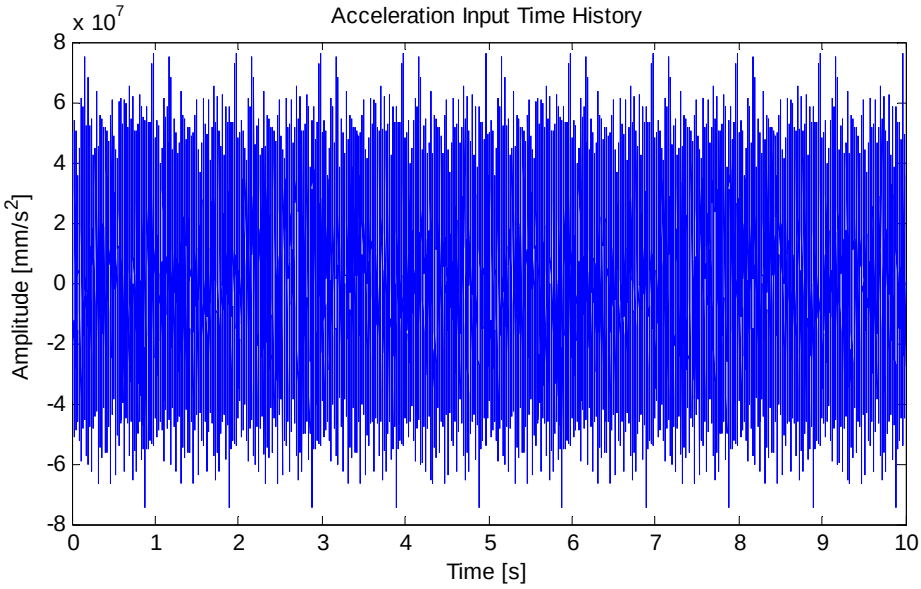

Figure 4.2 – Input Acceleration Loading Time History

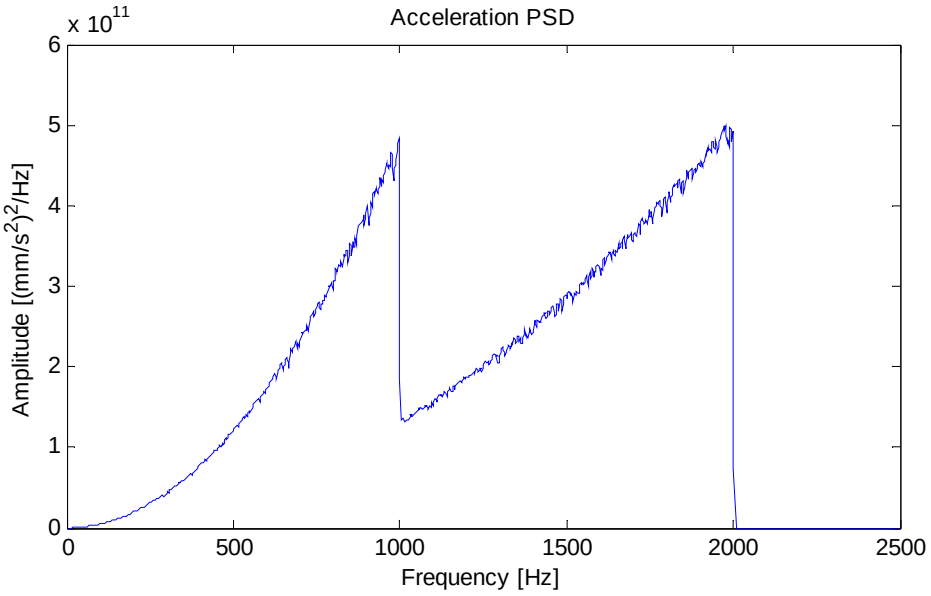

Figure 4.3 – Input Acceleration Loading PSD

4.2.1 Finite Element Analyses

The plate's finite element analyses are carried out using MSC-Patran pre-post processing tool, MSC-Nastran solver, and MSC-Fatigue pre-post processor and solver. The plate is modeled using hexahedral elements with 8 nodes (HEX8).

4.2.1.1 Modal Analysis

Modal analysis is carried out to determine the natural frequencies and mode shapes up to 2000 Hz which are taken into consideration in calculations. First 5 mode shapes of the cantilever plate are showed in Figures from 4.4 - 4.8.

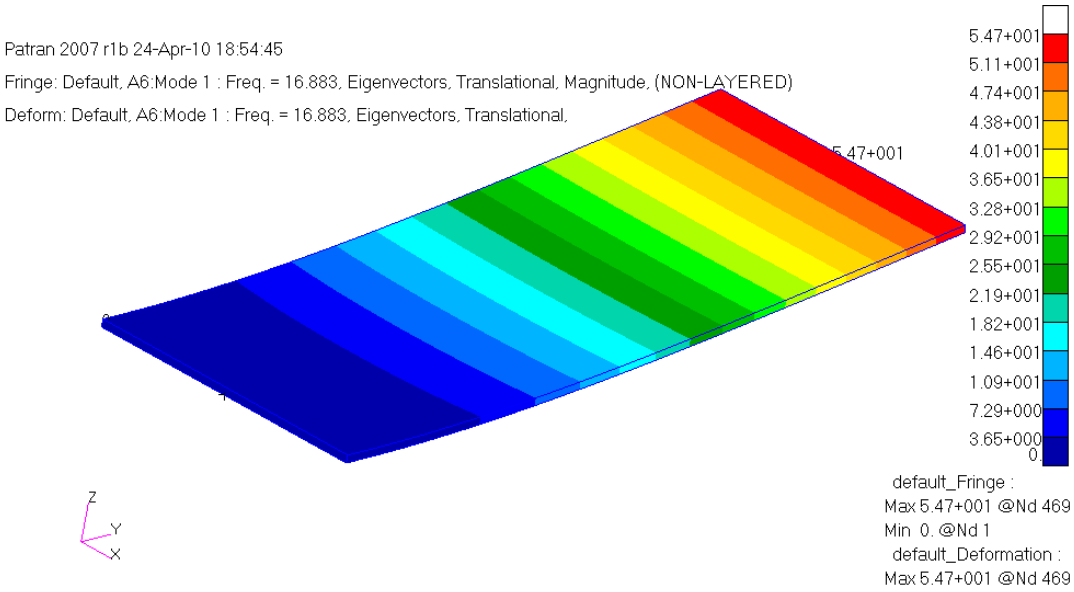

Figure 4.4 – First Mode Shape (1st Bending) of the Cantilever Beam

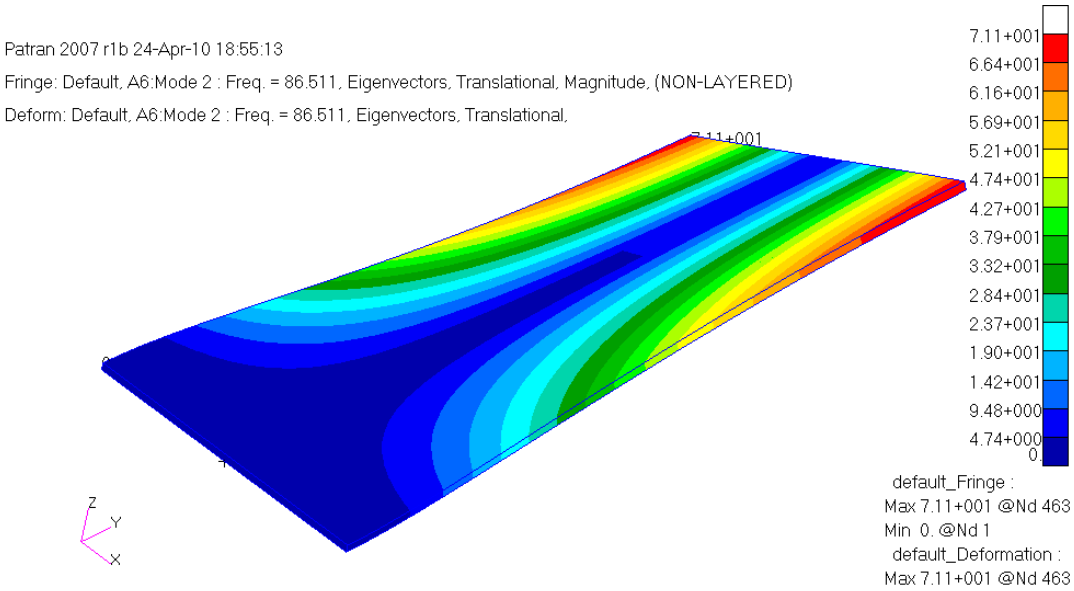

Figure 4.5 – Second Mode Shape (1st Torsion) of the Cantilever Beam

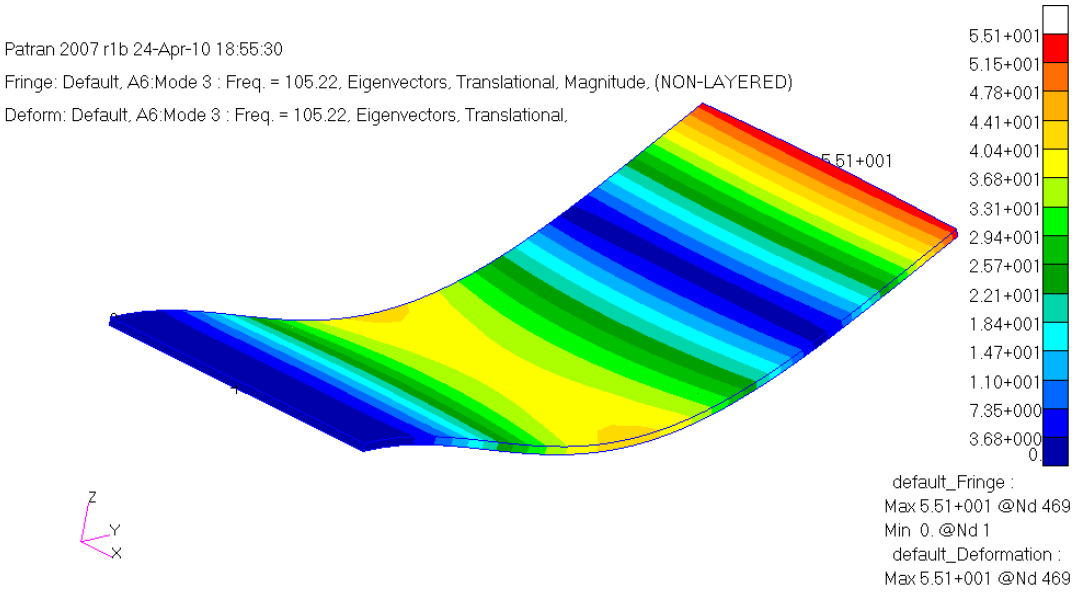

Figure 4.6 – Third Mode Shape (2nd Bending) of the Cantilever Beam

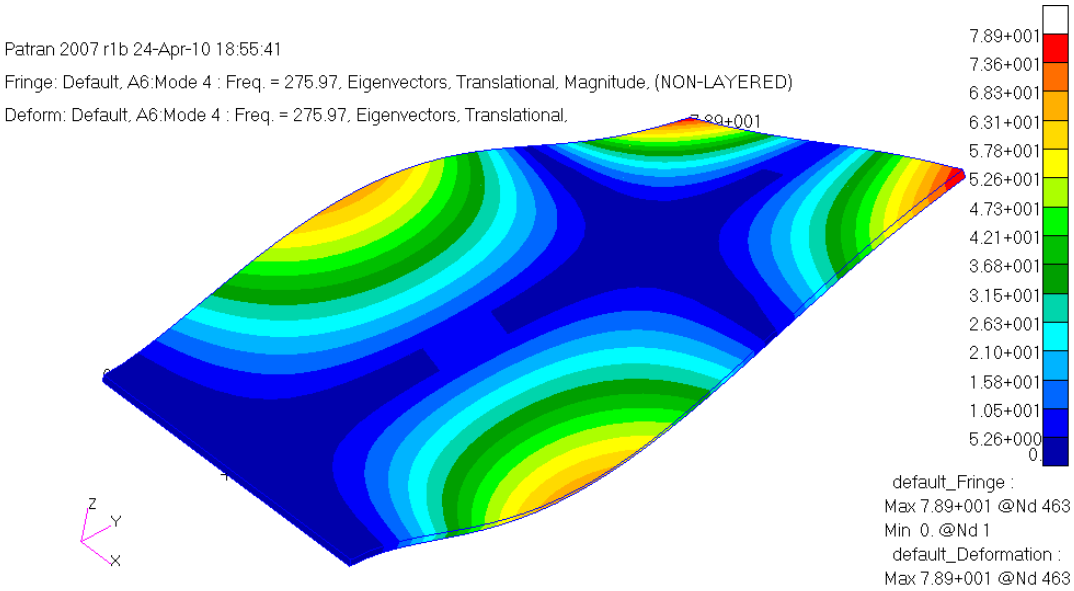

Figure 4.7 – Fourth Mode Shape (2nd Torsion) of the Cantilever Beam

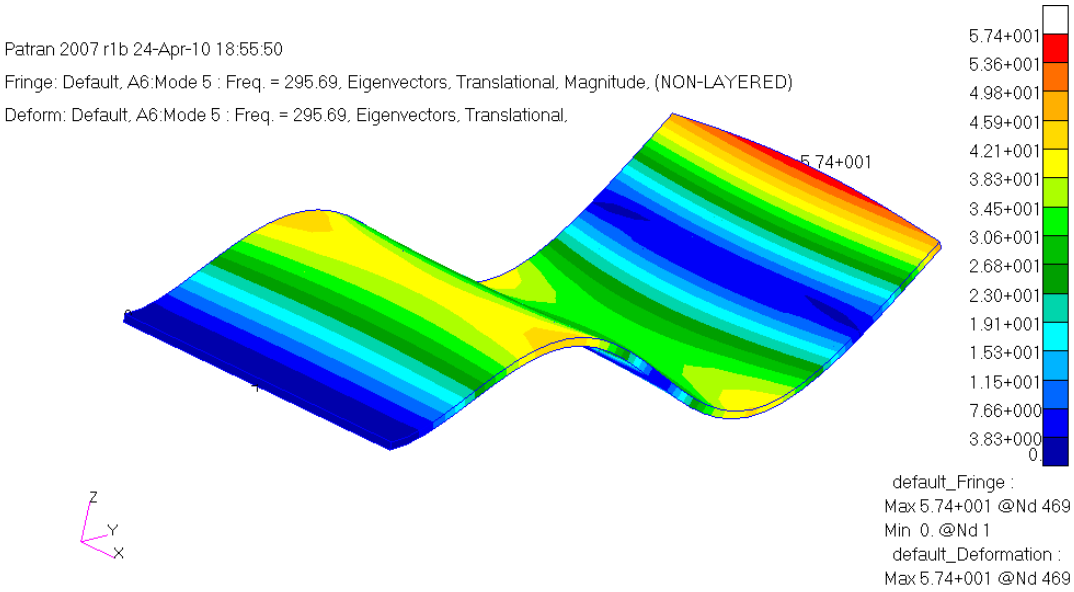

Figure 4.8 – Fifth Mode Shape (3rd Bending) of the Cantilever Beam

4.2.1.2 Frequency Response Analysis

Frequency response analysis is carried out to obtain transfer functions between input acceleration and output von Mises stresses needed for fatigue calculations. A unit amplitude, 1mm/s^2, sinusoidal loading is applied to the structure as a base excitation. Damping ratio is taken as %2 to be in the safe side and to compensate experimental errors which is also a typical value for aluminum applications [51]. Transfer functions which represent the relation between input acceleration and output stress at each frequency are determined up to 2000 Hz at every node. Frequency response analysis result is shown in Figure 4.9.

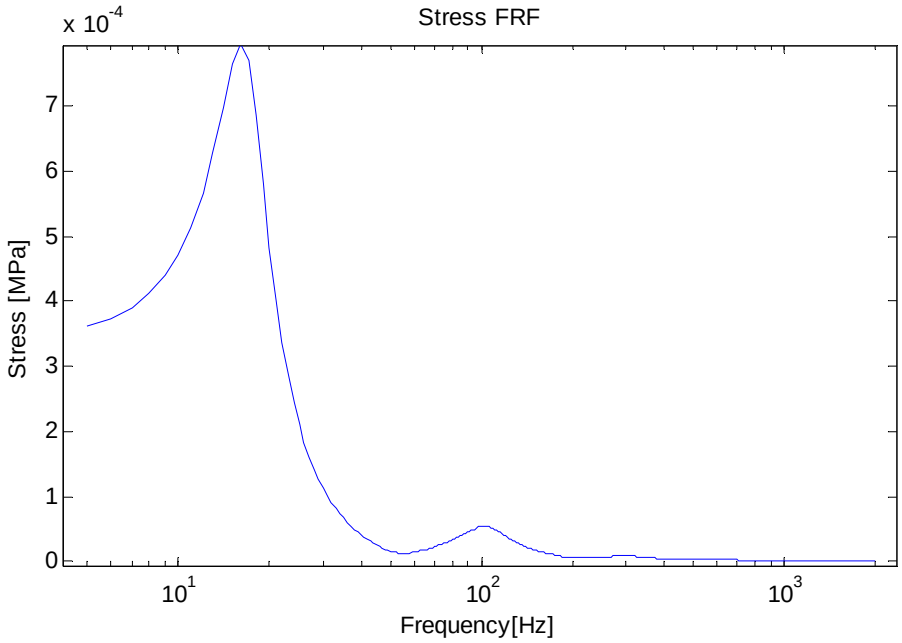

Figure 4.9 – Frequency Response Analysis Results of the Cantilever Plate for First Five Natural Frequencies for node 511 (Logarithmic Scale)

4.2.1.3 Static Analysis

Static analysis is conducted to find out von Mises stress at the desired vicinity to be used for mean correction. Linear static analysis is done with an inertial loading (Figure 4.10) of magnitude equal to the mean value of the input acceleration loading shown in Figure 4.2.

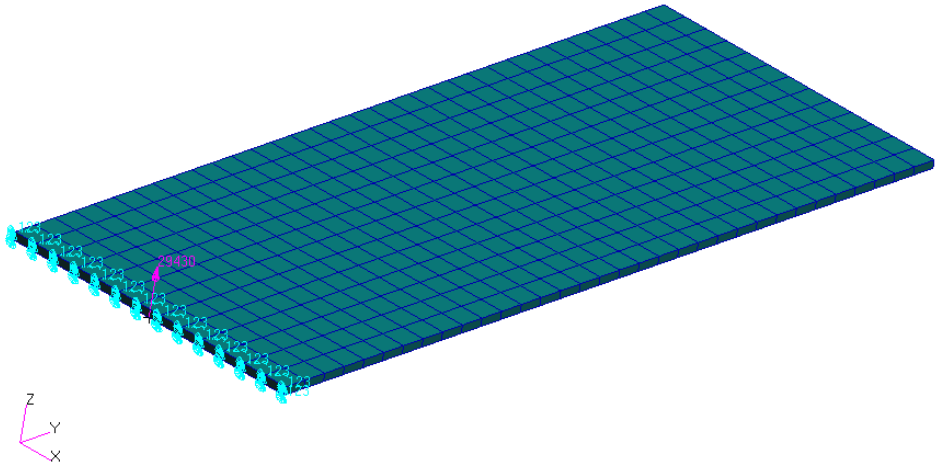

Figure 4.10 – Load and Boundary Conditions of Static Analysis

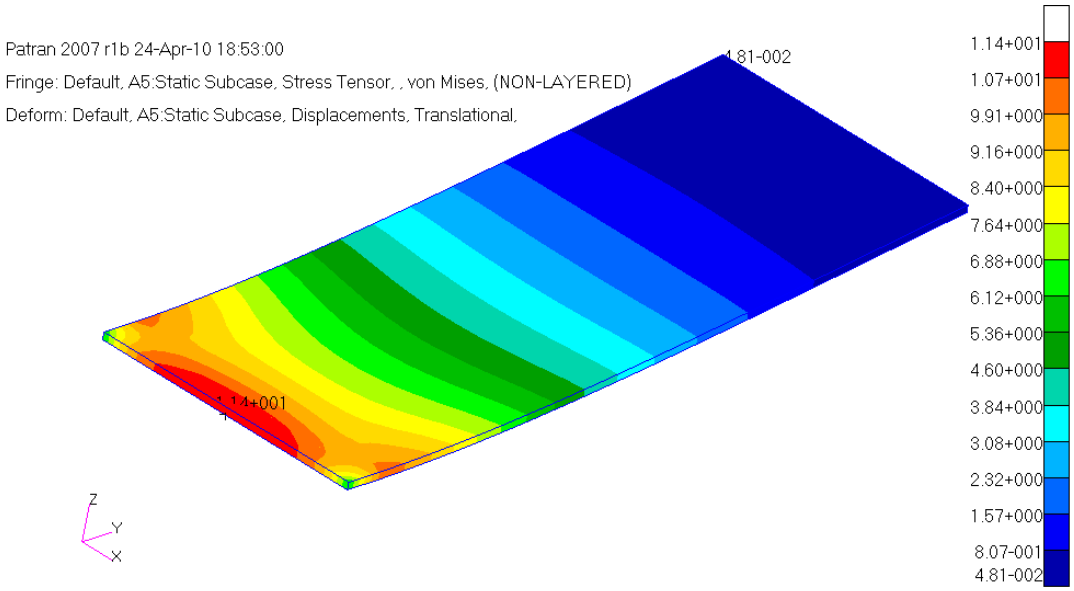

Figure 4.11 – Static von Mises Stress on the Cantilever Plate

4.2.1.4 Vibration Fatigue Analysis

Transfer functions obtained via frequency response analysis and excitation loadings are the inputs of fatigue analysis. The first analysis is conducted for determination of fatigue life using Dirlik's method without mean stress correction. Then, the second analysis is performed with Goodman mean stress correction proposed by MSC. Fatigue. Afterwards, mean stress correction technique mentioned in section 4.1 is performed using output von Mises stress PSD taken from the first analysis. Von Mises stress caused by mean acceleration of the input loading at the specific point whose life is the least is used for the mean stress correction. Specified point is actually close to the cantilever support for the given case study where fatigue failure is expected to occur. After calculating modified output stress PSD as described in section 4.1, corrected input loading PSD with amplified amplitudes (Figure 4.12) is determined via (4.4). Finally, fatigue analysis is performed using modified input loading PSD for comparison.

Finite element analysis results regarding fatigue life are presented in Figure 4.13 and compared for the points in the vicinity of the point of failure (nodes shown in Figure 4.14) in Table 4.2.

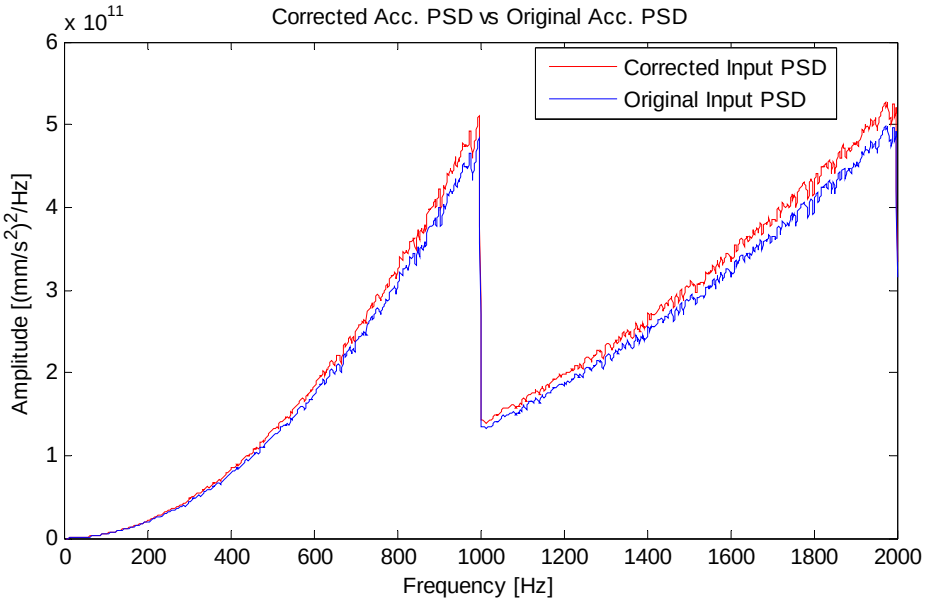

Figure 4.12 – Modified Input Loading and Original Input Loading for Cantilever Plate

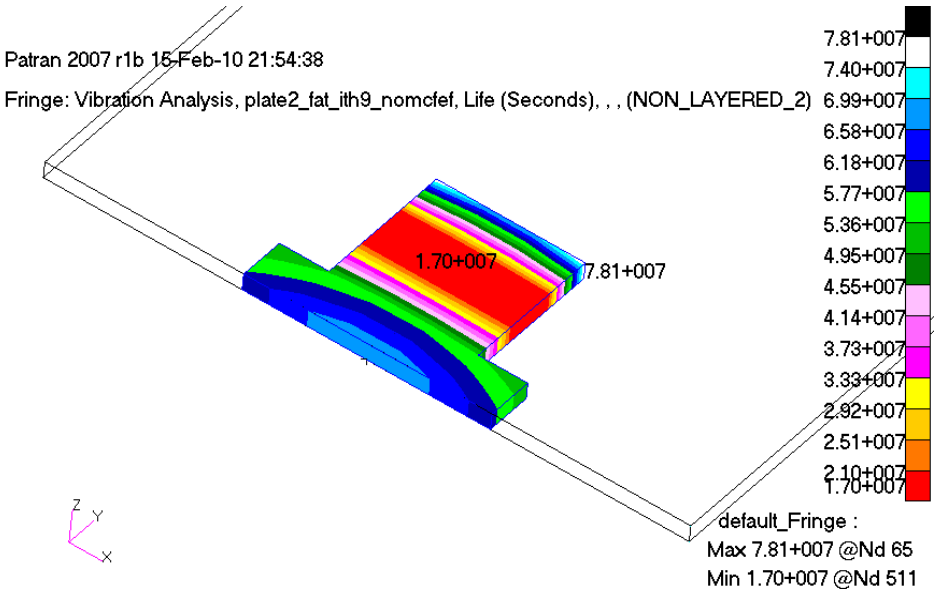

Figure 4.13 – Fatigue Life for the Plate (in seconds): a) without Mean Stress Correction.

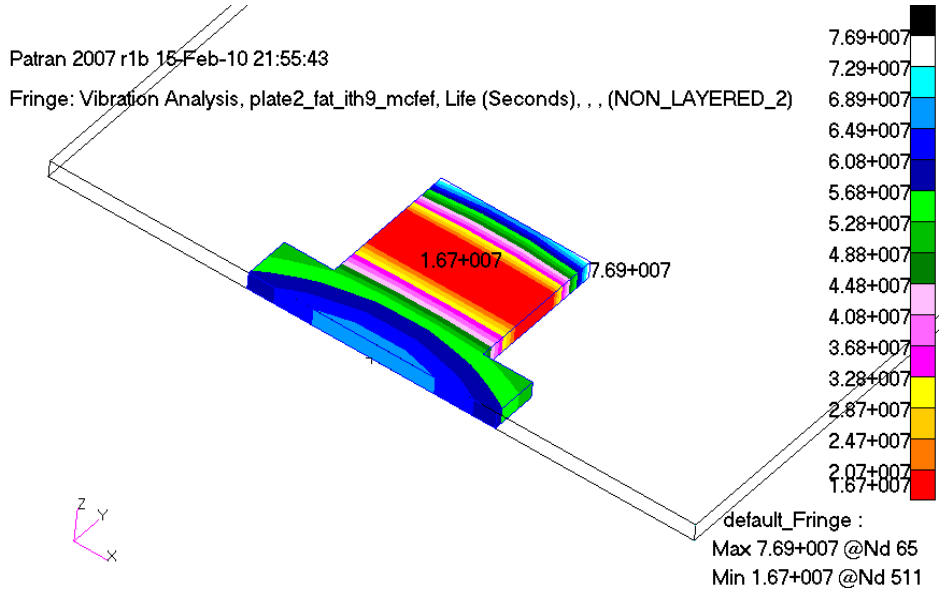

Figure 4.13 – Fatigue Life for the Plate (in seconds):

b) with Mean Stress Correction.

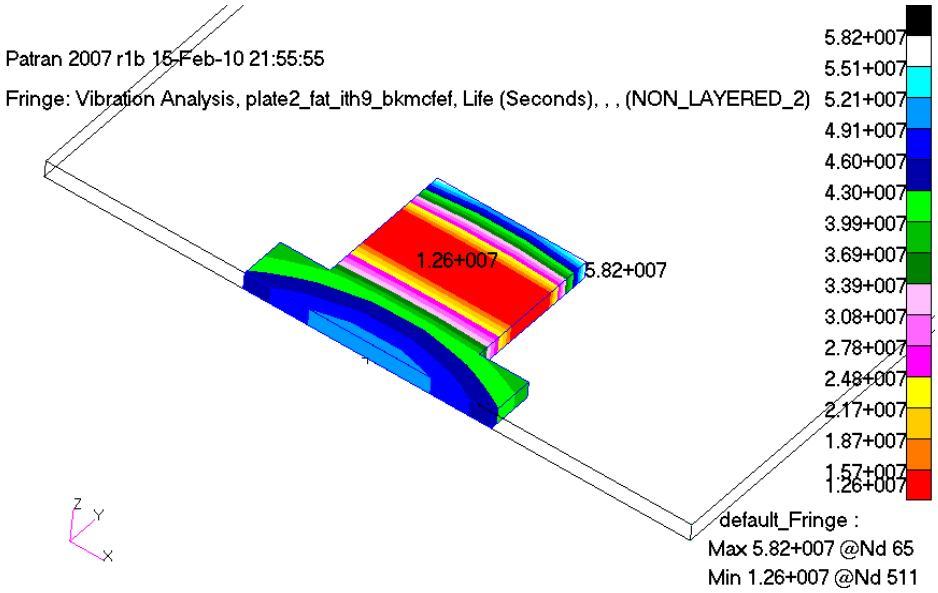

Figure 4.13 – Fatigue Life for the Plate (in seconds):

c) with Proposed Mean Stress Correction Method.

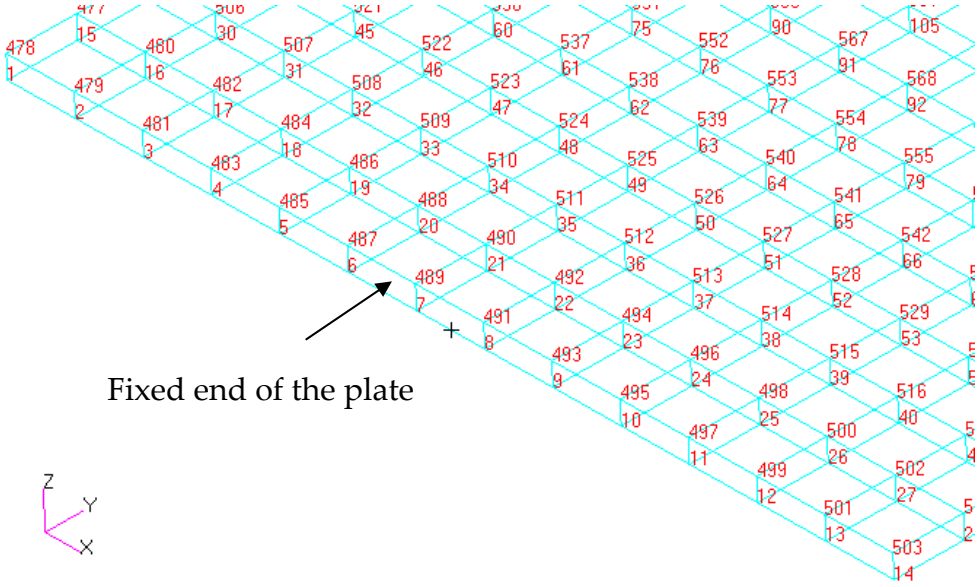

Figure 4.14 – Finite Element Model of Displaying the Plate-Node Numbers

Table 4.2 – Comparisons of Fatigue Life Values

	Analysis 1 (w/o mean stress correction)	Analysis 2 (w/ Goodman mean stress correction)	Analysis 3 (w/ proposed mean stress correction)
Node 511	1.696E7	1.671E7	1.264E7
Node 35	1.698E7	1.672E7	1.265E7
Node 512	1.7E7	1.675E7	1.267E7
Node 36	1.7E7	1.674E7	1.266E7
Node 510	1.716E7	1.69E7	1.278E7
Node 34	1.721E7	1.695E7	1.282E7

Developed method gives a more conservative fatigue life compared to that obtained by the Goodman mean stress correction used in the MSC Fatigue software. Therefore, the input loading obtained by means of the aforementioned method is concluded to be safe, practical and convenient for experimental applications.

CHAPTER 5

GENERATION OF A ZERO MEAN EXCITATION FOR MULTI-AXIAL LOADING

A machine component can be subjected to loadings in three axis perpendicular to each other that have a nonzero mean value. Then, the mean values appearing in loading sets will affect the stresses and thus the fatigue life of the component. In this chapter, a method is proposed to create a modified input loading set with zero mean which causes fatigue damage approximately equivalent to that created by input loading set with nonzero mean in three loading axis. For this purpose, a mathematical procedure is developed to apply mean stress correction to the output stress power spectral density matrix taking all stress components' effect into account. A modified input acceleration power spectral density matrix is generated by means of transfer functions between input and output calculated via frequency response analysis. This mathematical approach considers the multi-axial stresses at the point of interest and presents the needed input loading power spectral density. The modified input with zero mean value enables experimental verification while the mean value, other than 1g, of the input cannot be applied with standard vibration equipments.

The mean stress correction is accomplished with Goodman formula and Dirlik method is applied as vibration fatigue life calculation technique.

It is revealed that the proposed technique is useful in creating a modified input acceleration data set with a zero mean that can simulate the damage for a selected point in the structure under consideration. Equivalent input loading set is convenient and conservative for experimental applications. The developed technique is a time saving and appropriate method to be implemented for any type of loading.

Note that, some formulae and knowledge given in previous chapters are repeated in this chapter for the sake of integrity of the work presented.

5.1 Theory

The modification method to calculate zero mean loading set, $G_{im}(f)$, which leads to approximately equivalent fatigue damage on a structure which is subjected to a random loading with nonzero mean, is based on the frequency domain fatigue calculation techniques.

The linear relation between the input and the output of the system which are, in this chapter, acceleration, and stress, respectively, is given with (5.1) in frequency domain. Transfer function matrix elements are in complex form.

$$\{\sigma(f)\} = [H(f)]\{a(f)\} \tag{5.1}$$

where $\{a(f)\}$ is acceleration vector, $[H(f)]$ is transfer function matrix and $\{\sigma(f)\}$ is stress vector given in (5.2), (5.3), (5.4), respectively.

$$\{a(f)\} = \begin{Bmatrix} a_x(f) \\ a_y(f) \\ a_z(f) \end{Bmatrix} \tag{5.2}$$

$$[H(f)] = \begin{bmatrix} H_{\sigma_{xx},a_x}(f) & H_{\sigma_{xx},a_y}(f) & H_{\sigma_{xx},a_z}(f) \\ H_{\sigma_{yy},a_x}(f) & H_{\sigma_{yy},a_y}(f) & H_{\sigma_{yy},a_z}(f) \\ H_{\sigma_{zz},a_x}(f) & H_{\sigma_{zz},a_y}(f) & H_{\sigma_{zz},a_z}(f) \\ H_{\tau_{xy},a_x}(f) & H_{\tau_{xy},a_y}(f) & H_{\tau_{xy},a_z}(f) \\ H_{\tau_{xz},a_x}(f) & H_{\tau_{xz},a_y}(f) & H_{\tau_{xz},a_z}(f) \\ H_{\tau_{yz},a_x}(f) & H_{\tau_{yz},a_y}(f) & H_{\tau_{yz},a_z}(f) \end{bmatrix} \tag{5.3}$$

$$\{\sigma(f)\} = \begin{Bmatrix} \sigma_x(f) \\ \sigma_y(f) \\ \sigma_z(f) \\ \tau_{xy}(f) \\ \tau_{xz}(f) \\ \tau_{yz}(f) \end{Bmatrix} \tag{5.4}$$

Goodman's mean stress correction, Equation (3.6), is performed on the output stress vector, $\{\sigma(f)\}$, and the modified output stress vector, $\{\sigma_m(f)\}$, is obtained.

Power spectral density matrix of modified stress, $[G_{\sigma_m}(f)]$, is calculated via multiplication of stress vector conjugate and stress vector with $1/2T_p$ (5.5).

$$[G_{\sigma_m}(f)] = \frac{1}{2T_p}\{\sigma_m^*(f)\}\{\sigma_m^T(f)\} \tag{5.5}$$

where,

$$\left[G_{\sigma_m}(f)\right]=\begin{bmatrix} G_{\sigma_{xx},\sigma_{xx}}(f) & G_{\sigma_{xx},\sigma_{yy}}(f) & G_{\sigma_{xx},\sigma_{zz}}(f) & G_{\sigma_{xx},\tau_{xy}}(f) & G_{\sigma_{xx},\tau_{xz}}(f) & G_{\sigma_{xx},\tau_{yz}}(f) \\ G^{*}_{\sigma_{xx},\sigma_{yy}}(f) & G_{\sigma_{yy},\sigma_{yy}}(f) & G_{\sigma_{yy},\sigma_{zz}}(f) & G_{\sigma_{yy},\tau_{xy}}(f) & G_{\sigma_{yy},\tau_{xz}}(f) & G_{\sigma_{yy},\tau_{yz}}(f) \\ G^{*}_{\sigma_{xx},\sigma_{zz}}(f) & G^{*}_{\sigma_{yy},\sigma_{zz}}(f) & G_{\sigma_{zz},\sigma_{zz}}(f) & G_{\sigma_{zz},\tau_{xy}}(f) & G_{\sigma_{zz},\tau_{xz}}(f) & G_{\sigma_{zz},\tau_{yz}}(f) \\ G^{*}_{\sigma_{xx},\tau_{xy}}(f) & G^{*}_{\sigma_{yy},\tau_{xy}}(f) & G^{*}_{\sigma_{zz},\tau_{xy}}(f) & G_{\tau_{xy},\tau_{xy}}(f) & G_{\tau_{xy},\tau_{xz}}(f) & G_{\tau_{xy},\tau_{yz}}(f) \\ G^{*}_{\sigma_{xx},\tau_{xz}}(f) & G^{*}_{\sigma_{yy},\tau_{xz}}(f) & G^{*}_{\sigma_{zz},\tau_{xz}}(f) & G^{*}_{\tau_{xy},\tau_{xz}}(f) & G_{\tau_{xz},\tau_{xz}}(f) & G_{\tau_{xz},\tau_{yz}}(f) \\ G^{*}_{\sigma_{xx},\tau_{yz}}(f) & G^{*}_{\sigma_{yy},\tau_{yz}}(f) & G^{*}_{\sigma_{zz},\tau_{yz}}(f) & G^{*}_{\tau_{xy},\tau_{yz}}(f) & G^{*}_{\tau_{xz},\tau_{yz}}(f) & G_{\tau_{yz},\tau_{yz}}(f) \end{bmatrix}_{(m)} \tag{5.6}$$

It is desirable to express (5.6) in matrix form as (5.7) to improve computational efficiency and simplify the calculations [11].

$$\left[G_r(f)\right]=\left[H^{*}(f)\right]G_i(f)\left[H^{T}(f)\right] \tag{5.7}$$

Then, the relation between modified output stress and input acceleration PSD can be expressed with (5.8).

$$\left[G_{\sigma_m}(f)\right]=\left[H^{*}(f)\right]\left[G_{a_m}\right]\left[H^{T}(f)\right] \tag{5.8}$$

Finally, the needed modified input acceleration matrix power spectral density is obtained with (5.9) by reordering (5.8).

$$\left[G_{a_m}(f)\right]=\left[H^{*}(f)\right]^{-1}\left[G_{\sigma_m}(f)\right]\left[H^{T}(f)\right]^{-1} \tag{5.9}$$

A corrected multi-axial input loading with zero mean but modified alternating stress, which creates fatigue damage approximately equivalent to the damage caused by the unprocessed loading set with nonzero mean, is extracted by means of this technique. It should be noted that, this approach is focusing to find a modified loading set that simulates damage

for a selected point on the structure, which in turn will be acceptable in the vicinity of that point only.

5.2 Case Studies

5.2.1 Case Study I – Test Comparison

In this case study it is aimed to compare the proposed input loading generation method with test results. For this purpose a notched specimen is used since there would be lengthy test durations needed otherwise.

The dimensions of the 3 mm thick test specimen are given in Figure 5.1 with respect to the clamped end. The test specimen is manufactured from aluminum 5754 H111.

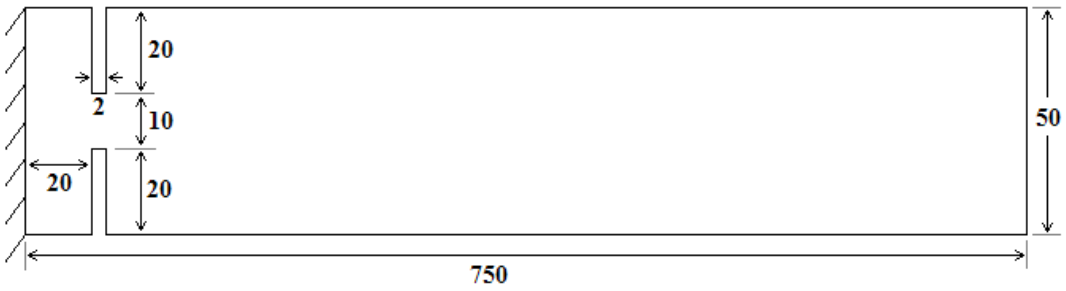

Figure 5.1 – Dimensions of the test specimen (Dimensions in [mm])

Standard vibration test systems do not have capabilities which enable mean stress application. Therefore a mean value of 1 g in the acceleration excitation is selected since it can be applied if the excitation direction is selected as vertical to make use of Earth's gravity.

Hence, tests are conducted in 2 different configurations. The first configuration is used for the actual mean stress test on a vertical vibration shaker armature as shown in Figure 5.2. The second configuration, shown in Figure 5.3 where a horizontal vibration shaker and slip table system is utilized, is used for both the pure alternating test and the test where modified loading corresponding to the proposed mean stress correction method is applied.

For these three tests, corresponding analysis are also conducted. Note that for the horizontal test condition, there is a 1 g mean stress acting in a direction perpendicular to the excitation direction. To show that this perpendicular mean stress does not affect the results critically, for the pure alternating test, another analysis is performed where this perpendicular mean stress is also taken into account. It is observed that the life reduction is less than %0.5 so the effect is negligible.

Figure 5.2 – Vertical test configuration

Figure 5.3 – Horizontal test configuration

The input is an acceleration PSD distribution over 20 Hz – 2000 Hz range which is given in Table 5.1 and plotted in Figure 5.4.

Table 5.1 – Input PSD Data

Frequency [Hz]	Amplitude [(mm/s²)²/Hz]
20	96.2
100	1.624E7
500	1.624E7
700	1.624E5
2000	1.624E5

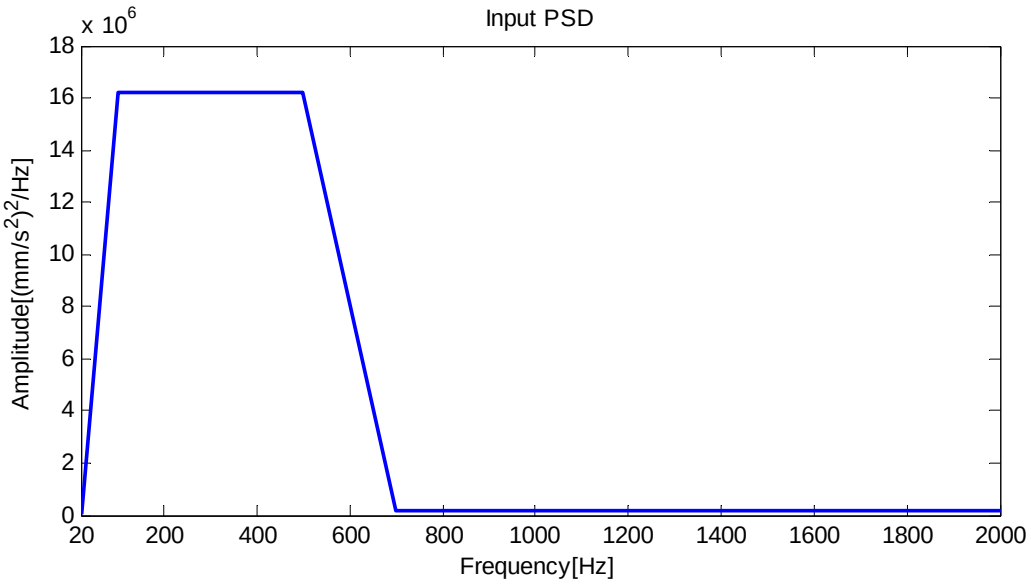

Figure 5.4 – Acceleration Input PSD

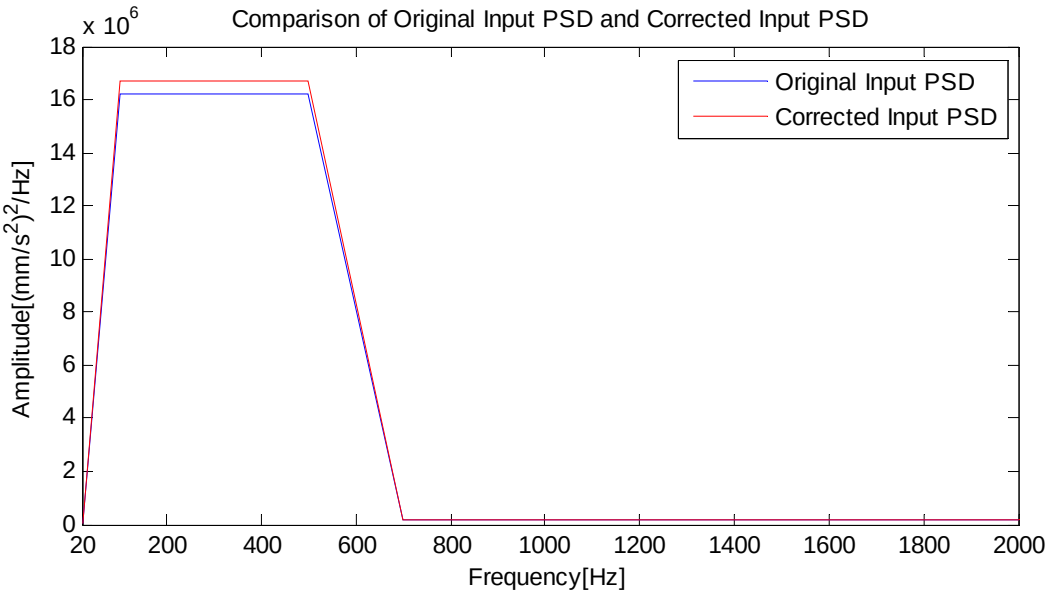

Figure 5.5 – Original and corrected acceleration input PSDs

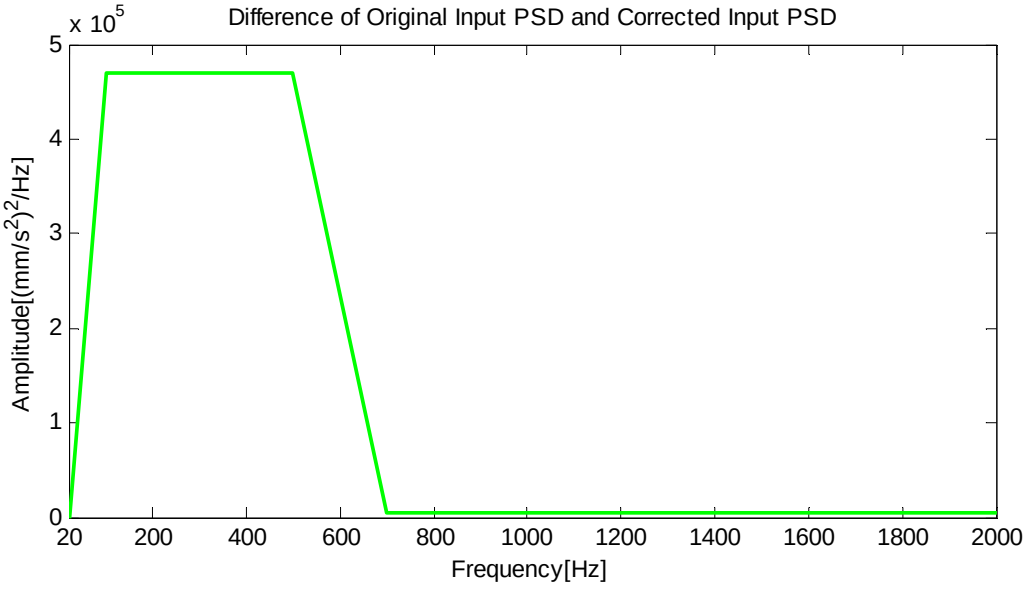

Figure 5.6 – Difference between corrected and original acceleration input PSDs (Corrected - Original)

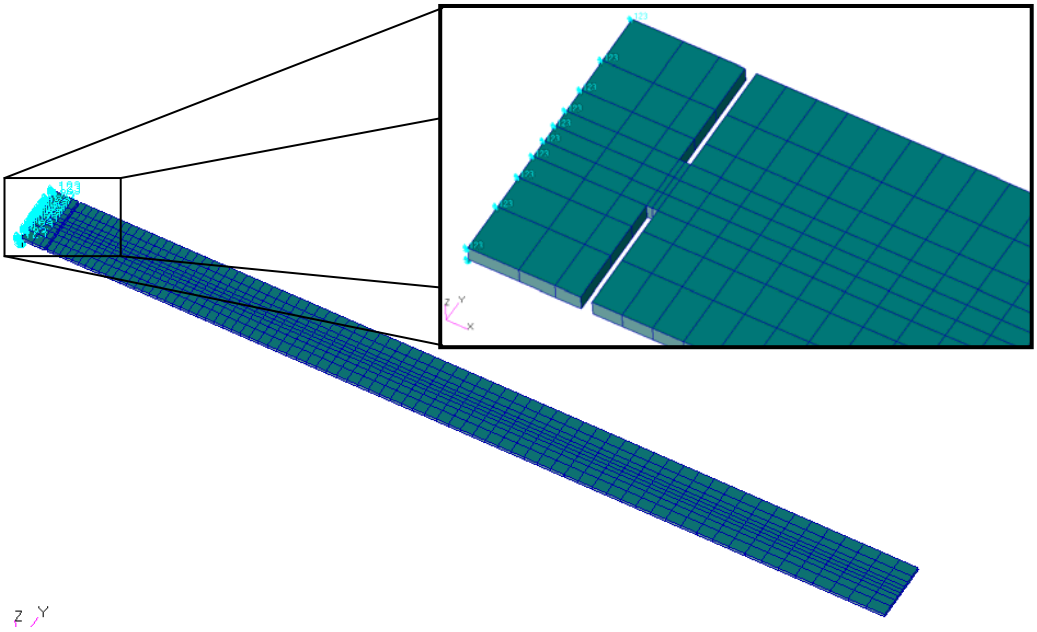

Figure 5.7 – Finite element model

The modified input loading and its difference from the original input loading are given in Figure 5.5 and Figure 5.6, respectively. A finite element model created with hexahedral solid elements with 8-nodes is used for the analysis step (Figure 5.7). The resulting fatigue life for the pure alternating input acceleration, neglecting input mean value so without mean stress correction, is given in Figure 5.8 and Figure 5.9, whereas Figure 5.10 and Figure 5.11 are the life plots for the Goodman mean stress correction case proposed by MSC Fatigue. Lastly, Figure 5.12 and Figure 5.13 are the fatigue life plots for the pure alternating loading resulting from the proposed mean stress correction method in Section 5.1 which is the corrected input PSD shown in Figure 5.5.

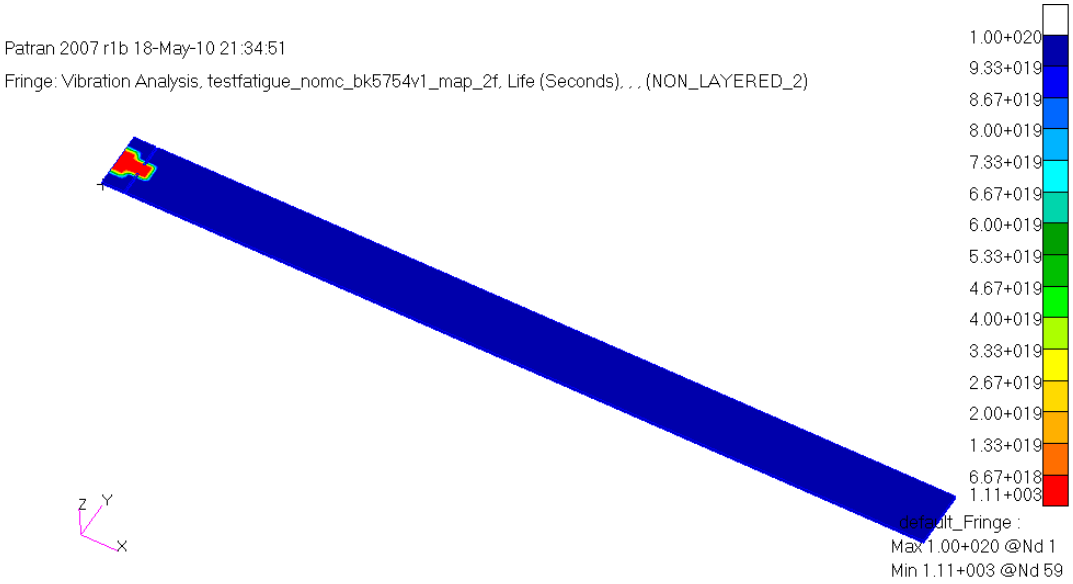

Figure 5.8 – Fatigue life for the plate: without mean stress correction

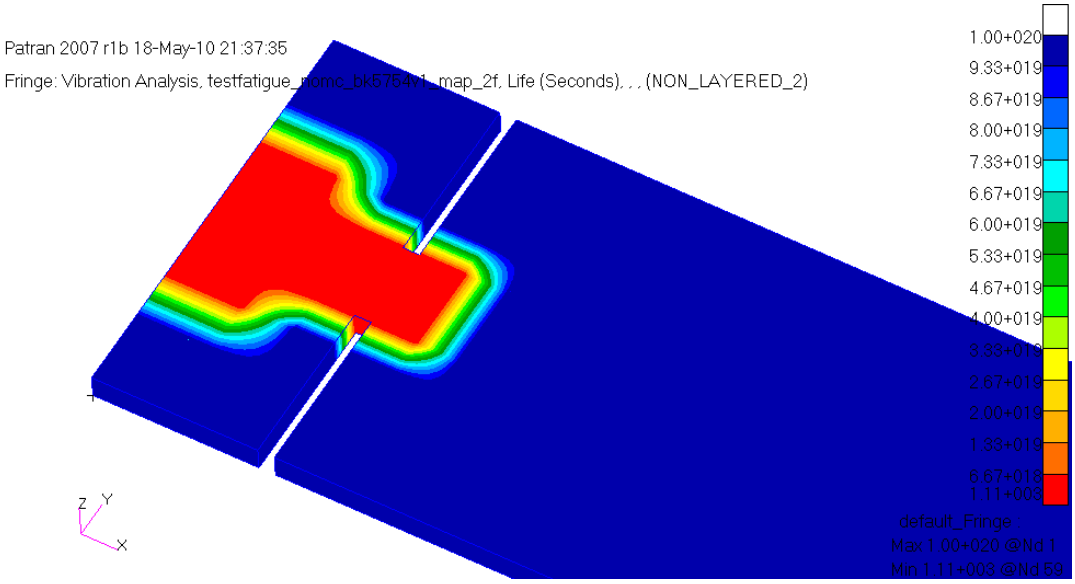

Figure 5.9 – Fatigue life for the plate: without mean stress correction (close-up)

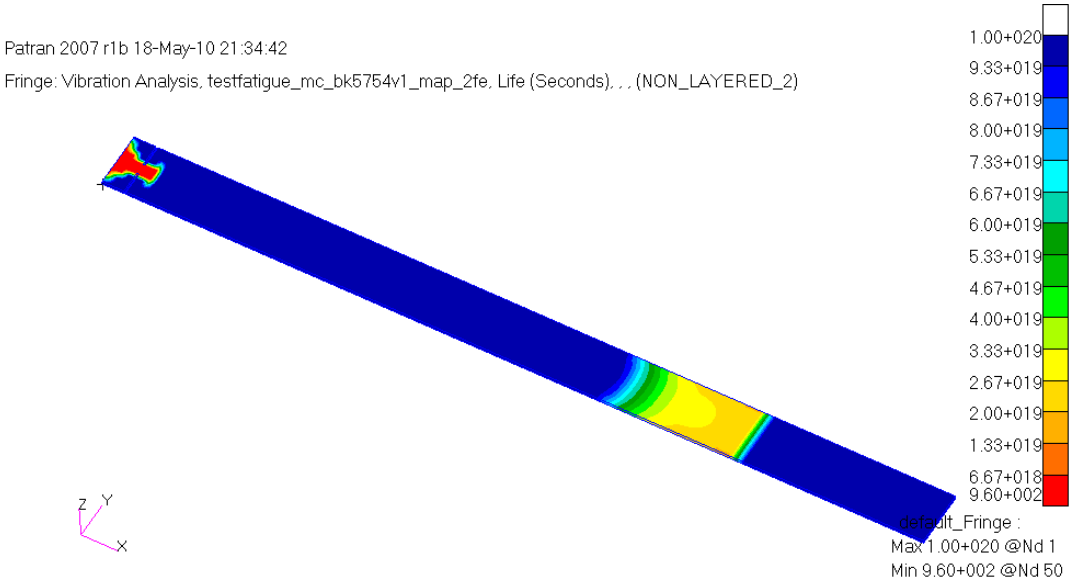

Figure 5.10 – Fatigue life for the plate: with mean stress correction

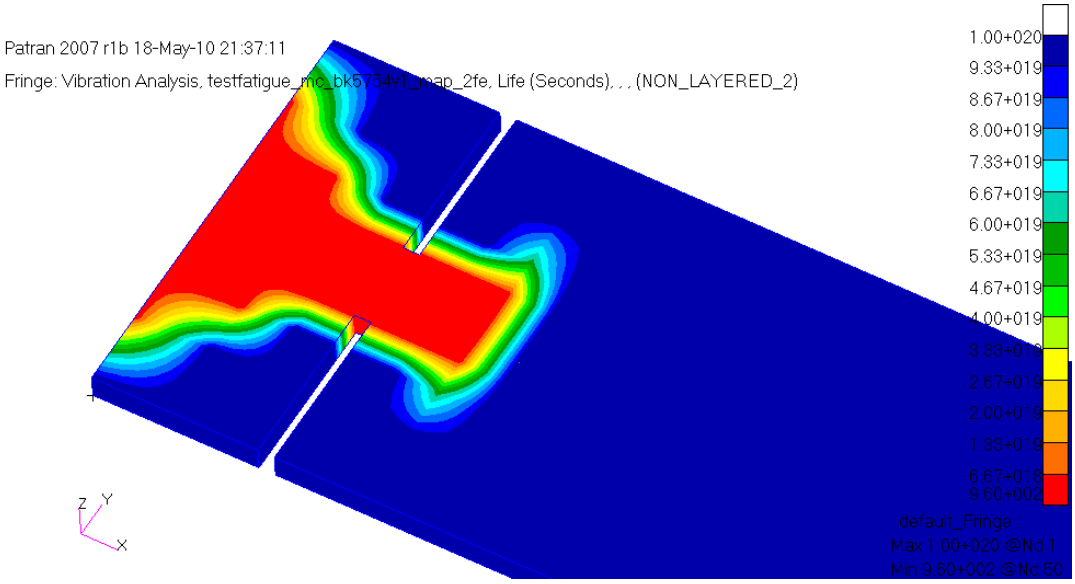

Figure 5.11 – Fatigue life for the plate: with mean stress correction (close-up)

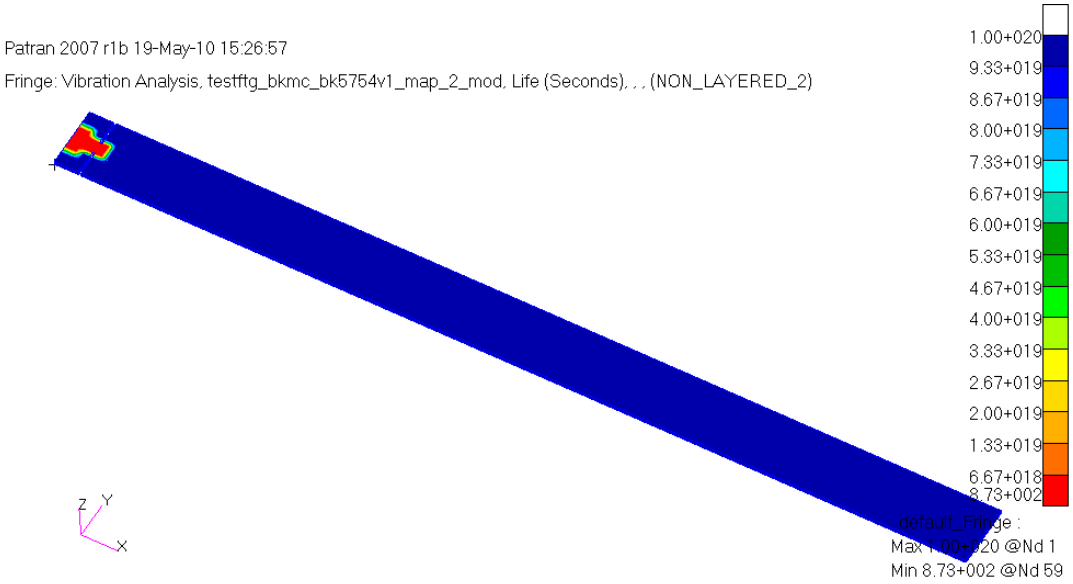

Figure 5.12 – Fatigue life for the plate: with mean stress correction via proposed method

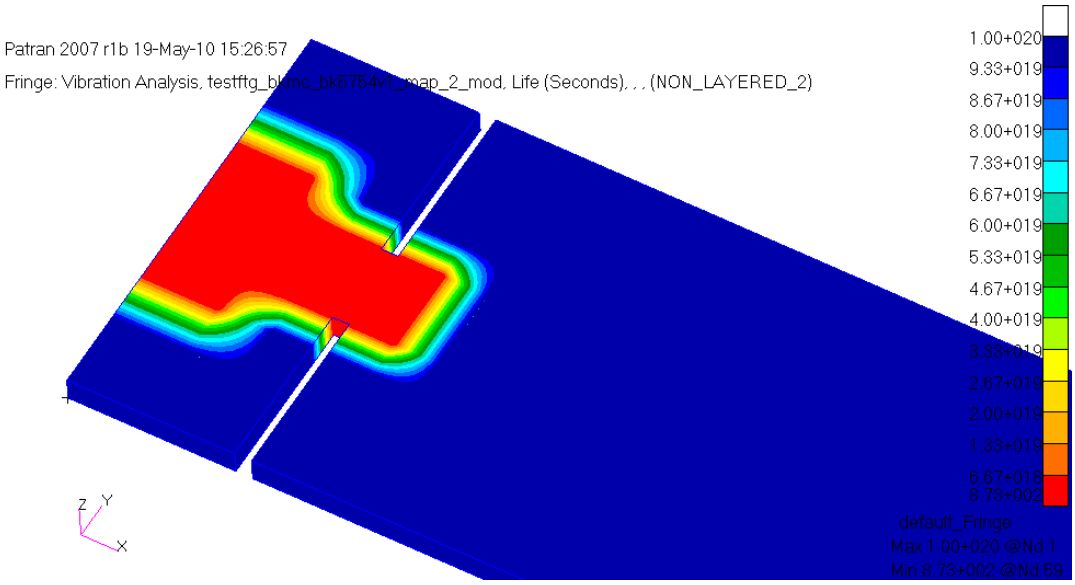

Figure 5.13 – Fatigue life for the plate: with mean stress correction via proposed method (close-up)

Table 5.2 lists the minimum life for all these analyses. The proposed mean stress correction method, which creates a modified pure alternating input, is able to match with the mean stress correction case and it is on the safe side. Also, the effect of the mean value of the loading can be seen from Table 5.2.

Table 5.2 – Life values from analysis

Loading	Life [s]
Without mean stress correction	1108
With mean stress correction	960
With proposed method	873

To clarify the most damaged nodes in the analyses given above, close-up life plots are also presented in logarithmic scale. It is clear from Figure 5.14, Figure 5.15 and Figure 5.16, failure is going to be on the notch for all of the three cases, as expected.

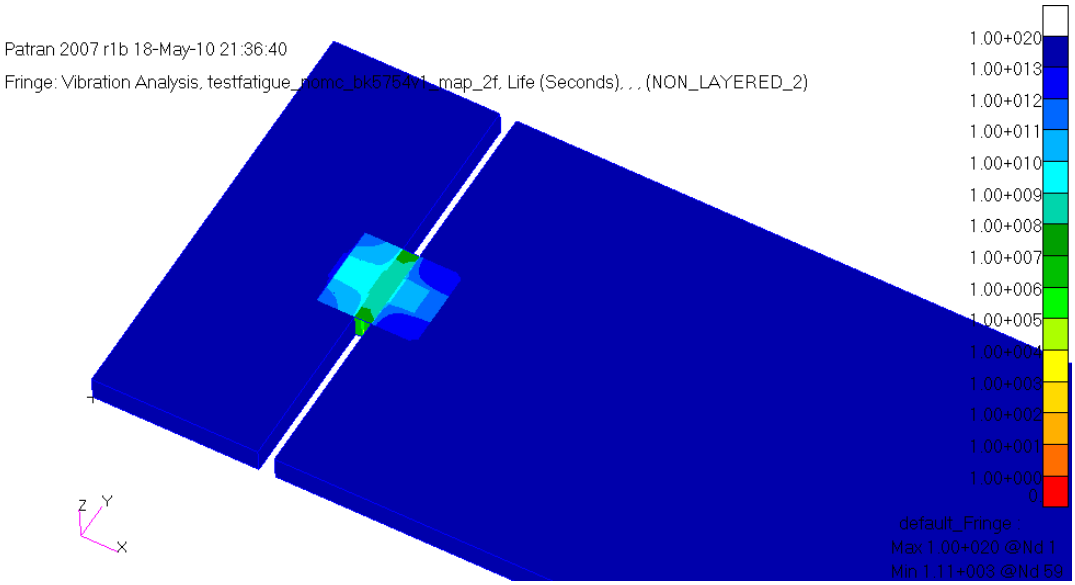

Figure 5.14 – Fatigue life for the plate: without mean stress correction (close-up, logarithmic scale)

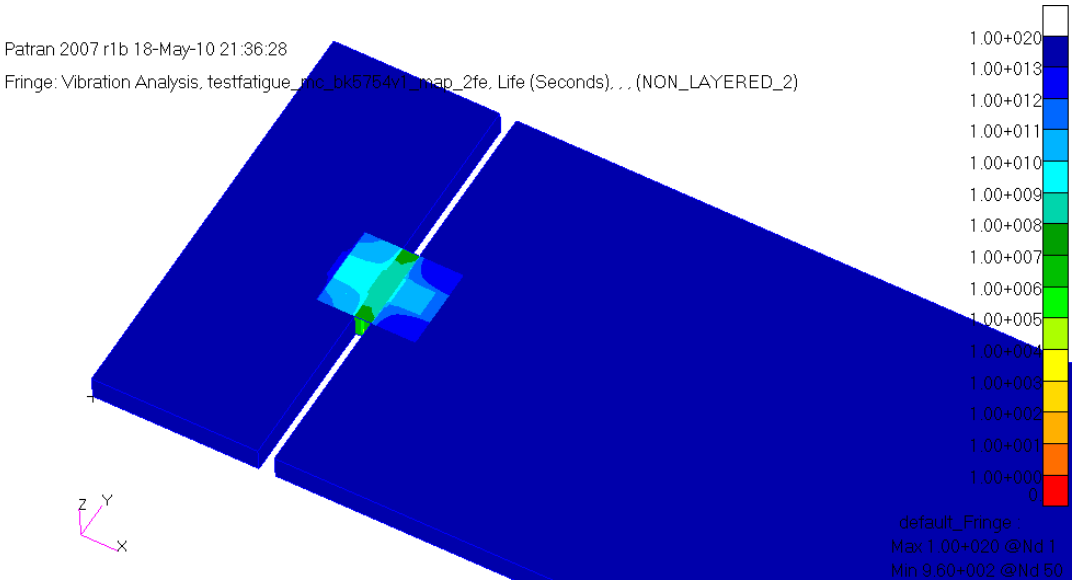

Figure 5.15 – Fatigue life for the plate: with mean stress correction (close-up, logarithmic scale)

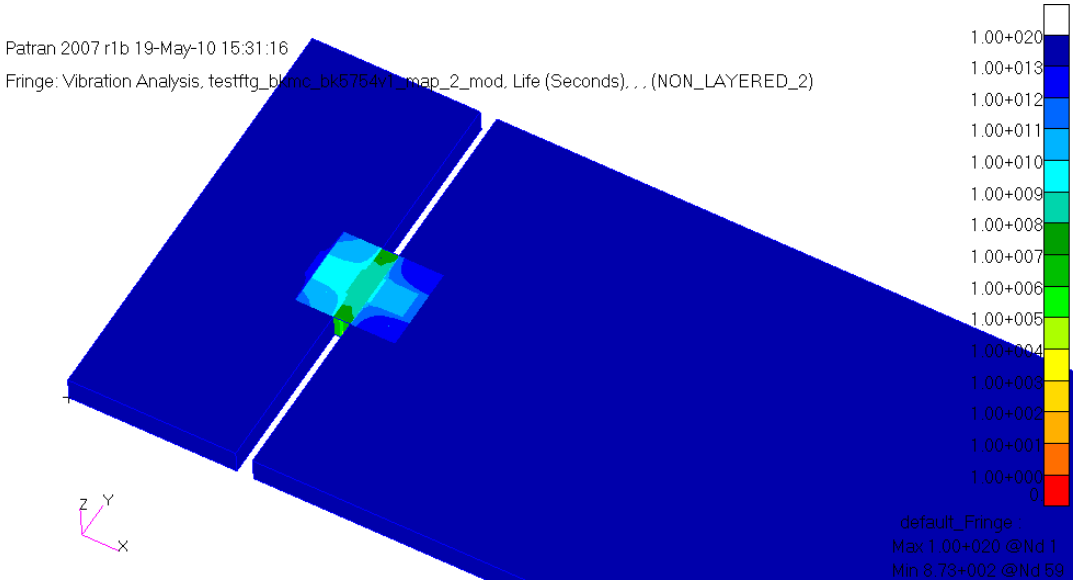

Figure 5.16 – Fatigue life for the plate: with proposed method (close-up, logarithmic scale)

As stated before, the tests for the three cases given in Table 5.2 are conducted such that the original loading without mean stress correction and the loading resulting from the proposed method utilizes the configuration given in Figure 5.3. and for the mean stress correction case, however, utilizes the configuration given in Figure 5.2 to make use of Earth's gravity as the mean stress acceleration component. During these three tests performed (each of which repeated for 3 times), it is seen that the plate vibrates for a while and suddenly fails around the notch, bending on one side. The life values (Table 5.3) for the test cases are determined such that it is the excitation time until this sudden damaging occurs. Mean values of these are given in Table 5.4.

Table 5.3 – Life values from tests

	Test 1	Test 2	Test 3
Without mean stress	1315	1450	1390
With mean stress	1285	1150	1234
With proposed method	1045	1090	1072

Table 5.4 – Mean value of life from tests

Loading	Life [s]
Without mean stress	1385
With mean stress	1223
With proposed method	1069

Figure 5.17 and Figure 5.18 show the damaged test specimen for the test case without mean stress, Figure 5.19 and Figure 5.20 are for the test case with actual mean stress applied using earth's gravity, and Figure 5.21 and Figure 5.22 depict the damaged specimen for test case excited with input obtained via proposed method.

Figure 5.17 – Damaged specimen 1: without mean stress

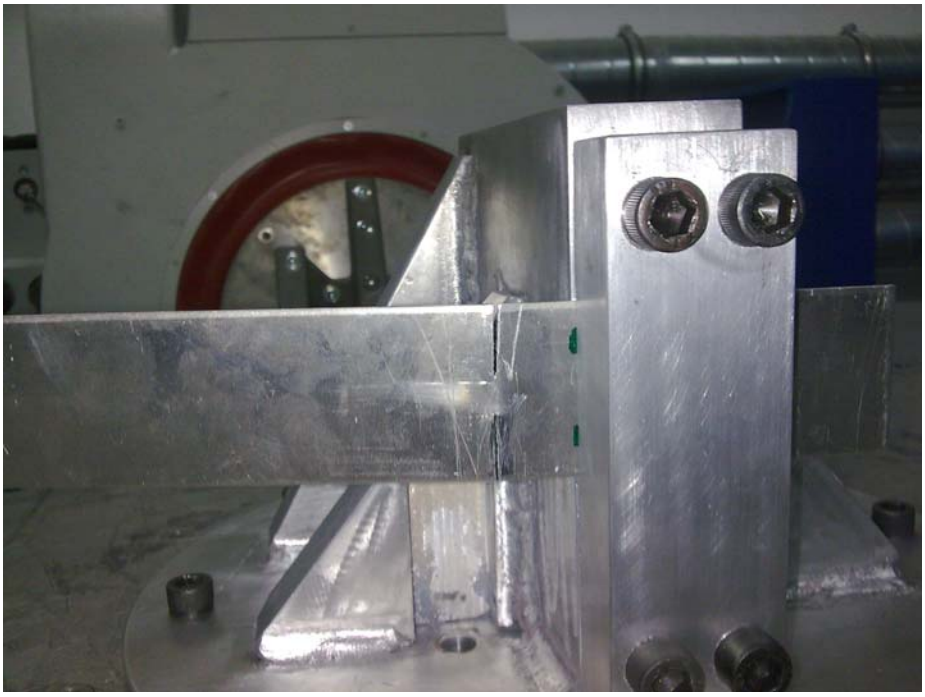

Figure 5.18 – Damaged specimen 1: without mean stress (close-up)

Figure 5.19 – Damaged specimen 2: with mean stress

Figure 5.20 – Damaged specimen 2: with mean stress (close-up)

Figure 5.21 – Damaged specimen 3: with proposed method

Figure 5.22 – Damaged specimen 3: with proposed method (close-up)

Finally, Table 5.5 compares the test and analysis cases based on life of the components. As expected, for all of the cases the analysis results are on the safe side and there is good correlation overall between the analysis and test cases since the percent difference between analysis and test case is almost the same for all of the three loadings.

Table 5.5 – Comparison of life values from test and analysis

Loading	Life [s] (Test)	Life [s] (Analysis)	Difference [%]
Without mean stress	1385	1108	20
With mean stress (correction in analysis)	1233	960	22
With proposed method	1069	873	19

5.2.2 Case Study II – Multi-axial Loading

The aim is to implement the proposed method for multiaxial loading in this case study. A fin like aerodynamic surface that is used in aerospace structures as a stabilizer during flight is excited at its attachment points in three axes. The solid model of the specimen is shown in Figure 5.23. The specimen is meshed with 8-noded solid elements. See Figure 5.24 for meshed finite element model.

The model is excited from fixed six holes in all degrees of freedom present on it. These holes serve for bolting the specimen on the flying equipment it is designed for.

Three inputs in x, y and z directions whose time history and power spectral density plots are given in Figure 5.25 and Figure 5.26 for x-axis, Figure 5.27 and Figure 5.28 for y-axis and Figure 5.29 and Figure 5.30 for z-axis respectively.

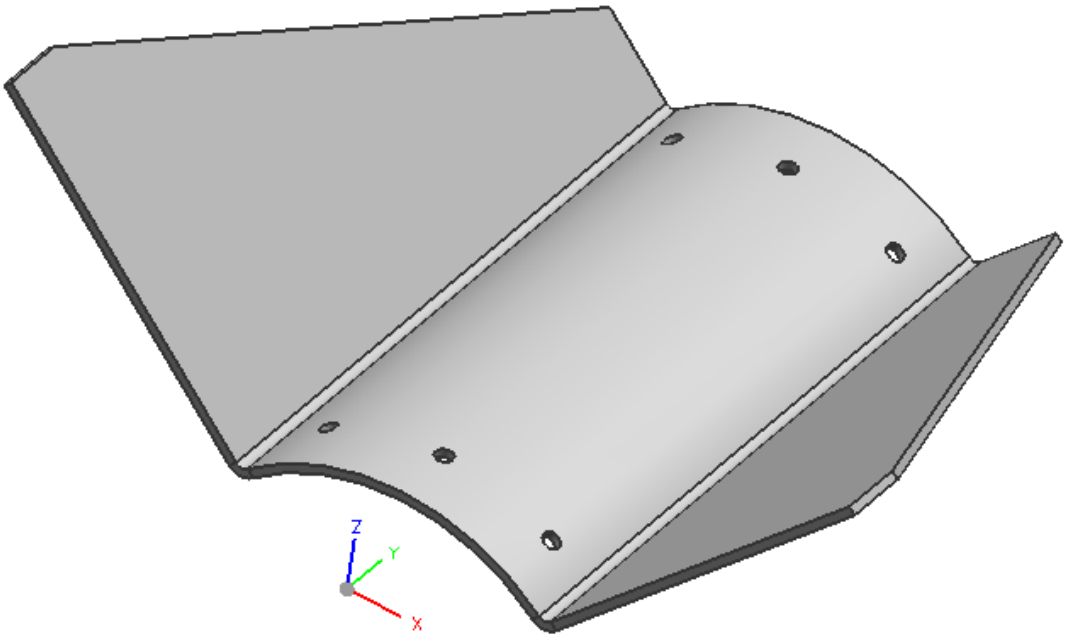

Figure 5.23 – Fin type aerodynamic surface

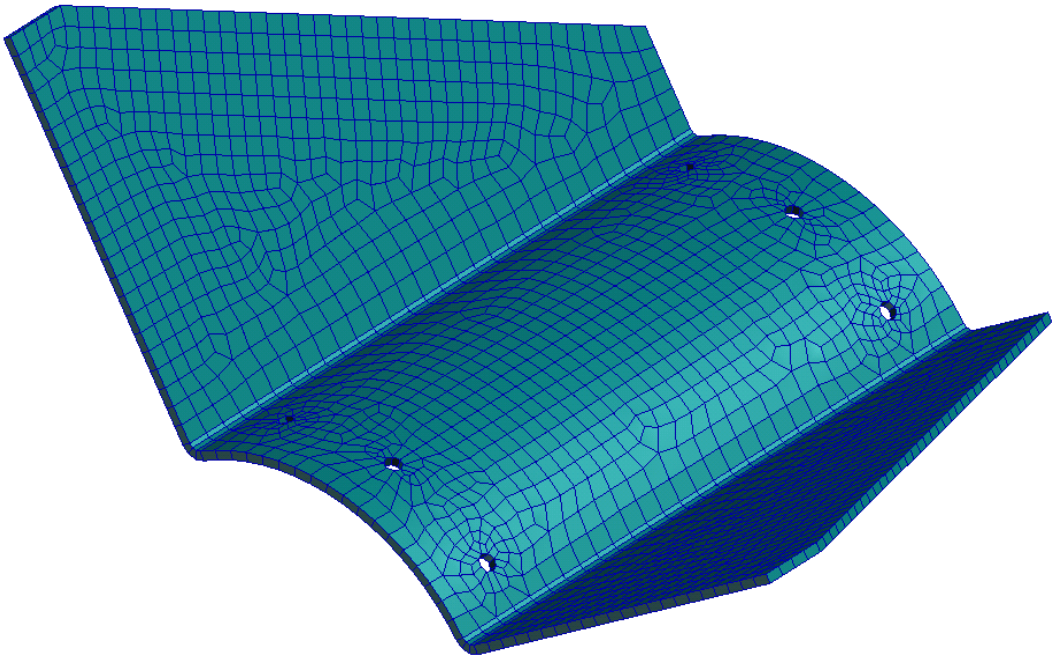

Figure 5.24 – FEM of the fin type aerodynamic surface

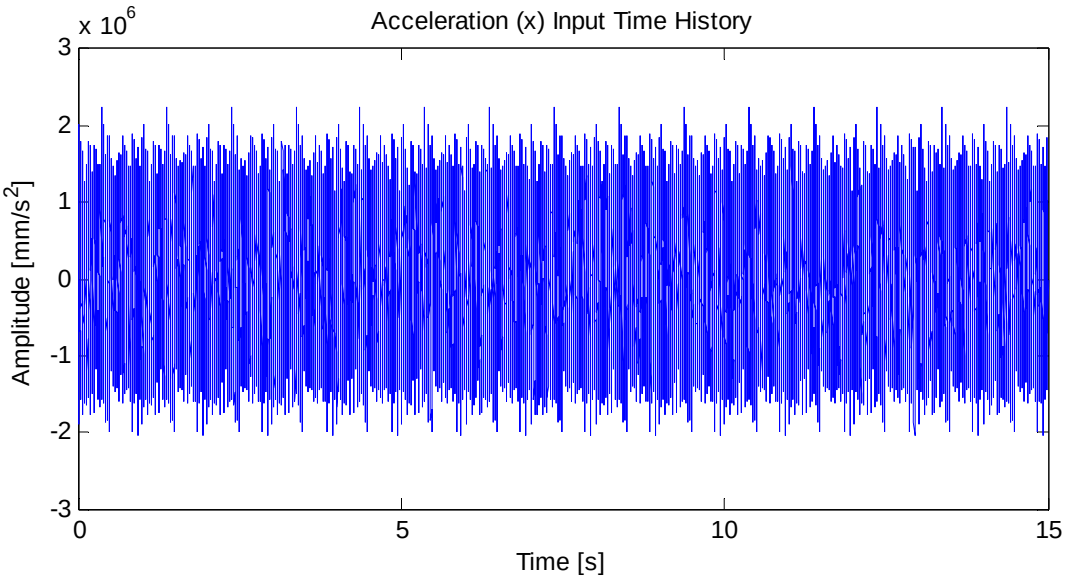

Figure 5.25 – Input time history in x-axis

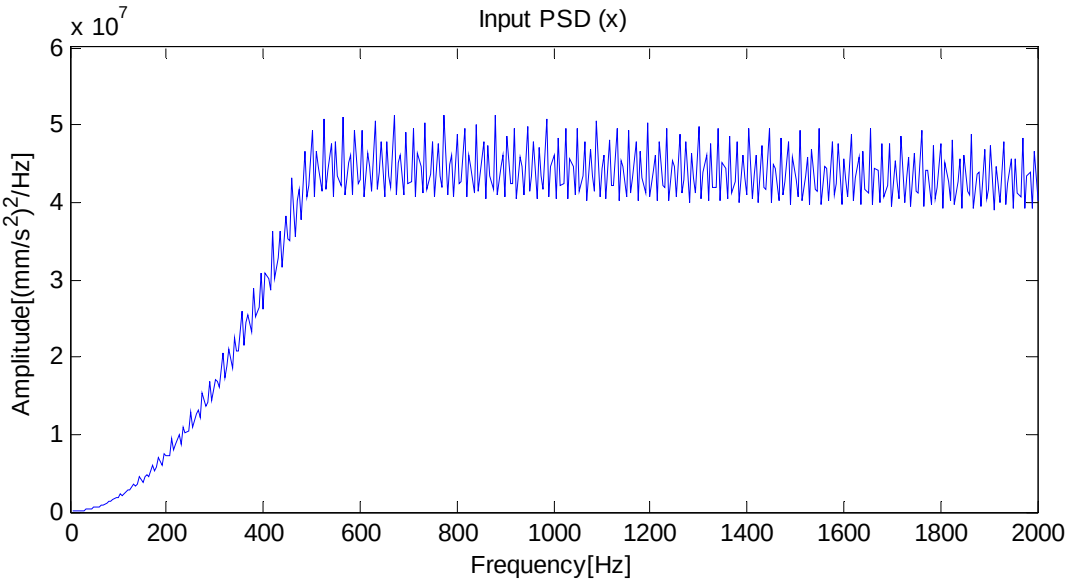

Figure 5.26 – Input PSD in x-axis

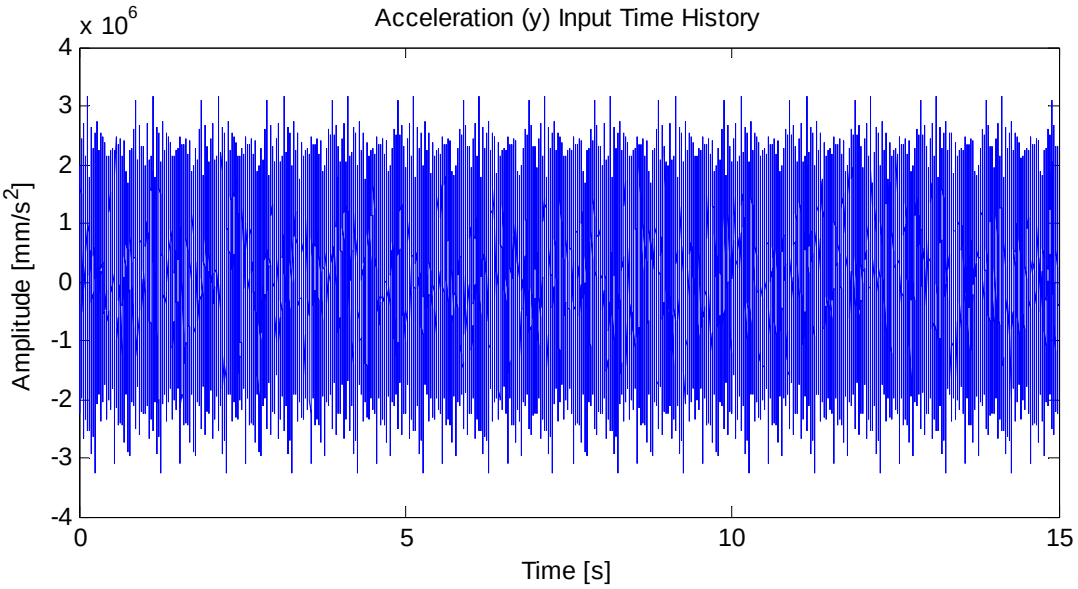

Figure 5.27 – Input time history in y-axis

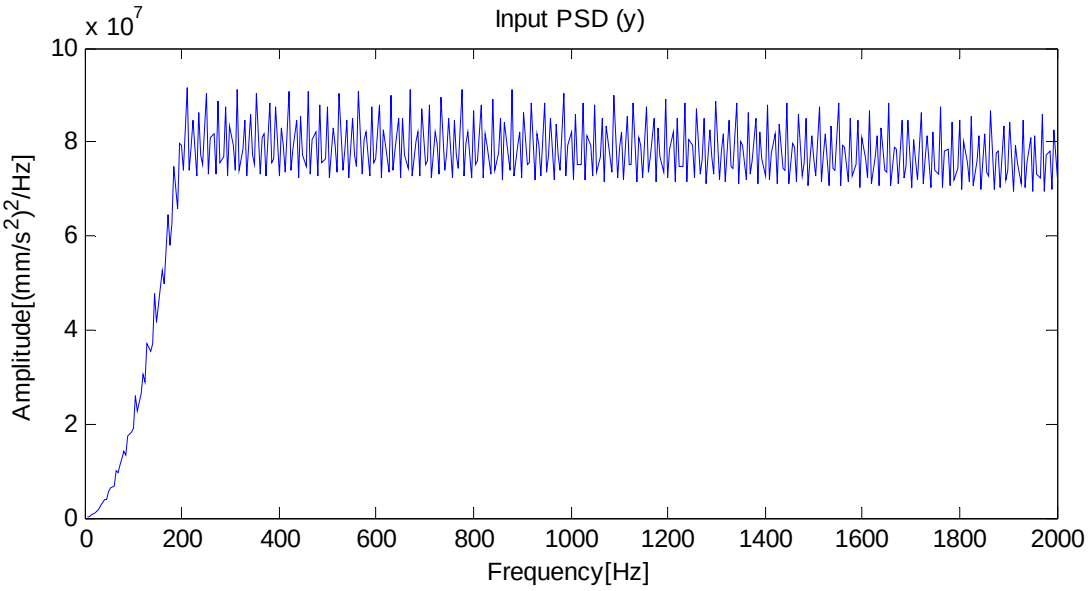

Figure 5.28 – Input PSD in y-axis

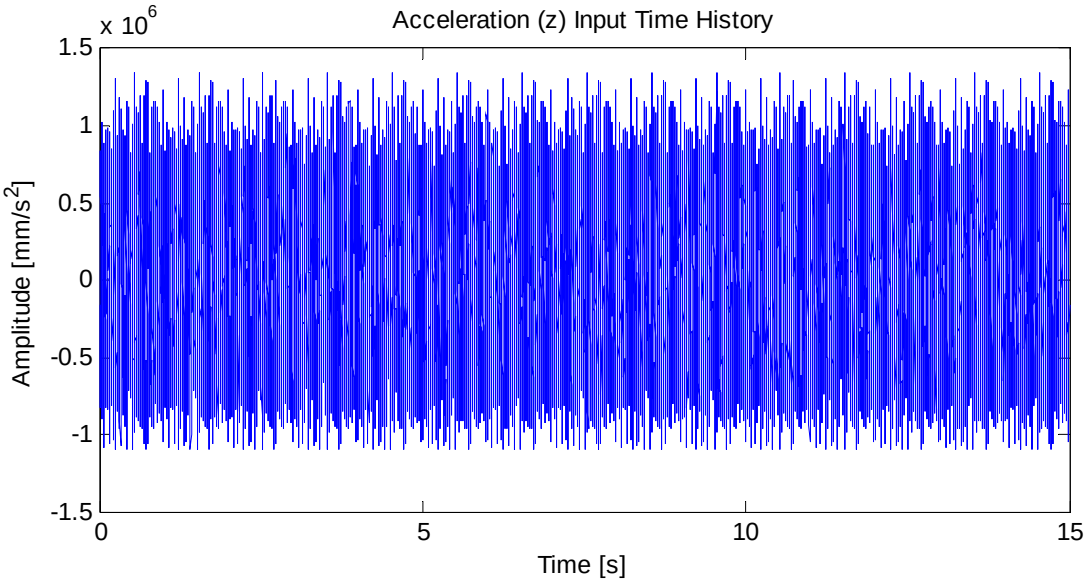

Figure 5.29 – Input time history in z-axis

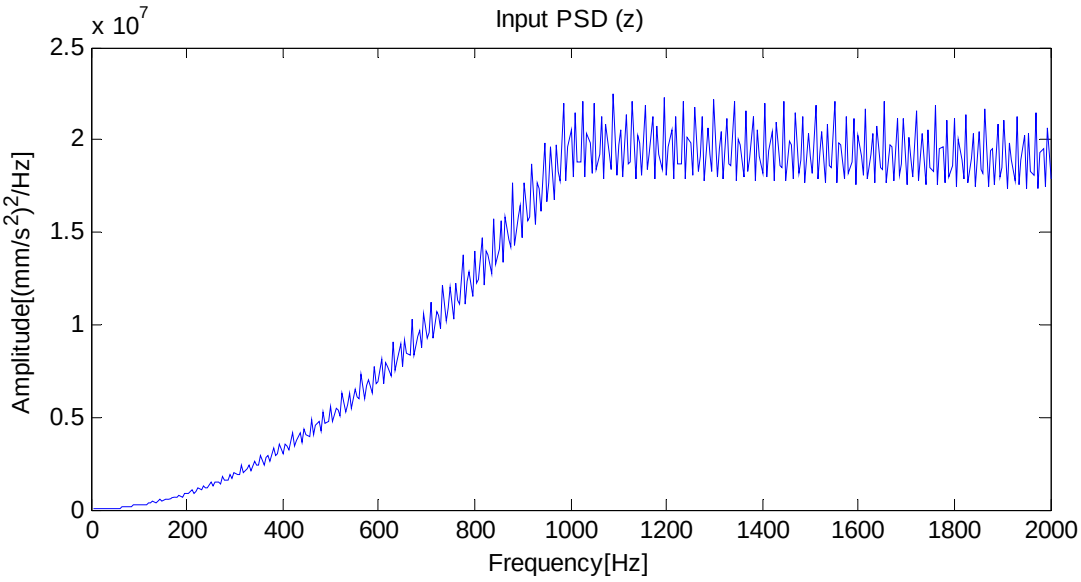

Figure 5.30 – Input PSD in z-axis

The inputs in all axes, namely x, y and z axes, have mean values of 2g, 3 g and 4g respectively.

Transfer functions obtained via frequency response analysis and excitation loadings are the inputs of fatigue analysis. The first analysis is conducted for determination of fatigue life using Dirlik's method without mean stress correction.

Then, the second analysis is performed with Goodman mean stress correction proposed by MSC Fatigue. Afterwards, inputs are corrected with the method proposed in section 5.1. Corrected inputs are plotted on top of the original inputs in Figure 5.31, Figure 5.32 and Figure 5.33. The interactions between matrix components and the influence of complex

transfer functions effect can be seen from the figures that there is no an obvious shift but the modifiation is changing in frequency band.

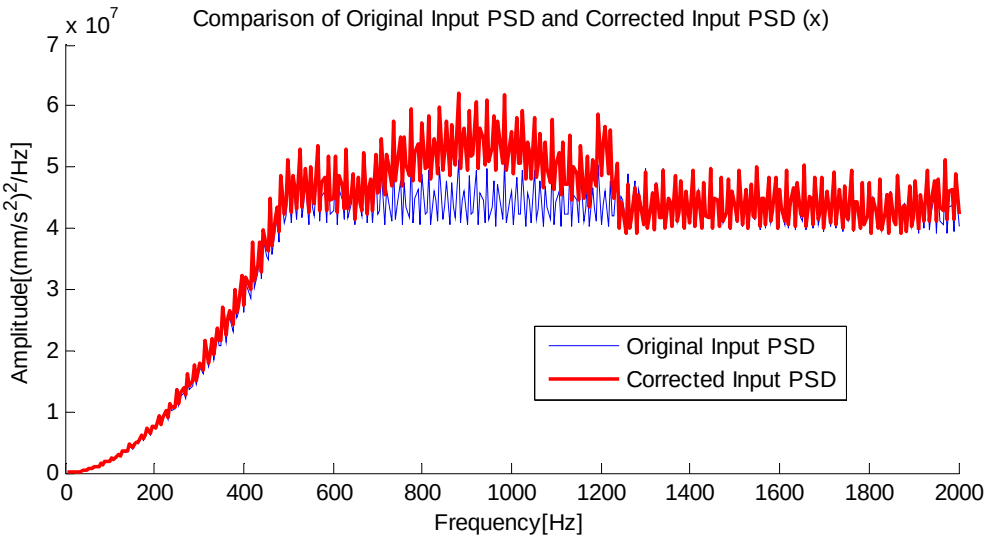

Figure 5.31 – Corrected and Original Input PSDs in x-axis

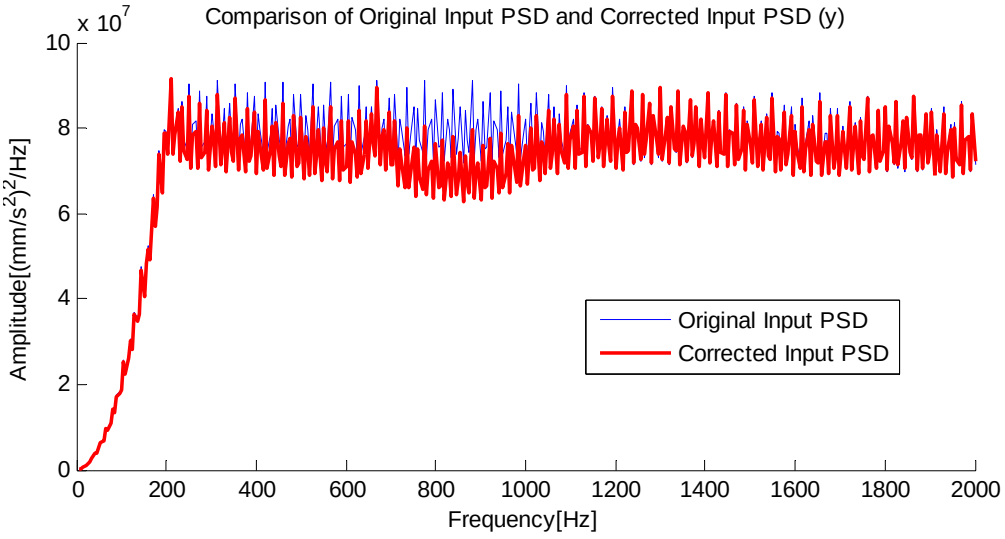

Figure 5.32 – Corrected and Original Input PSDs in y-axis

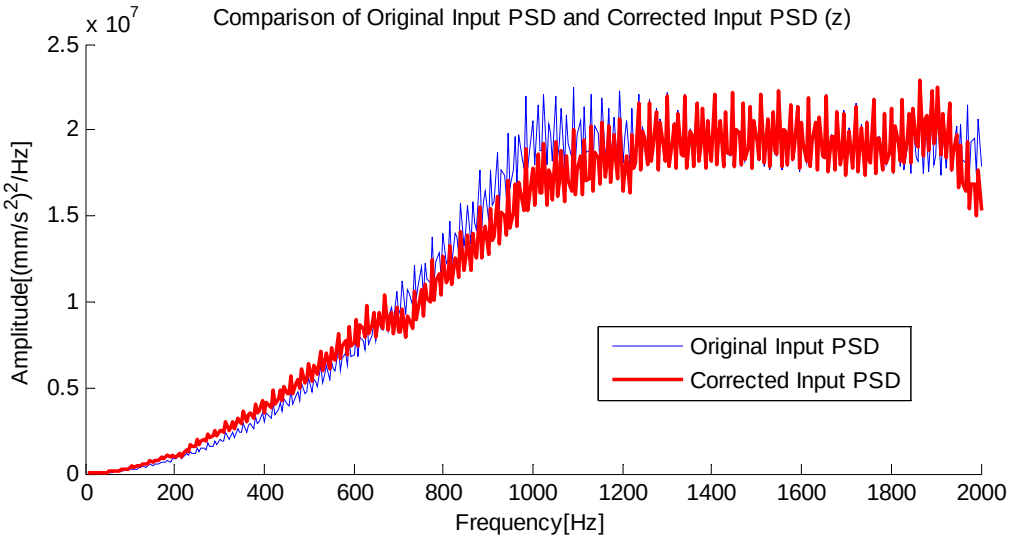

Figure 5.33 – Corrected and Original Input PSDs in z-axis

Finite element analysis results regarding fatigue life are presented in Figure 5.34, Figure 5.35, and Figure 5.36. Close-up plots of fatigue life are presented for the vicinity of the node that has the lowest life. These plots are given in Figure 5.37, Figure 5.38, and Figure 5.39.

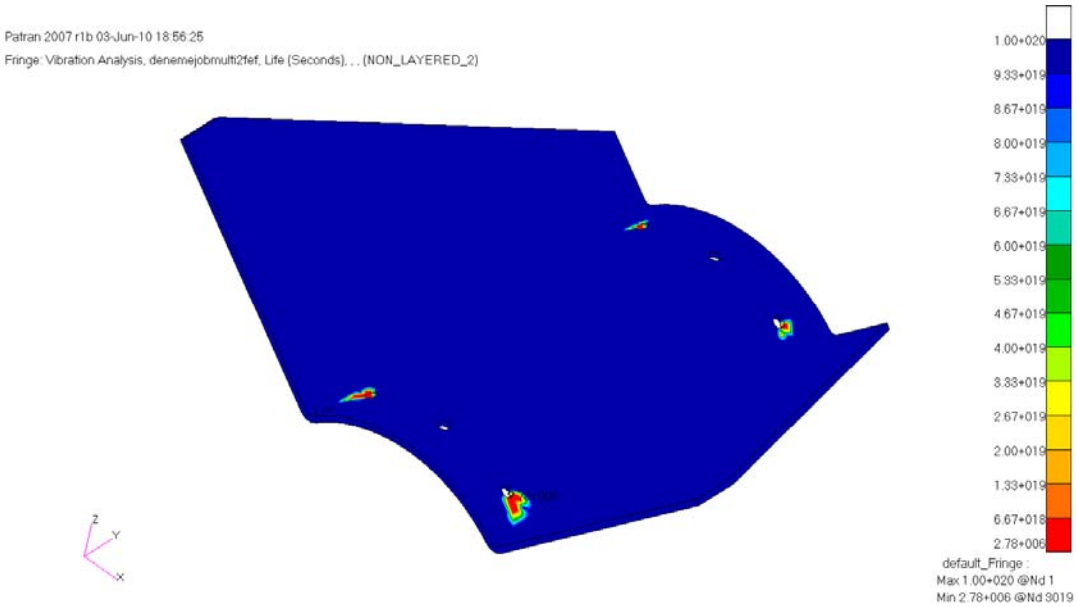

Figure 5.34 – Fatigue life for the fin: without mean stress correction

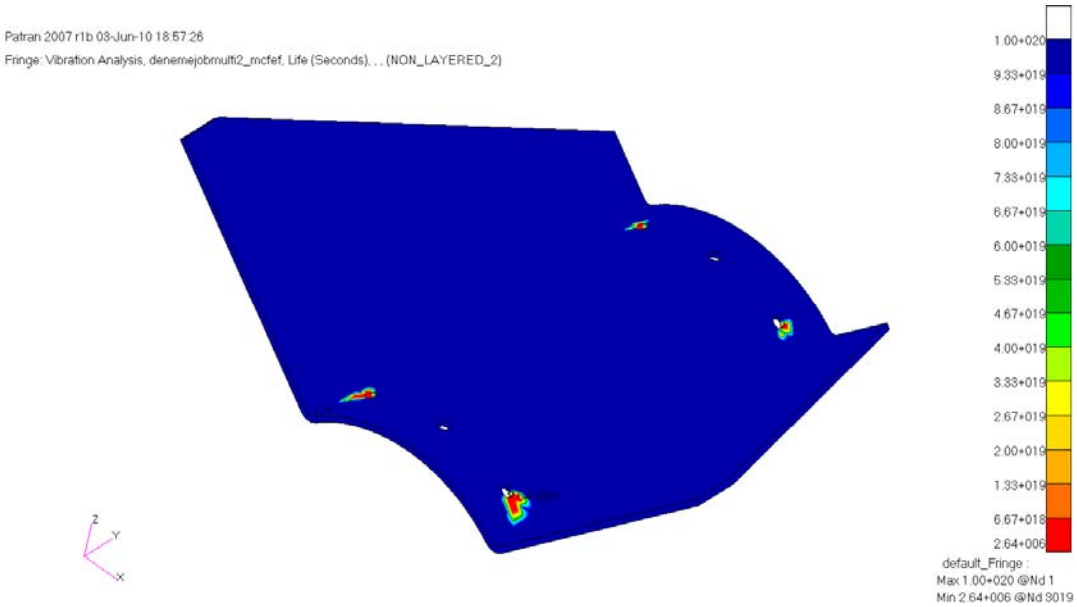

Figure 5.35 – Fatigue life for the fin: with mean stress correction

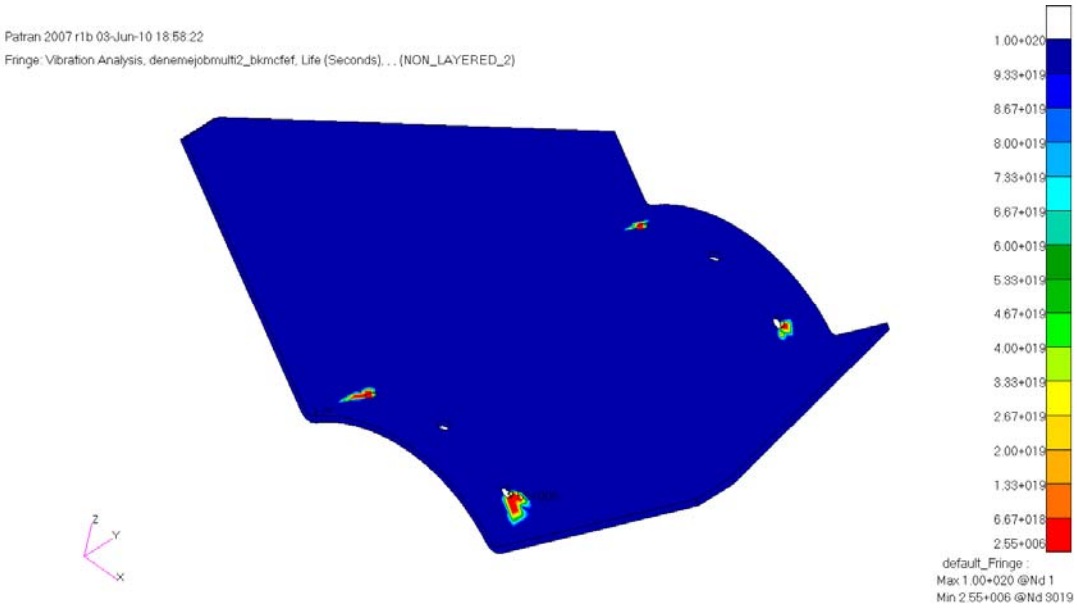

Figure 5.36 – Fatigue life for the fin: corrected with the proposed method

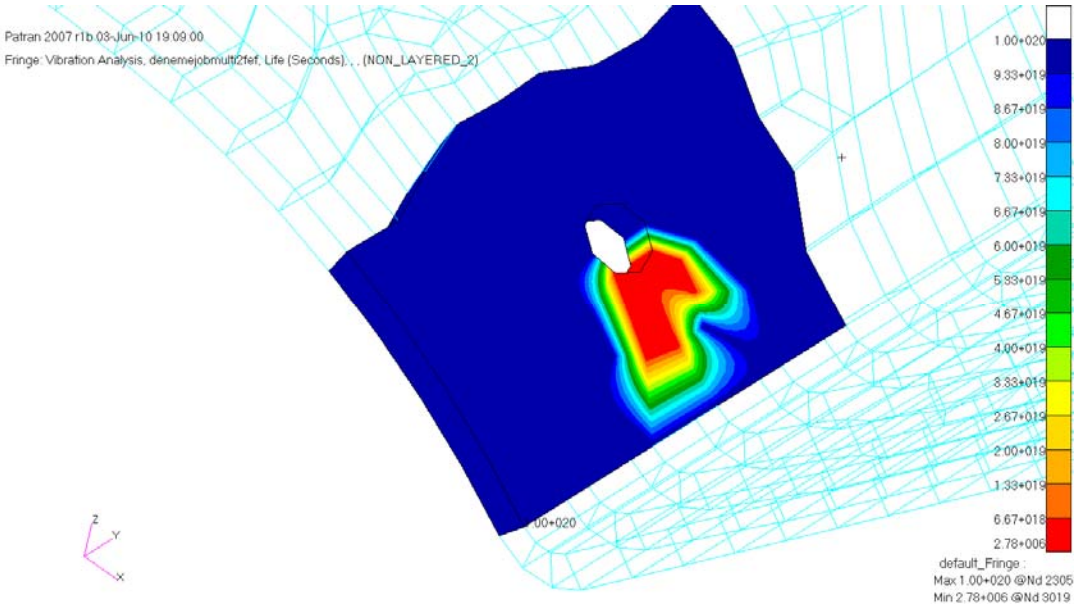

Figure 5.37 – Fatigue life for the fin: without mean stress correction (close-up)

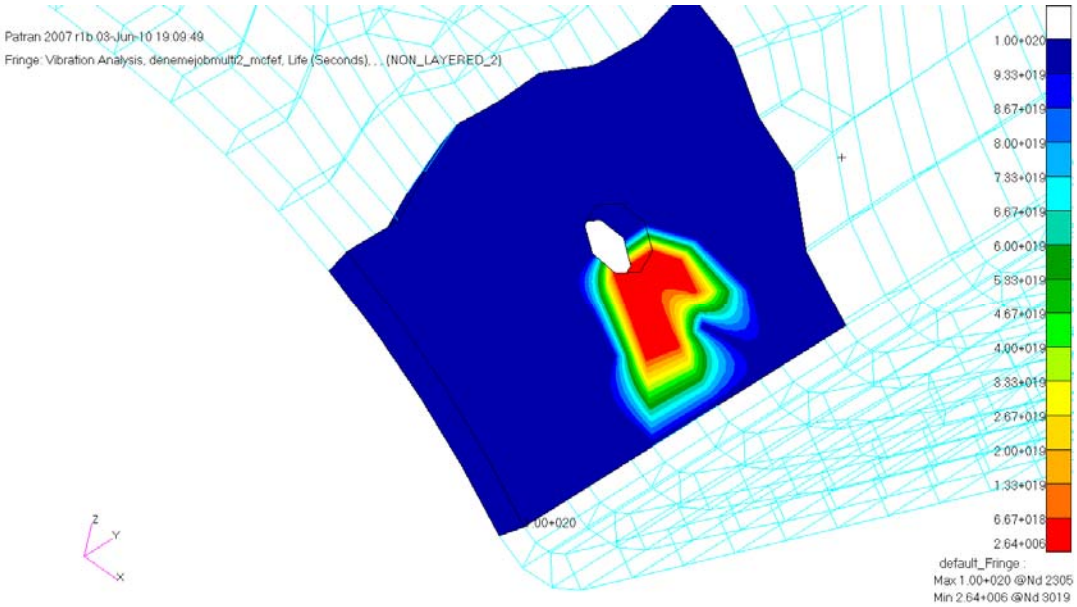

Figure 5.38 – Fatigue life for the fin: with mean stress correction (close-up)

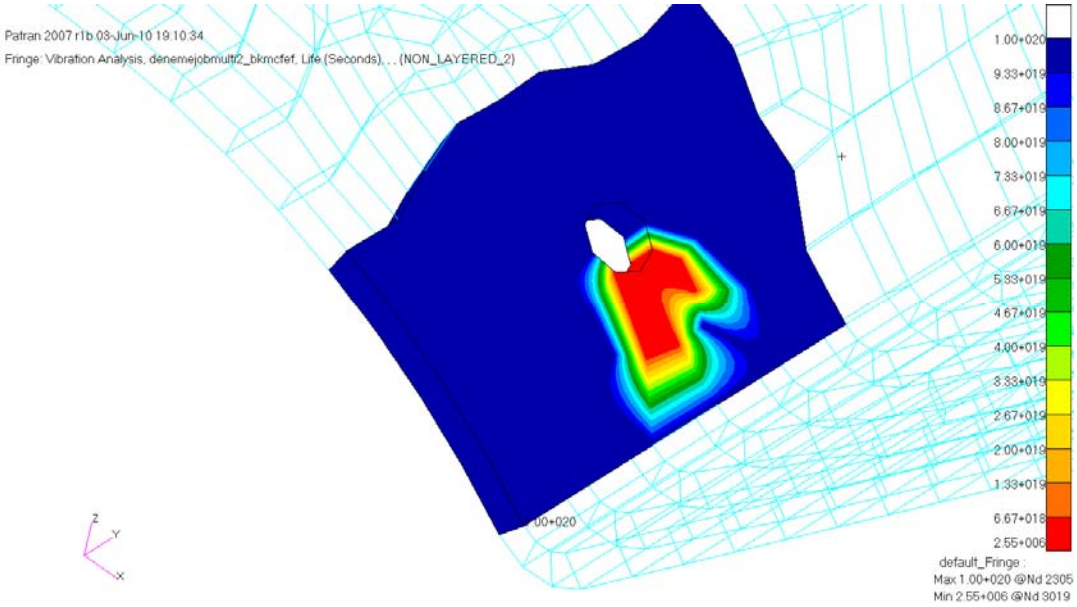

Figure 5.39 – Fatigue life for the fin: with the proposed method (close-up)

In this case study it is shown that the developed method is able to take care of multiaxial simultaneous inputs and yet gives a conservative fatigue life and comparable result considering that obtained by the Goodman mean stress correction.

CHAPTER 6

CONCLUSIONS AND DISCUSSION

In this thesis, vibration fatigue theory and its applications are examined. When the loading is dynamic and randomly fluctuating consisting of sine functions whose frequency content has a wide bandwidth, the resonance frequencies of the structure are likely to be excited under dynamic loading. Therefore, frequency domain fatigue analysis techniques are used in the investigation of such situations that consider the dynamic response of the structure.

In this study, fatigue theory is investigated in a chronological order and vibration fatigue approaches proposed up to now are presented. Narrow band solutions' theories and how to develop broadband solution technique are examined. Dirlik method is chosen as the broadband solution for vibration fatigue calculations. It is a well known approach and commonly used when the loading spectra has a wide bandwidth. It is easy to apply and time saving. Rainflow counting is applied to identify stress ranges and Goodman formula is used where mean stress correction is necessary throughout this thesis.

A method is developed throughout the thesis study to create a modified input loading history with zero mean value which leads to fatigue damage approximately equivalent to that created by input loading with a nonzero

mean value. A new perspective is brought to the implementation of mean stress correction by the application of Goodman mean stress correction on the output von Mises stress power spectral density data. Then, a modified input acceleration power spectral density is generated. This enables making fatigue tests with corrected input loading that has zero mean value to simulate a test input with mean value other than zero which cannot be applied in standard vibration tests. A case study is done to show that the developed method is useful. A plate is excited from its cantilevered base with acceleration time history possessing a mean value of 3 g. Two fatigue analyses are conducted using finite element method. First one is carried out with the original input by using Goodman mean stress correction offered by MSC Fatigue. The second analysis is performed with the corrected amplified input and no mean stress correction is applied. Finite element analysis results regarding fatigue life are compared for the points in the vicinity of the point of failure and the difference in fatigue life between two analyses comes out as about 24%. This part of the thesis has also been published in ICMFF9 [63].

Furthermore, this method is improved for the cases where the input loading multiaxial. By this means, a loading history power spectral density set with zero mean but modified alternating stress is obtained taking all stress components into consideration which causes fatigue damage approximately equivalent to the damage caused by the unprocessed loading set with nonzero mean. The proposed techniques' efficiency is discussed throughout case studies and fatigue tests. First case study is done to compare the proposed input loading generation method with test results. A test plate is excited at its clamped end and the mean value of acceleration

excitation is selected as 1 g since it can be applied where the excitation direction is parallel to Earth's gravity direction which enables test validation. Two types of analyses and tests are carried out such that first one uses the original input loading with mean stress effect and the second one uses the corrected amplified input loading without mean stress effect. The difference in fatigue life between analyses is about 9%. When the compatibility between tests and analyses are investigated, the difference comes out about 22%. The second case study is done to implement the proposed method in multiaxial fashion. A fin shaped aerodynamic surface is excited along the three axes. Two fatigue analyses are carried out using finite element method. First one is performed with the original input by using Goodman mean stress correction proposed by MSC Fatigue. The second analysis is conducted with the corrected amplified input without mean stress correction. Finite element fatigue life results are compared for the point of failure and the difference in fatigue life between two analyses comes out as about % 3.5.

The developed methods enable making fatigue tests with the inputs having mean value other than zero. The fatigue results are conservative therefore it is safe to use the modified input as the test input. The conservatism is lessened by means of improvements for multiaxial loadings which prevents oversafe design. This way, the optimization between safety and conservatism is improved.

As future work, the proposed methods developed using broadband fatigue solution can be adapted for narrowband excitation applications using narrowband solutions rather than Dirlik's method. Besides, the proposed

methods can be modified using Gerber mean stress correction which is less conservative when compared with Goodman formula. This way, the difference between fatigue life results of vibration fatigue tests and fatigue life results of finite element analysis is expected to decrease.

REFERENCES

[1] J. E. Shigley, C. R. Mischke, and G. Budynas, "Mechanical Engineering Design", *Mc Graw-Hill*, Seventh Edition, New York, 2004.

[2] P. J. E. Forsyth, "A two stage process of fatigue crack growth", *Proceedings of Crack Propagation Symposium*, vol. 1, pp. 76–94, Cranfield, 1961.

[3] P.J.E. Forsyth, "The Physical Basis of Metal Fatigue", *Blackie and Son Publications*, London, 1969.

[4] N. E. Frost, K. J. Marsh, and L. P. Pook, "Metal Fatigue", *Dover Publications*, Mineola, NY, 1999.

[5] R. A. Smith, "The Versailles railway accident of 1842 and the first research into metal fatigue", *Fatigue '90 MCE Publications*, vol. 4, pp. 2033–2041, Birmingham, 1990.

[6] W. Schutz, "A history of fatigue", *Engineering Fracture Mechanics*, vol. 54, pp. 263–300, 1996.

[7] R. H. Parsons, "History of the Institution of Mechanical Engineers", *Institution of Mechanical Engineers*, London, 1947.

[8] H. J. B. Schmidt, "Fatigue and Damage Tolerance", *Course Lecture Notes*, Ankara, 2008.

[9] C. Kilroy, "American Airlines Flight 191", *www.airdisaster.com*, 2008.

[10] "Aircraft Accident Report: Aloha Airlines, Flight 243", *www.aloha.net*, 1988.

[11] MSC Inc., "MSC. Fatigue User's Guide", Southfield, MI, 2008.

[12] R. E. Peterson, "Discussion of a Century Ago Concerning the Nature of Fatigue, and Review of Some of the Subsequent Researchers Concerning the Mechanism of Fatigue", *ASTM Bulletin*, no. 164, pp. 50, 1950.

[13] F. Braithwaite, "On the fatigue and consequent fracture of metals", *Institution of Civil Engineers, Minutes of Proceedings*, vol. 13, pp. 463–474, 1854.

[14] "Wöhler's Experiments on the Strength of Metals", *Engineering,* pp. 160, 1867.

[15] J. Bauschinger, "On the Change of the Position of the Elastic Limit of Iron and Steel Under Cyclic Variations of Stress", *Mitt. Mech.-Tech. Lab.*, Munich, vol. 13, no. 1, 1886.

[16] J. A. Ewing, and J. C. W. Humfrey, "The Fracture of Metals under Repeated Alterations of Stress", *Phil. Trans. Roy. Soc.*, London, vol. CC, pp. 241, 1903.

[17] O. H. Basquin, "The Experimental Law of Endurance Tests", *Proceedings of the ASTM*, vol. 10, part II, pp. 625, 1910.

[18] A. A. Grifith, "The Phenomena of Rupture and Fow in Solids", *Trans. Roy. Soc.*, London, vol. A221, pp. 163, 1920.

[19] A. Palmgren, "Die Lebensdauer von Kugellagern", *ZDVDI*, vol. 68, no. 14, pp. 339, 1924.

[20] H. Neuber, "Kerbspannungslehre", *Springer-Verlag*, Berlin, 1937.

[21] M. A. Miner, "Cumulative Damage in Fatigue", *Transactions of the ASME, Journal of Applied Mechanics*, vol. 67, pp. A159, 1945.

[22] G. R. Irwin, "Analysis of Stresses and Strains Near the End of a Crack Traversing a Plate", *Transactions of the ASME, Journal of Applied Mechanics*, vol. 24, pp. 361, 1957.

[23] W. Weibull, "A Statistical Distribution Function of Wide Applicability", *Journal of Applied Mechanics*, pp. 293, 1951.

[24] S. S. Manson, "Discussion of Ref. [25]", *Trans. ASME, J. Basic Eng.*, vol. 84, no. 4, p. 537, 1962.

[25] J. F. Tavernelli, and L. F. Coffin, "Experimental Support for Generalized Equation Predicting Low Cycle Fatigue", *Transactions of the ASME, Journal of Basic Engineering,* vol. 84, no. 4, pp. 533, 1962.

[26] T. H. Topper, B. I. Sandor, and J. Morrow, "Cumulative Fatigue Damage Under Cyclic Starin Control", *Journal of Materials,* vol. 4, no. 1, p. 189, 1969.

[27] M. Matsuishi, and T. Endo, "Fatigue of Metals Subjected to Varying Stress", *Japan Society of Mechanical Engineers*, Japan, 1968.

[28] W. Elber, "Fatigue Crack Closure under Cyclic Tension", Engineering *Fracture Mechanics,* vol. 2, pp. 37, 1970.

[29] P. C. Paris, "Testing for Very Slow Growth of Fatigue Cracks", *Closed Loop,* vol. 2, no. 5, 1970.

[30] S. O. Rice, "Mathematical Analysis of Random Noise", *Selected Papers on Noise and Stochastic Processes*, Dover, New York, 1954.

[31] J. S. Bendat, "Probability functions for random responses", *NASA report on contract NAS-5-4590*, 1964.

[32] P. H. Wirsching, M. C. Light, "Fatigue under wide band random loading", *Journal of Structural Division, ASCE*, pp. 1593-1607, 1980.

[33] G. K. Chaudhury, and W. D. Dover, "Fatigue Analysis of Offshore Platforms Subject to Sea Wave Loading", *International Journal of Fatigue*, vol. 7, 1985.

[34] J. M. Tunna, "Fatigue Life Prediction for Gaussian Random Loads at the Design Stage", *Fatigue Fact Engineering Mat. Struct.*, vol. 9, no. 3, pp. 169-184, 1986.

[35] J. C. P. Kam, and W. D. Dover, "Fast Fatigue Assessment Procedure for Offshore Structures under Random Stress History", *Proceedings of the Institution of Civil Engineers*, vol. 85, part 2, pp. 689-700, 1988.

[36] D. S. Steinberg, "Vibration Analysis for Electronic Equipment", *John Wiley & Sons*, 3rd edition, USA, 2000.

[37] T. Dirlik, "Application of computers in Fatigue Analysis", Ph.D. Thesis, University of Warwick, 1985.

[38] W. F. Wu, H. Y. Liou, and H. C. Tse, "Estimation of fatigue damage and fatigue life of Components under Random Loading", *International Journal of Pressure Vessels & Piping*, vol. 72, pp. 243-249, 1997.

[39] N. Bishop, A. Caserio, and C. Mesa, "Vibration Fatigue Analysis in the Finite Element Environment", *Americas User Conference*, California, 1998.

[40] H. Y. Liou, W. F. Wu, and C. S. Shin, "A modified model for the estimation of fatigue life derived from random vibration theory", *Probabilistic Engineering Mechanics*, vol. 14, pp. 281-288, 1999.

[41] X. Pitoiset, A. Preumont, and A. Kernilis, "Tools for Multiaxial Fatigue Analysis of Structures Submitted to Random Vibrations", *Active Structures Laboratory*, Brussels, 1999.

[42] G. Petrucci, and B. Zuccarello, "On the estimation of the fatigue cycle distribution from spectral density data", Department of Mechanics and Aeronautics, University of Palermo, Italy, 2004.

[43] G. Petrucci, and B. Zuccarello, "Fatigue Life Prediction under Wide Band Random Loading", Department of Mechanics and Aeronautics, University of Palermo, Italy, 2004.

[44] X. Pitoiset, and A. Preumont, "Spectral Methods for Multi-axial Random Fatigue Analysis of Metallic Structures", *International Journal of Fatigue*, vol. 22, pp. 541–550, 2000.

[45] R. Tovo, "Cycle Distribution and Fatigue Damage under Broad-band Random Loading", *International Journal of Fatigue*, vol. 24, pp. 1137–1147, 2002.

[46] N. A. Siddiqui, and S. Ahmad, "Fatigue and fracture reliability of TLP tethers", *Marine Structures 14*, pp. 331-352, 2001.

[47] P. L. Tu, Y. C. Chan, and J. K. L. Lai, "Effect of Inter-metallic Compounds on Vibration Fatigue of μBGA Solder Joint", *IEEE Transactions on Advanced Packaging*, vol.24, no.2, pp. 197-206, 2001.

[48] D. Benasciutti, and R. Tovo, "Spectral Methods for Lifetime Prediction under Wide-band", *International Journal of Fatigue*, vol. 27, pp. 867–877, 2005.

[49] I. Rychlik, "On the 'Narrow-band' Approximation for Expected Fatigue Damage", *Prob. Eng. Mech.*, vol. 8, pp. 1-4, 1993.

[50] H. O. Madsen, S. Krenk, and N. C. Lind, "Methods of Structural Safety", *Englewood Cliffs: Prentice-Hall*, 1986.

[51] M. Aykan, "Vibration Fatigue Analysis of Equipments used in Aerospace", M.Sc. Thesis, Middle East Technical University, Ankara, 2005.

[52] N. W. M. Bishop, and F. Sherratt, "Finite Element Based Fatigue Calculations", *NAFEMS*, Germany, 2000.

[53] "ASTM Designation E 1049-85: Standard Practices for Cycle Counting in Fatigue Analysis", *ASTM*, 1985.

[54] Y. Murakami, "The Rainflow Method in Fatigue", *Butterworth-Heinemann*, Oxford.

[55] E. Kreyszig, "Advanced Engineering Mathematics", Seventh Edition. *John Wiley & Sons*, 2005.

[56] J. W. Cooley, and J. W. Tukey, "An Algorithm for the Machine Calculation of Complex Fourier Series", *Math. Comp.*, vol. 19, pp.297-301, 1965.

[57] N. W. M. Bishop, N. Davies, A. Caserio, and S. Kerr, "Fatigue Analysis of an F16 Navigation Pod", *www.randomvibration.com*, 2000.

[58] J. C. P. Kam, and W. D. Dover, "Fast Fatigue Assessment Procedure for Offshore Structures under Random Stress History", *Proc. Instn. Civ. Engrs.*, Part 2, vol. 85, pp. 689-700, 1988.

[59] M. M. Rahman, A. K. Ariffin, N. Jamaludin, C. H. C. Haron, and R. A. Bakar, "Fatigue Life Prediction of Two-Stroke Free Piston Engine Mounting Using Frequency Response Approach", *European J. of Scientific Research*, vol. 22, pp. 480-493, 2008.

[60] J. S. Bendat, and A. G. Piersol, "Random Data: Analysis and Measurement Procedures", *John Wiley and Sons*, NY, 1986.

[61] T. Lagoda, E. Macha, and R. Pawliczek, "The influence of the mean stress on fatigue life of 10HNAP steel under random loading", *International Journal of Fatigue*, vol. 23, pp. 283-291, 2000.

[62] R. Hathaway, and K. W. Long "Transducers and Acquisition Data", *Elsevier Butterworth-Heinemann*, USA, 2005.

[63] B. Kocer, Y. Yazicioglu, S. Dag, "On the Generation of a Loading History with Zero Mean for a Structure Subjected to Multiaxial

Variable Stresses", *Proceedings of The Ninth International Conference on Multiaxial Fatigue & Fracture (ICMFF9)*, June 7-10, 2010, Parma, Italy.

[64] Leissa, A. W., "Vibration of Plates", *Aeronautics and Space and Administration*, Washington, 1969.

APPENDIX A. TEST FIXTURE

A fixture made of aluminum AA-5754 is designed to be used for vibration fatigue tests. The solid model of the fixture is given in Figure A.1. The design criterion is the functionality that allows for tests in both vertical and horizontal direction (Figure A.2) and the strength which sustain the test loadings. For this purpose, a fixture is designed such that its first natural frequency is above the biggest frequency appearing in the input loading which is 2000 Hz. The modal analysis results are given in Figure A.3 - Figure A.5 for the first three mode shapes with natural frequencies.

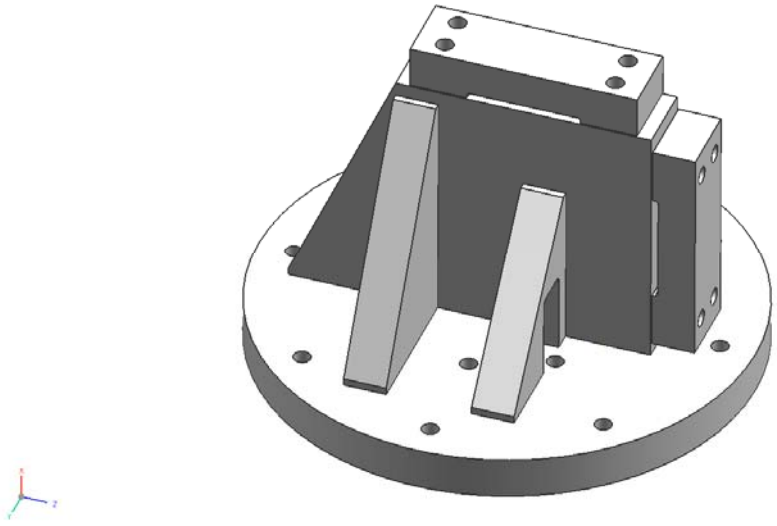

Figure A.1 – Test Fixture

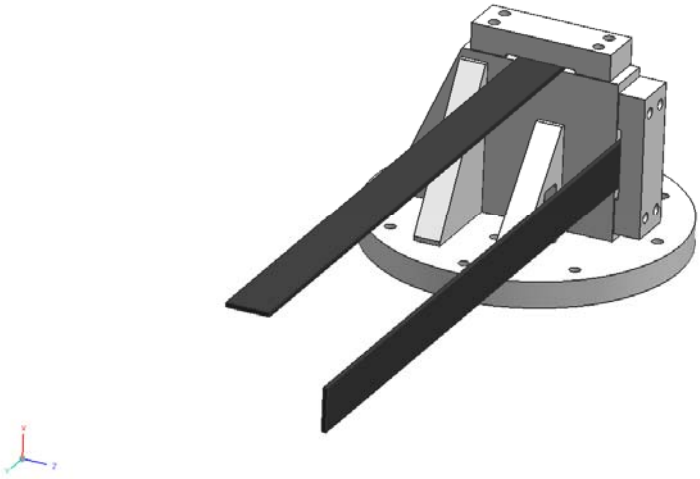

Figure A.2 – Test Fixture – Specimen Assembly Types

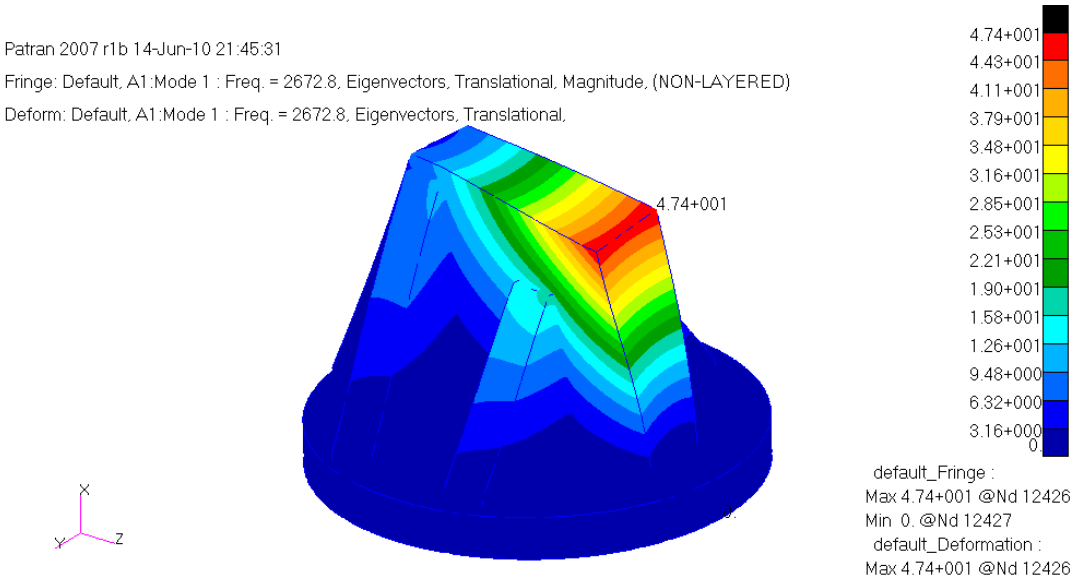

Figure A.3 – First Mode Shape of the Test Fixture

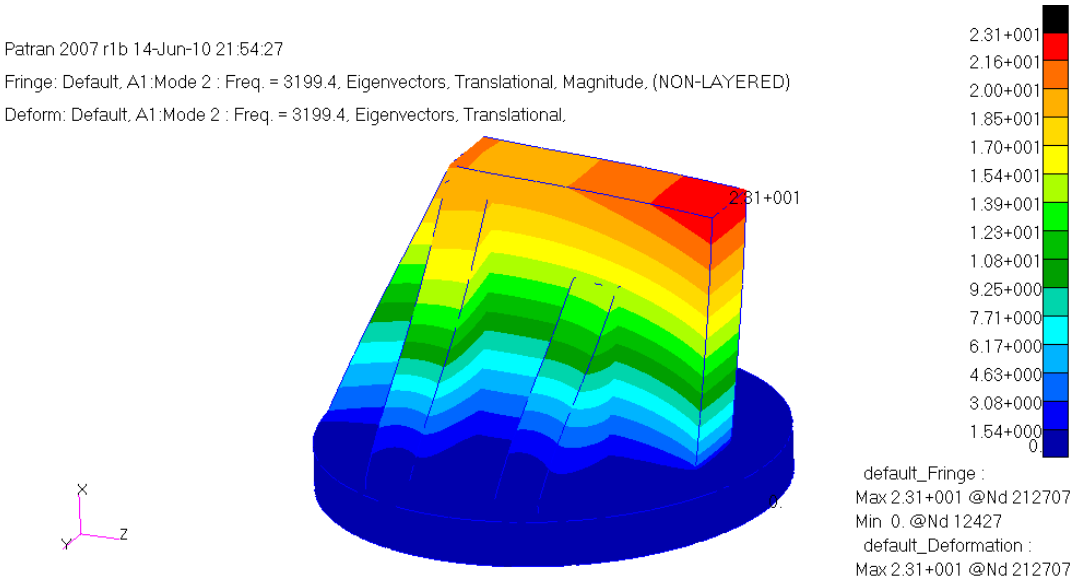

Figure A.4 – Second Mode Shape of the Test Fixture

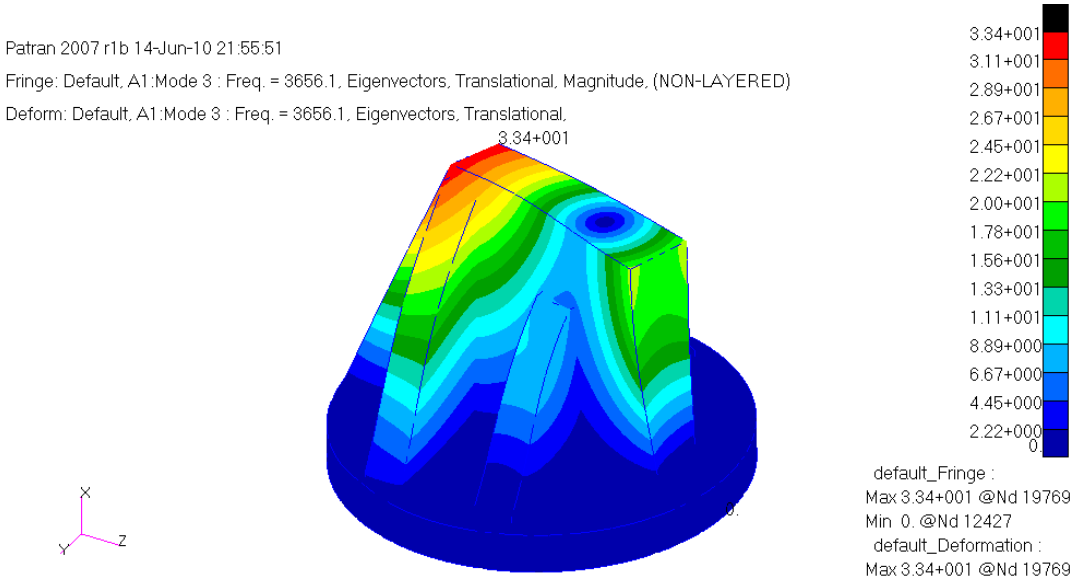

Figure A.5 – Third Mode Shape of the Test Fixture

APPENDIX B. COMPARISON OF SOLID AND SHELL FEM

The finite element model's compatibility with the specimen (Figure 4.1) is verified comparing the analytical solutions and finite element results for modal analysis. The analytical formula [64] used to calculate four natural frequencies of a plate (Figure B.1) is given in (B.1)-(B.3) and Table B.1.

Furthermore, the difference in accuracy between the results obtained from the model constituted with shell elements and the model constituted with solid element is presented in Table B.2. The solid element is chosen for the modeling rather than shell element since it gives more reliable results.

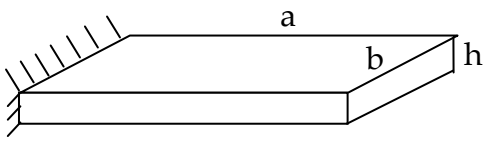

Figure B.1 – Plate Dimensions

Table B.1 – Constant A for a/b=5

Mode	A
First Bending	3.450
Second Bending	21.52
First Torsion	34.73
Second Torsion	105.9

$$\omega = A\sqrt{\frac{D}{K}}\frac{1}{a^2} \tag{B.1}$$

$$K = \rho h \tag{B.2}$$

$$D = \frac{Eh^3}{12(1-\nu^2)} \tag{B.3}$$

where

ρ : Density

h : Thickness

a : Length

b : Width

E : Elastic modulus

υ : Poisson ratio

Table B.2 – Natural Frequencies Errors

Mode	Analytical Solution (Hz)	Shell Model (Hz)	Solid Model (Hz)	Error (Shell-Analytical)	Error (Solid-Analytical)
First Bending	7.59	7.38	7.42	-2.89	-2.36
Second Bending	47.40	46.18	46.44	-2.58	-2.03
First Torsion	76.50	104.31	72.33	36.34	-5.45
Second Torsion	233.28	315.63	221.28	35.30	-5.14